12-31-2006

Data fusion of complementary information from parietal and occipital event related potentials for early diagnosis of Alzheimer's disease

Nicholas Stepenosky
Rowan University

Data Fusion of Complementary Information from Parietal and Occipital Event Related Potentials for Early Diagnosis of Alzheimer's Disease

by

Nicholas Stepenosky

A Thesis Submitted to the

Graduate Faculty in Partial Fulfillment of the

Requirements for the Degree of

MASTER OF SCIENCE

Department: Electrical and Computer Engineering
Major: Engineering (Electrical Engineering)

Approved:

In Charge of Major Work

For the Major Department

For the College

Members of the Committee

Rowan University
Glassboro, New Jersey
2006

ABSTRACT

Nicholas Stepenosky
DATA FUSION OF COMPLEMENTARY INFORMATION FROM PARIETAL AND OCCIPITAL EVENT RELATED POTENTIALS FOR EARLY DIAGNOSIS OF ALZHEIMER'S DISEASE
2005/06
Dr. Robi Polikar
Master of Science in Electrical Engineering

The number of the elderly population affected by Alzheimer's disease is rapidly rising. The need to find an accurate, inexpensive, and non-intrusive procedure that can be made available to community healthcare providers for the early diagnosis of Alzheimer's disease is becoming an increasingly urgent public health concern. Several recent studies have looked at analyzing electroencephalogram signals through the use of many signal processing techniques. While their methods show great promise, the final outcome of these studies has been largely inconclusive. The inherent difficulty of the problem may be the cause of this outcome, but most likely it is due to the inefficient use of the available information, as many of these studies have used only a single EEG source for the analysis. In this contribution, data from the event related potentials of 19 available electrodes of the EEG are analyzed. These signals are decomposed into different frequency bands using multiresolution wavelet analysis. Two data fusion approaches are then investigated: i.) concatenating features before presenting them to a classification

algorithm with the expectation of creating a more informative feature space, and ii.) generating multiple classifiers each trained with a different combination of features obtained from various stimuli, electrode, and frequency bands. The classifiers are then combined through the weighted majority vote, product and sum rule combination schemes. The results indicate that a correct diagnosis performance of over 80% can be obtained by combining data primarily from parietal and occipital lobe electrodes. The performance significantly exceeds that reported from community clinic physicians, despite their access to the outcomes of longitudinal monitoring of the patients.

ACKNOWLEDGMENTS

For more than two years, I have had the privilege of working on this project. For that I owe much appreciation to Dr. Robi Polikar. I would like to thank him for this amazing opportunity and for his patience and encouragement. If he hadn't believed in me and offered me this chance, I feel my abilities would not be at the level they are and I would not have had the same experiences in education and travel.

I want to thank my family. Without them, I would have never gotten this far. They have always believed in me and supported me in all my choices throughout my collegiate career and I love them very much. Also to the newest member to my family, Jennifer Berenato (soon to be Stepenosky), thank you for your support, your patience, and most of all for your love. You are my strength and my inspiration and I love you.

Special thanks goes out to Dr. Shreekanth Mandayam and Dr. Adrian Rusu for taking time out of their busy schedules to be a part of my defense committee. I would also like to thank Apostolos Topalis and Genevieve Jacques for their help and work throughout this research, Mark Turowski, Kyle Stockdale, Hussein Syed Mohammed, and everyone else that has supported me. Finally, I would like to thank the National Institute on Aging of the National Institutes of Health (under grant number P30 AG10124 - R01 AG022272) for supporting my graduate studies.

TABLE OF CONTENTS

LIST OF FIGURES

LIST OF TABLES

CHAPTER 1

INTRODUCTION

The number of the elderly population affected by Alzheimer's disease (AD) is rising and has become a major public health concern. Therefore, the need for an accurate, inexpensive and non-intrusive procedure for the early diagnosis of the disease that can be made available to local healthcare providers becomes increasingly urgent. Although once considered rare and part of normal aging, Alzheimer's disease is now the most common type of dementia, as it accounts for more than half of all dementia cases [1,2]. In general, evidence of dementia cases from well-planned, representative epidemiological surveys is scarce in many regions. According to [3], there are an estimated 24.3 million people suffering from dementia, with 4.6 million new cases of dementia every year. This means that there is approximately one new case of dementia every 7 seconds. According to data based on the number of cases detected in the 2000 United States census, the Alzheimer's Association and the National Institute on Aging in the United States estimate that approximately 4.5 million people have AD. This number is expected to increase substantially and reach approximately 16 million cases in the United States alone by the year 2050 [1].

The only definitive means for diagnosis is via autopsy, but clinical evaluations are the most common procedure for diagnosing AD. A study showed that local physicians have a significantly lower overall correct diagnostic accuracy than that of a skilled physician with access to longitudinal monitoring of patients [1,4]. Unfortunately, this

type of expertise, particularly that of neuropsychologists, is only available at major research and university hospitals and can be prohibitively expensive. There is currently no standard procedure or effective diagnostic tool available to community healthcare providers who serve as the first line of intervention for the disease. To have a meaningful impact on healthcare, an effective, accurate, inexpensive, and non-invasive procedure for the diagnosis of AD must be made available to community-based physicians. The goal of this study is to develop an automated diagnostic tool for the early diagnosis of AD that can be made available to local health clinics that is comparable to the diagnostic abilities of an expert.

The approach proposed in this study for creating such a diagnostic tool involves an analysis of EEG signals using signal processing techniques and automated classification. Several studies have been performed on EEG signals for the early diagnosis of AD using signal processing methods in order to establish a biomarker for AD, but these attempts have shown only varying degrees of success. The reason for using EEGs is practical and quite simple. EEGs are a well established technique, inexpensive and non-intrusive to acquire, and many local healthcare facilities already own or have access to the necessary equipment.

1.1 ALZHEIMER'S DISEASE

Alzheimer's disease is a progressive neurological disorder associated with aging, nerve degeneration, and neuron death. It gradually destroys a person's memory and their ability to learn, reason, make judgments, communicate, and carry out daily activities. In the pre-clinical stages of AD, there are no reliable and valid symptoms that can be detected to

allow a very early diagnosis before irreversible cognitive deficits manifest. In the mild stage, an impairment of learning and memory is usually noticeable. The declarative recent memory, or fact memory, which stores information from the "what," "who," "where," and "when" kinds of questions, is predominantly affected with early loss of memory for everyday events. Semantic difficulties with word generation and a deterioration of object naming are also prominent. In the moderate dementia stage, language difficulties increase and become more obvious [5]. Deficits in other cognitive abilities (abstract and logical reasoning, planning, organizing,etc.) appear during the progression of the disease [6]. As the disease progresses, individuals may also experience changes in personality and behavior, such as anxiety, suspiciousness or agitation, and some may experience delusions or hallucinations [1].

The likelihood of developing AD almost doubles every five years after the age of 65. This is often referred to as late-onset Alzheimer's disease. At this age range, approximately one out of ten individuals will develop the disease. By the age of 85, the odds of developing AD increases to one out of every two [1].

An AD patient may live eight to twenty years beyond diagnosis, if the disease is diagnosed and treated in its earliest stages. An early diagnosis allows an early start of a treatment plan, which can not only improve the life expectancy of the patient significantly, but also improve their quality of life. Therefore, the early diagnosis of Alzheimer's disease is of utmost importance.

1.1.1 BIOLOGICAL ASPECTS OF ALZHEIMER'S DISEASE

As previously mentioned, Alzheimer's disease is associated with nerve degeneration and neuron death. Scientists and researchers believe that factors that trigger the disease begins its damage to the brain years before any detectable symptoms appear. When symptoms do finally appear, nerve cells that process, store, and retrieve information, have already begun to degenerate and die. Typically, the damage of the nerve cells begins with those involved with learning and memory functions. The disease then gradually spreads to cells that control the abilities and aspects of thought, judgment, and behavior. The neuropathology of AD is characterized by widespread neuronal cell loss due to two types of unusual proteins: neurofibrillary tangles, and senile amyloid plaques in the hippocampus, neocortex, and other brain regions [7].

Amyloid plaques are clumps of protein fragments that accumulate outside of the brain's nerve cells. Beta amyloid, which is typically a harmless protein, is believed to cause these deposits of plaque which form *between* neurons early in the disease process, before neurons begin to die and any symptoms develop [8]. The role of amyloid deposits is uncertain as a part of the pathology of the disease because a variant form of the disease has no amyloid deposits present [2].

Neurofibrillary tangles, on the other hand, are clumps of altered proteins *inside* cells, mainly tau protein. During the progression of AD, threads of tau protein undergo alterations that cause them to become twisted forming "tangles". Some researchers believe that this seriously damages the neurons by breaking down their internal cellular structure and causes them to die [8]. Just like that of amyloid deposits, the role of tau in AD has also been questioned since mutations in the tau gene have been linked to a variety

of neurodegenerative diseases other than AD [2].

Some research efforts have focused on identifying genetic causes of the disease, while other scientists and researchers have focused on developing medications that slow and prevent the accumulation of suspected proteins. Many others yet believe that the cause of the disease is not necessarily as important as the fact that the course of the disease remains the same regardless of its cause [9].

1.1.2 CLINICAL DIAGNOSIS

Just as AD has no known single cause, there in no standard procedure for diagnosis. The only definitive means of diagnosis is via an autopsy. The disease is characterized by the above mentioned unusual proteins, which can only be seen by studying brain tissue under a microscope. Researchers have been working to discover early symptoms, a method for diagnosis, and medications to prevent possible causes and progression before the disease reaches its debilitating stages.

The current 'gold standard' for AD diagnosis is clinical evaluation, which has been used with considerable success for AD diagnosis. The evaluation process involves a series of clinical interviews between a neuropsychologist and the subject. Results from a thorough medical history, physical examination, and memory assessment and nervous system function tests are combined to determine if there are changes in the person's cognitive status. All of these tests are necessary to assess if a person has symptoms of AD. Overall, it is difficult to determine whether a person is actually suffering from AD, or from other possible forms of dementia such as vascular dementia, or if the symptoms are simply associated with normal aging [10].

Having access to the expertise of a skilled physician is usually not an option for the majority of dementia patients. Since most patients are evaluated at local community clinics and healthcare facilities. The expertise and accuracy of diagnosis at such facilities remains uncertain. Our only metric for these health care providers is a 1999 study, where a group of Health Maintenance Organization-based physicians reported a sensitivity of 83%, a specificity of 55%, and an overall accuracy of 75% [4]. This performance is the metric against which the results of this effort are compared.

1.1.3 OTHER DIAGNOSTIC TOOLS

Other methods besides conventional clinical evaluations are being considered for diagnostic tools. Spinal taps are used to extract cerebrospinal fluid (CSF), which contains known biomarkers for AD, but this is a highly invasive technique. One study has shown that concentrations of beta amyloid, total tau, and phosphorylated tau in CSF are strongly associated with the future development of Alzheimer's disease in patients with mild cognitive impairment [11]. Magnetic resonance imaging (MRI) scans can capture images of the lesions in the brain, but they are very expensive and are not always available at local health care facility.

Abnormalities in the brain are known to disrupt the brain's electrical signals and can theoretically be detected through electroencephalogram (EEG) signals. EEGs can be obtained in a non-invasive manner, and are a fairly inexpensive to acquire. Traditionally, EEG analysis was not used for AD diagnosis due to it poor spatial resolution. There were difficulties in EEG analysis in distinguishing changes attributed by AD and those by normal aging, other medical illnesses, and other factors associated with physiology [12].

Recently, there has been a revival of EEG analysis used for the diagnosis of AD and many techniques seem more promising then had originally been anticipated [13]. One reason behind this revival is that AD is a cortical dementia in which EEG abnormalities are more frequently shown. Subcortical dementias exhibit relatively normal EEG patterns compared with other cortical dementias [14]. The EEG abnormalities in AD directly reflect anatomical and functional deficits of the cerebral cortex after being damaged by the disease. Thus, it is anticipated that the analysis of EEG dynamics will provide useful and informative clues concerning the neuropathology of AD.

Again, an accurate, cost-effective, and non-intrusive diagnostic tool, that can be made available to local clinics is of critical importance. As we move the diagnostic process earlier within the natural history of the disease, it is very important to maintain current levels of sensitivity and specificity of the AD diagnosis. [15]. An approach based on EEG analysis can potentially satisfy all of the mentioned requirements, if its accuracy can be established. The EEG itself is an established and dependable technology, easy and cost-effective to operate, and hence ideally suited for a health clinic setting. Overall, a reliable method for diagnosing the illness in its early stages is essential so that medications may be administered in a timely fashion to reduce the progression of the disease to its later devastating stages.

1.2 OBJECTIVES OF THIS STUDY AND ORGANIZATION OF THE THESIS

The goal of this study has been the design and development of an automated algorithm for the early diagnosis of Alzheimer's disease. The specific research objectives were:

1. Develop an automated classification procedure for the early diagnosis of

Alzheimer's disease through the analysis of EEG signals that is comparable in accuracy to a clinical diagnosis by an expert.

2. Compare the diagnostic performance of different frequency subbands from the wavelet analysis of data from all available electrode recordings acquired during both the target and novel stimuli.
3. Combine features from electrodes using data fusion techniques in an effort to provide the most informed decision for classification and enhance the overall generalization performance.

The organization of this thesis is as follows. Alzheimer's disease and difficulties associated with its diagnosis were introduced in this chapter. Chapter 2 provides specific background on EEG signals, event related potentials, and their acquisition. Chapter 3 describes previous approaches on using EEGs and ERPs for AD diagnosis. Chapter 4 includes the implementation of our approach as well as the data acquisition process, and subject statistics. The theory behind the multiresolution wavelet analysis which is used as the feature extraction technique is also covered in Chapter 4. Chapter 5 describes the theory behind the classifier and ensemble based algorithms and techniques used throughout the experiments of this research. Chapter 6 presents the results from all experiments which include using single MLP neural networks, and different ensembles and combination rules. Finally, Chapter 7 summarizes the accomplishments of this study, discusses possible sources of error, and presents recommendations for future work as a conclusion for this thesis.

CHAPTER 2

THE ELECTROENCEPHALOGRAM AND THE EVENT RELATED POETENTIAL

2.1 ELECTROENCEPHALOGRAM

Electroencephalogram (EEG) signals represent the electrical activity of the brain as voltage (typically microvolts) over time. EEGs are recorded using a series of electrodes placed on the scalp. These signals have traditionally been used to determine illnesses associated with brain activity, such as schizophrenia [16], and epilepsy [17]. Changes in the brain's electrical activity can reflect changes in cognitive status. Hence, the main goal of this study is to determine whether our method of automated analysis can detect changes in EEG signals that reflect the earliest changes caused by Alzheimer's disease.

Hans Berger, a neuropsychiatrist, is credited for the discovery of human EEG signals [18]. Berger started studying humans in 1924 using various galvanometers. In the following years, he identified different features within the brain's signals such as sleep spindles, fluctuations of consciousness, the first evidence of alpha rhythms, as well as a several disorders [19]. He was also the first to observe pathological EEG sequences in a historically verified AD patient [18,20].

Thereafter, the EEG developed as a method for investigating mental processes and was quickly adopted for use in clinical applications. The EEG became more popular with the introduction of event-related potentials (ERPs), which are components of the EEG that result from specific sensory and cognitive processes.

Many advances in EEG studies led to breakthroughs in neurophysiology. The idea that different neurological disorders could be explored further through the use of EEGs caused research to shift in that direction [19,21].

2.1.1 EEG RECORDINGS

EEG recordings are acquired using electrodes placed in different locations on the scalp. EEGs can be recorded as bipolar recordings where electric potentials are recorded between pairs of active electrodes, or as a monopolar recording where potentials are recorded with respect to a single passive reference electrode. These measures are primarily performed on the surface of the scalp (scalp EEG), but special electrodes can also be placed on the surface of the brain during a surgical operation (intracranial EEG). Better resolution can be achieved with the intracranial implanted electrodes, but a surgical procedure is required for placement of the electrodes. Hence, intracranial recordings are impractical for most human studies [21].

The standard system in use for the placement of scalp electrodes is the International 10-20 system, which was developed to keep a consistent placement scheme for comparison studies. The system is termed 10-20 because EEG electrodes are placed on the scalp at 10 and 20 percent of a measured distance (the circumference of one's head). The system involves a number of electrodes connected at key scalp locations. The electrodes are usually referenced to two electrodes on the earlobes to obtain signals from particular regions of the brain.

One problem with scalp electrode recordings is that artifacts alter the EEG signal. Artifacts are easily created due to head and eye movements, muscle activity, etc. Since

the EEG signals have such low amplitudes, artifacts from these added stimuli contaminate recordings. These artifacts are typically removed as a preprocessing procedure by the EEG technician. Synchronized and repeated signals are then averaged to make the components within the signal more pronounced [21].

Figure 2.1 shows an expanded version of the International 10-20 system. It displays the possible electrode names and their positions on the scalp. Note that these extra electrodes are added in between the usual electrodes for a more thorough analysis and higher resolution. The notation in Figure 2.1 is as follows: F = frontal, C = central (cortex), P = parietal, T = temporal, O = occipital, and A = auditory reference corresponding to the regions of the brain where the electrodes are placed. Convention calls for odd numbers on the left and even numbers on the right [19].

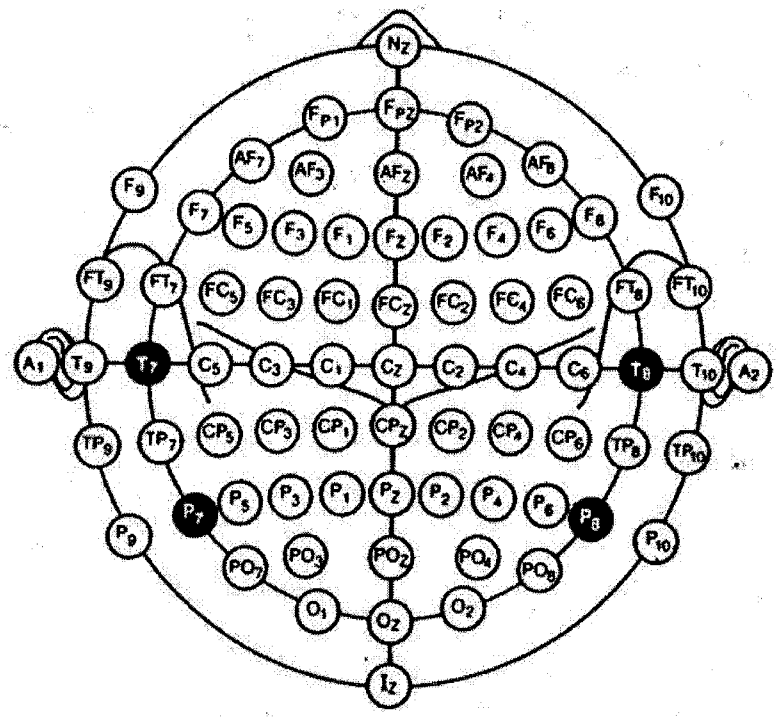

Figure 2.1: Example of the expanded International 10-20 system for scalp electrode placement.

2.1.2 SPECTRAL CONTENT OF THE EEG

An EEG signal can be broken into different frequency bands. Each band has been shown to be associated with different brain functions. As reported in [22], the five main frequency bands are as follows:

- The delta band (0.5 – 3.5Hz) is characteristic of deep sleep stages. An increase in the amplitude of the delta response has been found during experiments using an oddball paradigm (refer to Section 2.2). This suggests that the response may be linked to signal detection and the corresponding decision [23,24].

- The theta band (3.5 – 7.5Hz) has been correlated with higher cognitive and associative brain processes [24,25]. The event related potential (refer to Section 2.3) components in the theta band are prolonged after target stimuli in oddball paradigm experiments. This latency indicates a relationship with selective attention [23,24].

- The alpha band (7.5 – 12.5Hz) is sometimes divided into two subbands, alpha1 (7.5 – 10Hz) and alpha2 (10 – 12.5Hz). In some cases, results have indicated that the working memory is associated with alpha oscillations [23,26].

- The beta band (12.5 – 30Hz), like the alpha band, can also be divided into subbands, beta1 (12.5 – 20Hz) and beta2 (20 – 30Hz). The beta rhythms have been found to elicit a stronger response in recordings from the central and frontal electrodes. Beta rhythms have also shown enhancement during states of expectancy and tension [21].

- The gamma band (30 – 60Hz) became popular after cellular level experiments showed a relationship with the linking of stimulus features into perceived information. Basar-Eroglu *et al.*, 1996, suggested that the gamma band activity is part of the common language elements of the brain. This activity may also be associated with mutual information transfer between subcomponents of the brain just as it is with other oscillations such as theta, alpha, or beta [27,28].

2.2 DATA ACQUISITION PROTOCOLS

In certain protocols for EEG acquisition, the patient is exposed to a sensory stimulus in order to elicit a particular response. These responses are known as event related or evoked potentials. There are three common modalities, or types of stimuli, used: auditory, visual, and somatosensory. The auditory modality uses single tones of a preset frequencies or clicks with a broadband frequency distribution as stimuli. For the visual type, stimuli are produced by a single light or sometimes by the reversal of a pattern such as a checkerboard. For the somatosensory modality, stimuli are a combination of the visual and auditory types [29].

Sequences of stimuli are arranged in paradigms to study the responses to tasks in order to test such factors as memory, reaction time, awareness, etc. The tasks involved could vary from simple tasks such as pressing a button to harder tasks such as the memorization of an extensive list. The oddball paradigm, one of the most common paradigms, has been used in experiments conducted for this study.

The traditional oddball paradigm involves two different stimuli presented in a pseudo-random order. The oddball, or target, tone is presented randomly in a series of

frequently occurring, or standard, tones. The standard tone is presented in 75-80% of the trials, and the oddball stimuli in the remaining 20-25% of the trials. The oddball stimulus is usually a different frequency than the standard, set far enough apart to be distinguishable from the frequent stimuli [12,21]. The subjects are instructed to perform a simple task such as pressing a button, keeping a mental count of the number of oddball tones, etc., after hearing each oddball tone [12,21,30].

Yamaguchi *et al.*, 2000, developed a variation of this paradigm with the use of novel tones consisting of 60 unique environmental sounds, recorded from Disney movies edited to be 200ms in duration. In this variation, standard stimuli occur 65%, target stimuli occur 20%, and novel tones occur 15% of the time. Again, subjects are asked to respond only to the oddball stimulus by performing a simple task defined at the beginning of the experiment. This type of experiment is performed in efforts to differentiate between different types of dementia [31,32].

2.3 EVENT RELATED POTENTIALS

The potential evoked in the EEG as a response to a stimulation is called an event related potential (ERP) or an evoked potential [29]. ERPs are a series of positive and negative peaks that occur in response to a specific event to which the subject is usually asked to respond. Each element of the ERP has a name that denotes its sign, such as P for positive or N for negative, and its latency after the stimulus is perceived by the subject. Some of these elements are explained below and Figure 2.2 shows the labeled components of an ERP.

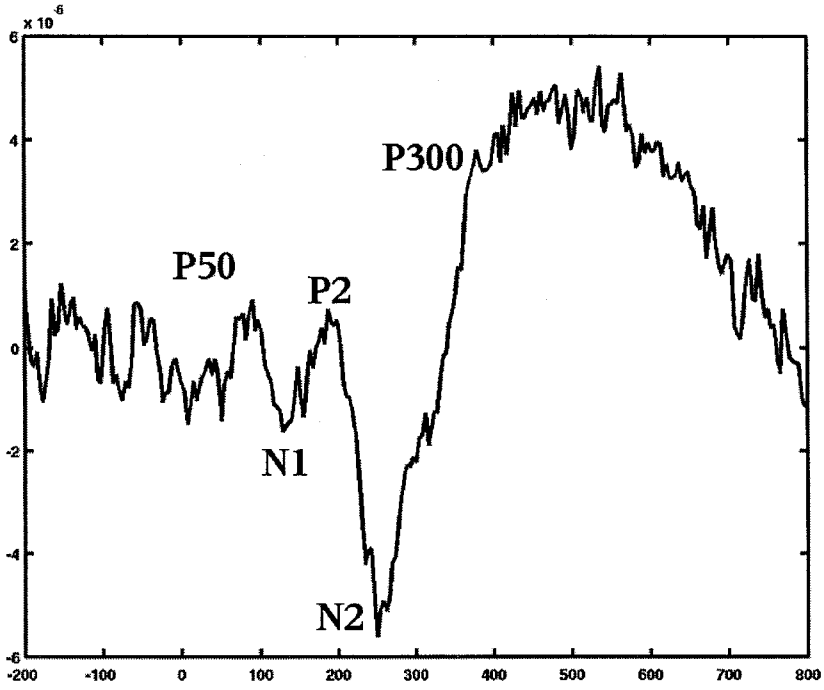

Figure 2.2: ERP signal and components

P50 is a positive peak that occurs around 50ms after the stimulus. N1 is a negative peak occurring around 100ms after the stimulus. Golob and Starr, 2000, showed in a study that changes in the amplitude and latency of the N1 peak may be observed during memorization tasks [33].

P2 is a positive peak at approximately 200ms after the stimulus. P2 response is stronger due to standard stimulus in an oddball paradigm as opposed to target stimulus, implying that it contains a component due to sensitivity of the sensory processes other than cognitive processes [32].

N2 is a negative peak at approximately 200ms. This response is found to be stronger in response to target tones in the oddball paradigm, however given its close proximity to the P3 component, it is hypothesized that the amplitude and latency of the N2 may be affected by the P3 generation [32].

P3 or P300 is a positive peak occurring around 300ms. The P300 has been shown to occur in response to oddball tones, and has also been associated with mental activity. The P300 is measured by quantifying its amplitude and latency, where amplitude is defined as the voltage difference between the pre-stimulus baseline and the largest peak with latency between 250-400ms. The latency is the time measured from stimulus onset to the point of maximum positive amplitude within the particular latency window [32,34]. The latency and amplitude of the P300 component have been shown to be related to age and the cognitive ability of the individual [19,32]. The P300 can be attributed to a manifestation of central nervous system activity involved with the processing of new information when attention is engaged in updating memory. The latency of the P300 in the discrimination task provides an indication of individual ability in mental processing capability and speed [12].

In 1999, Katayama and Polich conducted an experiment involving 12 young adults. EEG recordings were acquired using the oddball paradigm with both visual and auditory modalities. The P300 was largest for the parietal and mid-line electrodes and occurred in response to both target and non-target stimuli during both modalities [35].

A second P300 is created in experiments involving the novel tones. The target P3, or P3b, is the traditional P300 with the strongest area of detection from the parietal region. The novelty P3 or P3a is in response to an alarming or novel stimulus and originates in the frontal region. The use of the novel tones is said to increase the P3b and elicit a P3a. However, the P3a is only readily observed in about 20% of normal subjects which, although this peak may be the most sensitive to changes in cognitive function, tends to be limited in use [22,31,32].

Due to the low amplitude of the ERPs compared with the ongoing EEG, averaging several responses is a common practice to visualize the ERP. The ERPs have a similar pattern of response which is predictable under similar conditions [21,22]. Sufficient numbers of artifact-free trials have been shown to stabilize ERP measures in both amplitude and latency [31].

2.4 EEG OF ALZHEIMER'S PATIENTS

Different studies have shown abnormalities in the EEG of AD patients. The hallmark of EEG abnormalities in AD patients is slowing of the rhythms. An increase in theta and delta activities and a decrease in beta activities are repeatedly observed [36,37,38]. The severity of the disease is also correlated with these abnormalities [39, 40].

The P300, as mentioned in the previous sections, has been related to cognitive processes that require attentional allocation and immediate memory processes. It has been observed that the P300 latency is prolonged and that the amplitude is decreased in AD patients. Sometimes this can occur so that the peak is not at all obvious as shown in Figure 2.3 [31, 41]. The P300 directly reflects currents triggered by cortical post-synaptic potentials and seems to be primarily generated in the temporal-parietal cortex. This makes sense because this area shows pronounced synaptic loss in AD [42].

The P300 has been found to be affected by dementia, but there are many other factors that affect this particular peak. Contrary to what has been stated thus far, Figure 2.4 shows a nearly nonexistent P300 for a normal subject and a prominent P300 component for an AD subject.

The factors known to affect the P300 are kept to a minimum such as no food

intake prior to EEG, no medication of certain types taken within 48 hours of EEG, etc. Some guidelines are put in place to keep variations in the P300 to a minimum [12, 43]. In this study, criteria to control the factors known to affect the P300 response, such as those listed above, were added to limit the effects on the P300. The P300 in Figure 2.4 is most likely affected by other factors beyond those controlled in this study. Experiments conducted in this study do not specifically analyze the P300; however the frequency range in which the P300 and other ERP components occur are explored.

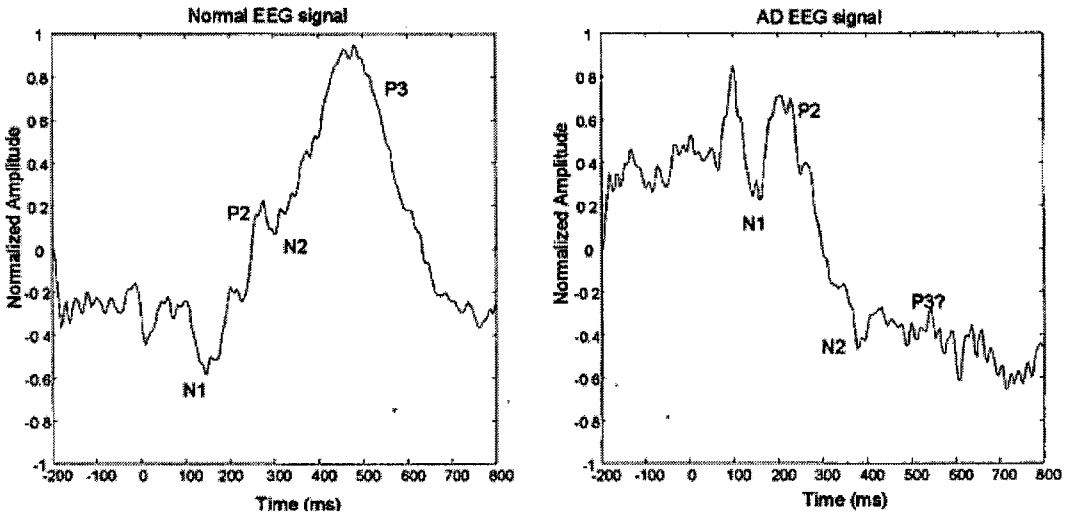

Figure 2.3: Normal subject EEG with obvious P3 (left), AD subject EEG with missing P3 (right).

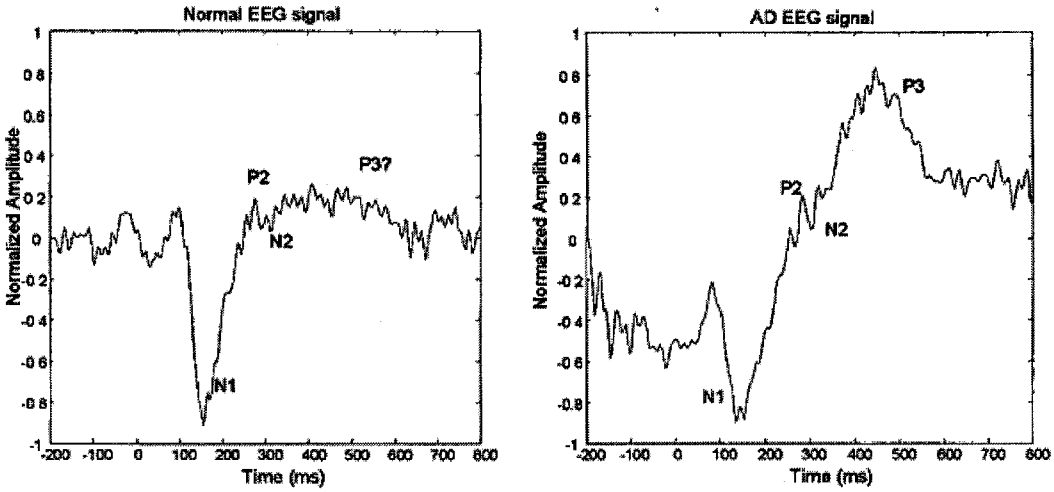

Figure 2.4: Normal subject EEG with P3 not obvious (left), AD subject EEG with prominent P3 (right).

CHAPTER 3

EEG & ERPs IN ALZHEIMER'S DISEASE DIAGNOSIS

The methods described in this chapter present previous efforts investigating EEG analysis as a potential biomarker for Alzheimer's disease. Some of the techniques that have been explored by fellow researchers within this project's previous studies including power spectral density analysis, ERP analysis, P300 analysis, statistical measures, and frequency analysis are also included. These techniques are discussed to represent a basis for this work and to present a comparison among different factors of this study and the work being done by fellow researchers.

3.1 P300 ANALYSIS

Demiralp *et al.*, 1999, applied a time–frequency decomposition to the event-related potentials elicited in an auditory oddball test. The goal was to assess differences in cognitive information processing. An analysis in the time domain revealed that cognitive processes are reflected by various ERP components. These reflections were most noticeable in the N1, P2, N2, and P300 ERP components. The wavelet transform allowed the time-dependent and frequency-related information in the ERPs to be captured and more precisely measured. A four-octave quadratic B-spline wavelet was selected as the wavelet function and the transform was applied to the acquired auditory oddball paradigm ERPs. The analysis showed that the frequency components in the delta, theta, and alpha ranges reflected specific aspects of cognitive information processing [44].

Demiralp *et al.*, 2001, assessed how target and standard discrimination difficulty and the degree of stimulus "novelty" affected target and non-target P300 scalp distributions for a visual modality in a three-stimulus oddball task. A wavelet analysis was performed on the non-target (P3a) and target (P3b) ERPs to assess how the underlying EEG activity was affected by both the difficulty and novelty factors. When the discrimination between target and standard stimuli was easy, amplitudes were higher for the target P3b than the non-target P3a across all electrode sites. Both responses also demonstrated parietal maximums. In contrast, when the target and standard stimuli discrimination was difficult, non-target P300 (P3a) amplitudes were higher and earlier over the frontal and central electrode sites for both levels of novelty, whereas target P300 (P3b) amplitudes were greater in parietal recordings and occurred later than the non-target components. The wavelet analysis indicated that theta activity was related to the more novel non-target stimuli. Delta coefficients during target stimuli were affected by the discrimination difficulty. These results suggest that target and standard discrimination difficulty, rather than stimulus novelty, determines P3a generation for visual stimuli. However, the theta oscillations are affected by stimulus novelty [45].

Basar *et al.*,2001, analyzed the effects of the wavelet transform and digital filtering on the underlying ERP data of the EEG. The compound ERPs are portrayed as the superimposition of evoked rhythms in EEG frequencies ranging from the delta to gamma bands. These frequency ranges are often referred to as the 'natural frequencies of the brain'. A wavelet analysis was implemented on the ERPs and confirmed the results of the combined analysis procedure obtained by using the amplitude frequency characteristics and digital filtering. The results obtained by wavelet analysis underline

and extend the view that alpha-, theta-, delta-, and gamma-responses are related to psycho-physiological functions. The properties of the wavelet analysis imply that it may be used to evaluate experiments where physiological tasks will be altered without informing the subjects [46].

Demirapl *et al.*, 2001, applied a comparative wavelet analysis to oddball P300 results. The results obtained confirm those obtained by using adaptive digital filtering. The delta response dominates the P300 potential while the theta response is prolonged in a second late window [47].

Aviyente *et al.*, 2004, performed an analysis of event-related potentials collected during a psychological experiment where two groups of subjects, spider phobics and snake phobics. Both groups are shown the same set of stimuli which consist of a blank stimulus, a neutral stimulus and a spider stimulus. The study introduces a new approach for ERP analysis based on distance measures in time-frequency distributions. The difference in brain activity before and after a presented stimulus is quantified using distance measures. Three different distance measures are applied on the time-frequency plane to discriminate between the responses of the two groups of subjects. The results illustrate the effectiveness of using distance measures combined with time-frequency distributions in differentiating between the two classes of subjects and the different regions of the brain [48].

3.2 EEG AND ALZHEIMER'S

Since Hans Berger first observed pathological EEG sequences in a historically verified AD patient [18,20], a large number of studies about the EEG of AD have been

performed. Goodin *et al.*, 1978, first demonstrated the slowing of P3 event-related potentials (ERPs) with aging [49]. Since then, a number of studies have suggested that ERPs are a useful indices for assessing age-related changes in cognitive brain functions.

Although ERP latency and its variability may be useful in describing group differences (i.e. Alzheimer's disease patients from age-matched controls), they are not sufficiently sensitive to classify individuals into subgroups of dementia [50]. Polich *et al.*, 1986, tested the ability of ERPs in distinguishing AD from other dementias and failed to find significant differences in either P3 latency or amplitude [51]. Neshige *et al.*, 1988, was unable to differentiate AD patients from VD patients using P3 latency obtained from a conventional auditory oddball paradigm [52]. However Polich *et al.*, later found in 1990, that increased latency and decreased amplitude of P300 was associated with AD when compared to normal ERPs [53]. For the next several years, researchers used a variety of stimuli to increase the diagnostic sensitivity of ERPs [54,55]. It was demonstrated that the latency, amplitude, and scalp topography of the P3 are affected by aging processes [55,56,57]. Yamaguchi *et al.*, 2000, proposed a modified auditory oddball paradigm to generate a maximum parietal P3, and found that the response to novel stimuli is affected by dementia [32].

Jeong, 2004, summarizes important findings about EEG abnormalities in AD patients obtained from linear and nonlinear methods, and considers the clinical neurophysiology of AD underlying the EEG abnormalities [13]. The following is an excerpt from the article.

> "Conventional visual analyzes of the EEG in AD patients have demonstrated a slowing of the dominant posterior rhythm, an increase in

diffuse slow activity [58,59,60,61], a reduction in alpha [62,63] and beta activities [63,64]. There is a good correlation between the degree of the EEG abnormality and cognitive impairment [58,59,60,61,64,65,66,67,68, 69,70]."

The above is just a sample of the topics covered in [13]. The extent of topics on EEG analysis related to Alzheimer's disease exceeds the scope of this thesis but those topics provided above are the foundation upon which this research is built.

3.3 EEGS, WAVELETS, AND NEURAL NETWORKS

Polikar *et al.*, 1997, applied the Daubechies 4 wavelet to EEG data collected from 14 normal subjects and 14 subjects diagnosed with probable AD. The ERP response in the oddball paradigm was analyzed to determine if the use of the wavelet transform was feasible for the detection of AD with a multilayer perceptron (MLP) neural network. Half the signals, 7 AD and 7 normal, were used for training while the rest were used for testing the network. The generalization performance of the network was 93%. The results confirmed that the approach is feasible for classifying ERPs, but the authors indicated that a more diverse database with a larger variety of signals would be necessary to allow statistically valid generalizations [30].

Petrosian *et al.*, 1999, used a method involving recurrent neural networks (RNN) and wavelet processing to distinguish between EEG recordings of six age-matched subjects, 3 probable AD and 3 controls. The eye-closed continuous 9-channel EEGs were recorded from each patient, and approximately 2 minute segments of artifact free recordings from occipital channels were selected to train and test neural networks. The

Extended Kalman Filter-based algorithm was used for training RNNs. This algorithm adapts the weights of the network in an instance-by-instance fashion. It accumulates important information in approximate error covariance matrices, and provides individually adjusted updates for each of the network's weights. The EEGs were encoded with target values of -0.85 and +0.85 for control and AD EEGs, respectively. The network training and testing procedures were implemented on both original EEGs as well as wavelet filtered subband signals with the Daubechies 4 wavelet. The network performed reliably when trained on a pair of AD and control recordings and tested on four recordings [71].

Petrosian *et al.*, 2001, also explored wavelet transform by using specifically designed and trained recurrent neural networks (RNNs) to discriminate between EEGs of ten mild AD patients and ten age-matched control subjects. The EEG recordings were taken during resting state without the use of a paradigm. The Daubechies 4 wavelet was chosen due to its good localization properties in the time and frequency domains. The RNNs used in the study belong to a type of discrete-time recurrent MLPs. This type of network has better temporal capabilities than that of a regular feedforward MLP, and is capable of representing and encoding strongly hidden states. Training on three AD subjects and three controls and testing on the remaining controls yielded performance that was better than chance with 80% sensitivity and 100% specificity. Five out of seven of the AD subjects were correctly classified. The authors suggest that their approach may be extended to include more classes such as other types of dementia [72].

Yagneswaran *et al.*, 2002, investigated signal power frequency and wavelet characteristics for differentiating between EEGs of 9 subjects diagnosed with probable

AD and 10 age-matched controls. The EEGs were recorded from 9 scalp electrodes placed according to the international 10-20 system. A bandpass FIR filter using the Hamming window was applied to each recording to segment each EEG into four significant subbands – delta (1-4Hz), theta (4-8Hz), alpha (8-13Hz) and beta (13-22Hz). The theta, alpha, and beta subbands were used for training and testing of a learning vector quantization (LVQ) classifier. These subbands displayed significant group differences in average power, relative power (RP), and slower wave ratio (SWR). The wavelet coefficients were obtained by a decomposition of the EEG recordings with the Daubechies 5 wavelet. The averages of the coefficients at each level were then used in the training and testing of an LVQ classifier. Out of 37 recordings (17 from AD and 20 from controls), 18 were used for training and 19 for testing. The power frequency input vector contained 9 spectral features (the average power, RP, and SWR of the theta, alpha and beta subbands), while the wavelet based feature vectors had 7 features (averages of the six detail level and the one approximation level coefficients). The network was able to correctly classify 18 of the 19 test recordings when using the spectral features, and 17 of the 19 test recordings when using the wavelet features [15].

In 2002, de Trad performed a study using the resonant recognition model (RRM) to predict characteristic frequencies for both beta-amyloid protein, its precursor, and functionally important amino acids for beta-amyloid as mentioned in Chapter 1. Amyloid plaques in the brain are a prominent and diagnostic feature of AD. One possible approach to preventing AD is to block the production of amyloid in the brain. The RRM is a physico-mathematical model that analyzes the interactions of protein and its target using digital signal processing methods. Once the RRM characteristic frequency for a

particular biological function or interaction has been determined, it is possible to identify the individual amino acids that contribute mostly to the characteristic frequency. Different wavelet functions (Morlet, Coiflets, Daubechies, Symlets, and Meyer) were used and compared in de Trad's study to detect active sites of beta-amyloid and beta-amyloid precursor proteins. Results linked frequencies with the proteins and predicted high energy domains but depended on the wavelet function used. In conclusion, better results may be obtained if a specific wavelet were designed for this application [73].

Cho *et al.*, 2003, proposed an automatic recognition method for Alzheimer's disease with a single channel EEG recording combined with the genetic algorithm (GA) and artificial neural networks (ANN). Sixteen probable AD patients and sixteen age-matched control patients were recruited. The EEGs were recorded from an Ag-AgCl electrode placed at P4. The ERPs were acquired during an auditory oddball task with standard sine-wave tones (75%) of 1 kHz and target tones (25%) of 1.5 kHz, each lasting 300ms. The subjects were instructed to count internally the number of target tones. The EEGs and ERPs were analyzed to generate a feature pool of 118 features which included 88 power spectral measurements, 28 statistical measurements, 2 chaotic features (central tendency and the boc-counting dimension), and 10 ERP features. The GA method consisted of making chromosomes of 35 features from the feature pool and assigning a fitness value to each. Genetic operations were used to create new generations of the chromosomes to find dominant features. The combined GA/ANN was applied to find the minimal set of dominant features from the feature pool that were the most effective in classifying the two groups. Hence, these dominant features were then used as the training and testing data for an ANN. 137 EEG segments from 11 AD patients and 10 normal

subjects were used as training data. The GA/ANN approach found the 35 dominant features including 24 spectral, 8 statistical, 1 nonlinear and 2 ERP features. 72 EEG segments for tests were from 5 AD patients and 6 normal subjects. The recognition rate was 81.9%. In conclusion, the selection of dominant features by the genetic algorithm was used to optimize input for a neural network, and appears to have an impact on the effectiveness of the network [74].

In the earlier stages of our own study, Jacques *et al.*, 2004, used a multiresolution wavelet analysis on ERPs followed by automated classification. The cohort consisted of 32 subjects, 14 probable AD patients and 18 cognitively normal patients. The ERPs were collected using an oddball paradigm based on [30]. The cohort produced a total of 75 ERP recordings in which 30 were from AD subjects and 45 were from normal subjects. Two types of wavelet functions were used, Daubechies 4 and Quadratic b-splines. The average overall performance of the Daubechies 4 wavelet was $84.1 \pm 0.6\%$, and $82.4 \pm 1.0\%$ for the b-splines. The results suggest that this method could provide a stable and effective method for a diagnostic tool but needs further investigation [75].

Table 3.1 shows a summary of the automated methods for the diagnosis of Alzheimer's disease from Section 3.3 and includes the author's name, the year of their study, the size of the cohort the acquired and analyzed, the method by which they performed their analysis, the training and testing set sized, and the resulting performance.

Table 3.1: Summary of automated methods for AD diagnosis

Author and Year	*Cohort Size*	*Method*	*Training*	*Testing*	*Recognition Rate*
Polikar *et al.*, 1997	7 AD 7 normal	Multiresolution wavelet analysis (Daubechies 4), MLPs	7 AD 7 normal	7 AD 7 normal	93.00%
Petrosian *et al.*, 1999	3 AD 3 normal	Wavelet analysis (Daubechies 4) Recurrent Neural Networks and Extended Kalman Filtering	2AD 2 normal	1 AD 1 normal	Reliable
Petrosian *et al.*, 2001	10 AD 10 normal	Wavelet analysis (Daubechies 4) Recurrent Neural Networks	3 AD 3 normal	7 AD 7 normal	AD: 5/7 normal: 4/7
Yagneswaran *et al.*, 2002	9 AD 10 normal	LVQ classifiers, power analysis, wavelet analysis (Daubechies 5), 37 ERP recordings (17 AD, 20 normal), 2 feature vectors (one of 9 average power, relative power, and slower wave ratio features; the other, the average of 6 detail and 1 approx. level coefficients for 7 features)	18 random recordings	19 random recordings	9 features: 18/19 7 features: 17/19
Cho *et al.*, 2003	16 AD 16 normal	Genetic algorithm, neural networks, 118 feature pool (88 power spectral, 28 statistical measures, 2 chaotic measures), chromosome of 35 dominant features	11AD 10 normal	5 AD 6 normal	81.90%
Jacques *et al.*, 2004	14 AD 18 normal	Multiresolution wavelet analysis (Daubechies 4 and quadratic b-splines), MLPs, 75 ERP recordings (26 AD, 49 normal)	17 AD 25 normal	13 AD 24 normal	db4: 84.1±0.6% b-splines: 82.4±1.0%

3.4 OTHER EEG AND ERP METHODS

Park and Cho *et al.*, 2001, performed an ERP analysis of the amplitude and latency of the P3 component in 4 cohorts. These cohorts consisted of 25 mild AD, 12 severe AD, 17 age-matched normal-aged controls and 7 young controls. The ERPs were obtained using an auditory oddball paradigm. Stimuli consisted of a series of computer-generated tones with 85dB, 300ms in duration. Tones of 1kHz (75%) and 1.5kHz (25%) were presented randomly for the 100 trials. Subjects were asked to count the number of

target tones and report it after the session. The EEG was recorded from Ag-AgCl electrodes placed at the F3, F4, CZ, P3, and P4 scalp locations. The N2, P3a, and P3b components of the ERP were measured for both the standard and target stimuli. The P3a and P3b were defined as the largest positive peak in the interval of 200-280, and 284-500ms post stimulus. The N2 component was the largest negative peak in the 109-196ms post stimulus. Correct response rates to target tones showed a significant difference between groups. While the normal aged group (88%) and young group (100%) showed high accuracy, the mild AD group (20%) and severe AD group (0%) had problems counting the stimuli. Major findings in this study showed the latency in the P3 component was prolonged in AD patients, whereas the amplitude of P3 was not different than that of the normal controls. This study suggests that the P3 components of the ERPs could be useful in the detection of AD [76].

Abasolo *et al.*, 2003, applied Approximate Entropy (ApEn) in the analysis of EEG background activity of 7 patients with a clinical diagnosis of Alzheimer's disease and 7 control subjects to determine whether there are differences between the groups. The EEGs were recorded while subjects were awake, relaxed in a quiet state with their eyes closed. EEGs were organized in frames of 5 seconds (1280 points). The P3 electrode was chosen for analysis at the advice of an electroencephalographer, because there are less artifacts and the rhythmical activity is more apparent. ApEn quantifies regularity in sequences and time series data. It assigns a non-negative number to a sequence or time series, where larger values correspond to more instances of recognizable features or patterns in the data. When applied to EEG data, larger values indicate higher complexity. Results showed with a statistical difference from ANOVA tests that the ApEn was higher

in control subject's EEGs when compared to the ApEn values of the EEGs of patients with probable AD. This experiment suggests that the non-linear analysis of EEG data might be useful to physicians since it shows the potential application of ApEn in reflecting differences in the complexity of EEG data time series of patients with a diagnosis of Alzheimer's disease and control subjects [77].

Melissant, *et al.*, 2005, studied an automatic EEG classification technique. They first implement a preprocessing technique for artifact-removal using independent component analysis (ICA). An ICA-processed multichannel EEG measurement does become more interpretable when compared to the raw data. They further proceed to show that detection of anomalies is also better after ICA-processing. The method is evaluated on measurements of a length of 8 seconds from two groups of patients. The first group of 28 patients show signs of the initial stages of the disease, whereas the 15 patients in the second group show signs of the later, more progressed stages of the disease. Both groups include a normal control group of 10 and 21, respectively. Three different classification methods were used: Bayes classifiers, *k*-NN classifiers, and feed-forward back-propagation neural networks. The results for the group with severe Alzheimer's disease are comparable to the best results from literature (upwards of 90%). The study shows that ICA-based reduction of artifacts improves classification results for patients in an initial stage [78].

CHAPTER 4

APPROACH

In our prior efforts [79-83], our approach consisted of performing a multiresolution wavelet analysis using the Daubechies 4 wavelet on the signals of our patient cohort. The coefficients obtained from the wavelet analysis were used as the features for the classification algorithm. The classification algorithm then resulted in a decision or diagnosis based on the features from the patient signal being analyzed.

This research used the same basic approach on our final cohort of 71 patients and on a subset of the final cohort consisting of 66 patients. All 19 available electrodes have been analyzed in this study, whereas only the PZ, CZ, or FZ electrodes had been explored in our previous works [79-83]. Single classifiers for each electrode/stimulus/frequency subband were trained and analyzed. The resulting performances from these classifiers give insight to the most informative electrode/stimulus/frequency subband combinations. Different classifier fusion techniques (specifically weighted majority vote, product rule and sum rule) were then used in an ensemble approach to combine the classifiers trained on the most informative electrode/stimulus/frequency subband features to increase the generalization performance. Feature-level fusion was also analyzed by concatenating the informative features for input into the classifiers.

The details of our approach are split between Chapters 4 and 5. Chapter 4 consists of details about the patients, the data acquisition protocol, and the process of the multiresolution wavelet analysis. Chapter 5 consists of the details of the classification algorithm including the multilayer perceptron, data fusion techniques, and combination rules. Figure 4.1 is a diagram overview of the approach of this project.

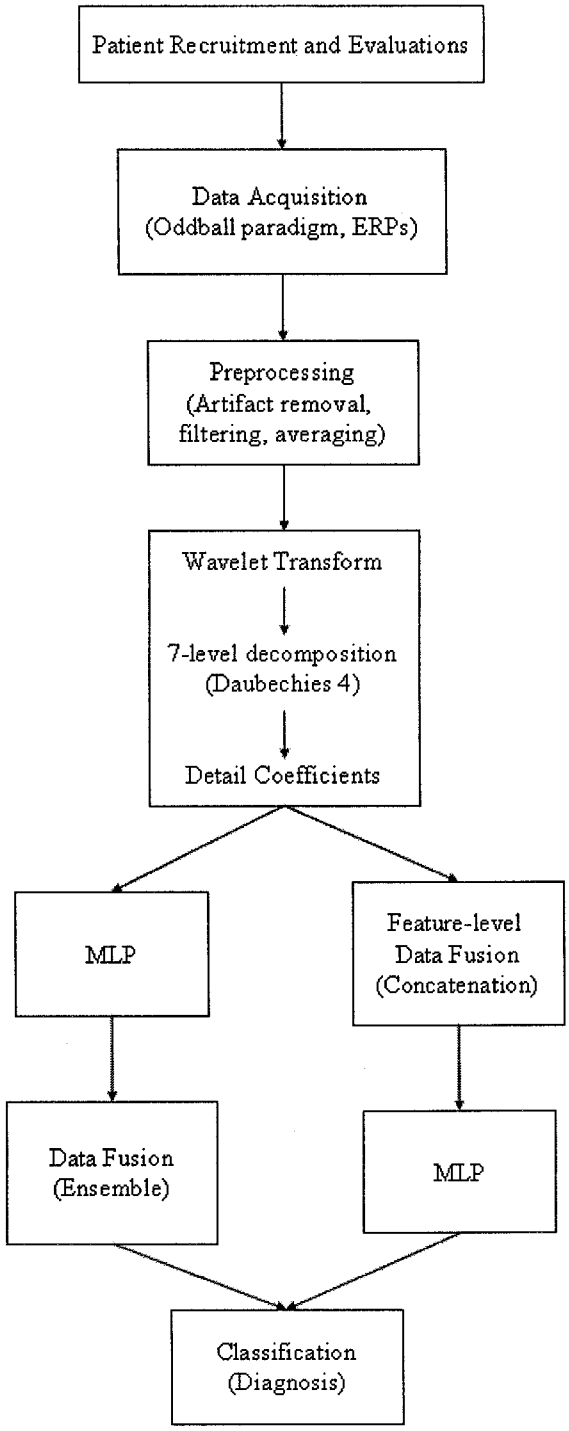

Figure 4.1: Overview of the project

4.1 RESEACH SUBJECTS

The data used for this research consisted of EEG data gathered at Drexel University from patients recruited by the University of Pennsylvania. Two cohorts have been analyzed in this research. The first set is the final cohort of this combined effort of seventy-one patients, 34 diagnosed with probable AD and 37 cognitively normal controls. The second cohort has excluded 5 patients from the 71 patient cohort because of suspected noisy data with artifacts from remnants of eye movement rendering unclassifiable results. This second cohort consists of sixty-six patients, 30 diagnosed with probable AD and 36 cognitively normal controls. Subjects were verified to be free of any evidence of other neurological disorders by history or by exam.

Mini-mental State Exam (MMSE), a test for memory, language and praxis skills is often used as one of the diagnostic tests during clinical evaluation. It is scored on a scale of 0-30, with decreasing scores (particularly below 19) indicating increased impairment. Other tests include Severe Impairment Battery (SIB), and the Clinical Dementia Rating (CDR) Scale, all of which are part of the NINCDS-ADRDA (National Institute of Neurological and Communicative Disorders and Stroke – Alzheimer's Disease and Related Disorders Association) criteria for probable AD [84]. Since our interest is in early diagnosis, the AD cohort was selected from those who has the highest MMSE scores. Table 4.1 shows details about both cohorts.

While recruiting the probable AD and cognitively normal cohorts, the following inclusion and exclusion criteria was used:

Inclusion criteria for cognitively normal cohort: (i) age > 60; (ii) Clinical Dementia Rating score = 0; (iii) Mini Mental State Exam Score > 26; (iv) no indication

of functional or cognitive decline during the two years prior to enrollment based on a detailed interview with the subject's knowledgeable informant.

Exclusion criteria for cognitively normal cohort: (i) evidence of any central nervous system neurological disease (e.g. stroke, multiple sclerosis, Parkinson's disease, etc.) by history or exam; (ii) use of sedative, anxiolytic or anti-depressant medications with 48 hours of ERP acquisition.

Inclusion criteria for AD cohort: (i) age > 60; (ii) Clinical Dementia Rating score = 0.5; (iii) Mini Mental State Exam Score ≤ 26; (iv) presence of functional and cognitive decline over the previous 12 months based on a detailed interview with a knowledgeable informant; (v) satisfaction of NINCDS-ADRDA (National Institute of Neurological and Communicative Disorders and Stroke – Alzheimer's Disease and Related Disorders Association) criteria for probable AD.

Exclusion criteria for AD cohort: Same as that for the cognitively normal controls.

Table 4.1: Cohort details including the number of patients, average ages and standard deviations, and average MMSE scores and standard deviations.

Cohort 1 (71 Patients)					
	Number of Patients	Average Age	Standard Deviation	Average MMSE Score	Standard Deviation
AD	34	74.9706	7.0860	24.6765	2.9513
Normal	37	76.1351	7.2845	29.2432	1.1880
Cohort 2 (66 Patients)					
	Number of Patients	Average Age	Standard Deviation	Average MMSE Score	Standard Deviation
AD	30	74.8333	7.2734	24.6667	2.9981
Normal	36	75.9722	7.3192	29.3056	1.1419

4.2 DATA ACQUISITION

The ERP recordings were obtained from each subject using the oddball paradigm. Subjects were comfortably seated facing a computer screen in a specially designated room. The protocol originally described by [32] was followed with slight modifications. Binaural audiometric thresholds were determined for each subject using a 1 kHz tone. The evoked response stimulus was presented to both of the subject's ears using stereo speakers with an amplitude level comfortable for their hearing. The stimulus consisted of tone bursts 100 ms in duration. Standard tones of 1000 Hz and target (oddball) tones of 2000 Hz were presented in a random sequence with the tones occurring in 65% and 20% of the trials, respectively. The remaining 15% of the trials consisted of novel sounds presented randomly. These included 60 unique environmental sounds that were recorded digitally and edited to duration of 200 ms.

A total of 1000 stimuli, including the standard (frequent) tones of 1000 Hz (n=650), target (infrequent) tones of 2000 Hz (n=200) and novel sounds (n=150), were delivered to each subject with an inter-stimulus interval of 1.0-1.3 seconds. The subjects were instructed to press a button each time they heard the target tone of 2000 Hz. With frequent breaks (approximately three minutes of rest every five minutes), the data collection process lasted about 30 minutes per subject with each session preceded by a 1 minute practice session without the novel sounds. Each recording is 1 second in duration with a 200ms pre-stimulus interval.

The ERPs were recorded from 19 tin electrodes embedded in an elastic cap. The electrode impedances were kept below 20 kΩ to yield a good signal. Artifacts were identified and rejected by the EEG technician. The remaining scalp potentials were

amplified, digitized at 256 Hz/channel (19 channels) and stored. The averaging protocol involved averaging 30-85 recordings per patient yielding 1-3 recordings per patient. All averages have been notched filtered at 59-61 Hz and baselined with the pre-stimulus interval. The 1-3 recording per patients were then averaged to create an overall average per patient (71 or 66 total) and normalized. Below in Figure 4.1 is example of the overall average ERP for the normal and AD cohorts during the target and novel stimuli. Figure (4.1a) is from the target recordings of the PZ electrode while Figure (4.1b) is from the novel recordings. Appendix B contains similar figures for all electrodes during both stimuli.

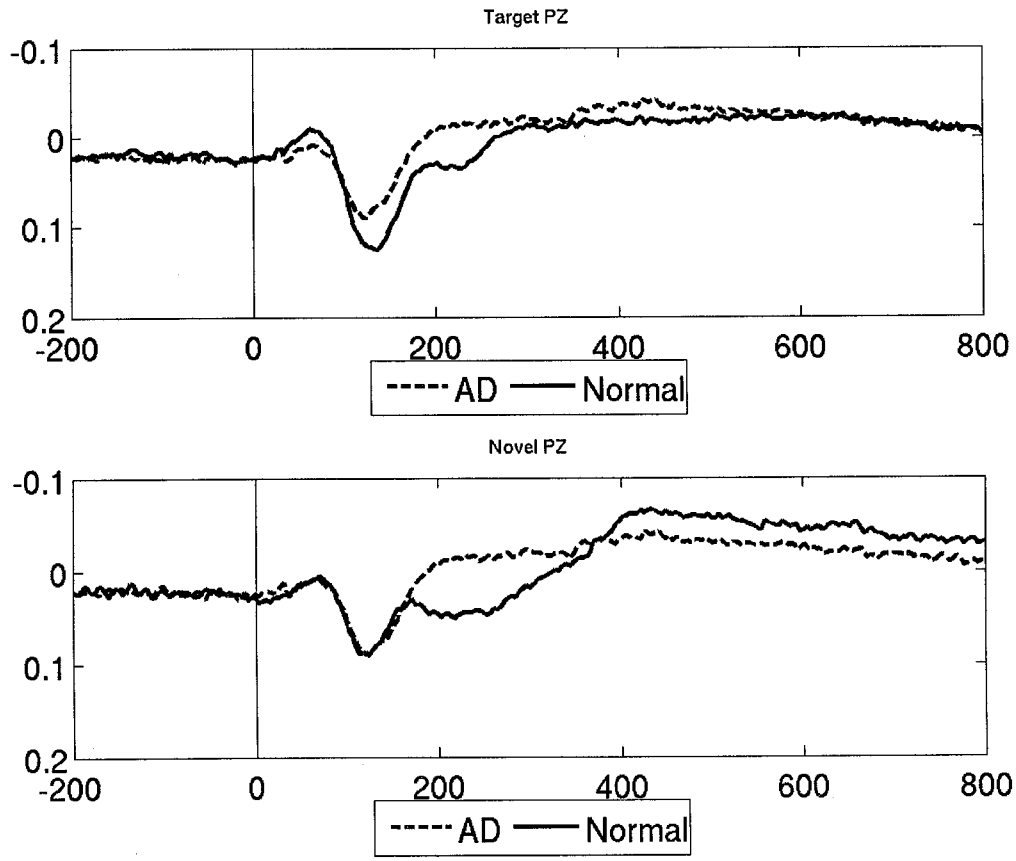

Figure 4.2: Overall average ERP from the PZ electrode during (top) target and (bottom) novel stimuli.

4.3 MULTIRESOLUTION WAVELET ANALYSIS FOR FEATURE EXTRACTION

Frequency analysis is an alternative and informative method for describing time domain signals. One advantage of the frequency domain representation over the time domain representation is the ability to visualize the frequency content of the signal. The Fourier Transform involves a correlation between a time signal and complex exponentials of different frequencies. However, the FT requires that a signal be stationary as it provides a global representation of frequencies in the signal and therefore results in the loss of time information.

The short time Fourier transform (STFT) tries to overcome this limitation and provides localized frequency information by windowing the complex exponential kernel of the FT. This gives a time evolution of the frequencies of the signal by shifting the window throughout the signal. The STFT consists of correlating the original signal with the time-windowed and modulated complex exponentials. If the window is too narrow, the STFT provides good time resolution and poor frequency resolution; conversely, if the window is too wide, good frequency resolution and poor time resolution is obtained. Ideally, low frequencies need a wide window while higher frequencies require a narrow window in order to appropriately capture the signals behaviors. The STFT is suited for analyzing non-stationary signals but its abilities are limited by a fixed window length throughout its analysis. This inability to adapt with the changing frequency content of a non-stationary signal is insufficient for our analysis [85,86].

An alternative approach to the FT and STFT, is the wavelet transform, particularly the discrete wavelet transform. The discrete wavelet transform is obtained through a process call multiresolution wavelet analysis. Multiresolution wavelet analysis

determines time localizations of spectral components, providing a time-frequency representation of the signal being analyzed. Such an analysis is particularly well-suited for non-stationary signals, such as ERPs, whereas the Fourier and short-time Fourier transforms lack time localization capabilities and adaptable resolutions for the appropriate frequency content, respectively. Therefore, a multiresolution wavelet analysis, by means of the DWT, will used in this study to extract features from the ERPs.

4.4 THE WAVELET TRANSFORM

The wavelet transform was developed as an alternative approach to overcome the fixed resolution problem of the short time Fourier transform. The main advantage of the wavelet transform is the varying window size which allows wide windows for low frequencies and narrow windows for high frequencies, leading to optimal time-frequency resolution for all frequency ranges [85,86,87].

4.4.1 THE CONTINUOUS WAVELET TRANSFORM

The continuous wavelet transform (CWT) is calculated in a similar way to that of the FT and STFT. The signal is multiplied with a wavelet kernel function, similar to the complex exponential kernel function in the FT. Just as the FT is calculated for different frequencies, the wavelet transform is computed for different segments of the signal with respect to its two parameters, scale and translation.

There are two main differences between the STFT and the CWT. First, the FTs of the windowed signals are not taken whereas the FT is computed for every windowed portion of the signal in the STFT. Secondly, the width of the window is changed as the

transform is computed for every single spectral component whereas the window is a fixed width throughout the entire calculation of the STFT [87].

A wavelet family $\psi_{b,a}$ is a set of functions created by dilations and translations of a unique mother wavelet $\psi(t)$:

$$\psi_{b,a}=|a|^{-1/2}\psi\left(\frac{t-b}{a}\right) \tag{4.1}$$

where $a \neq 0$, and $a, b \in \Re$ are the translation and scale parameters, respectively. Thus, the wavelet transform is a function of two variables. The constant number $|a|^{-1/2}$ is for energy normalization purposes so that the transformed signal will have the same energy at every scale. Translation is a time shift and scale is a parameter inversely proportional to frequency, where larger scales analyze global behavior and small scales analyze local behavior. a controls the support of the wavelet function; for example, by increasing a, the wavelet becomes narrower. b controls the position of the wavelet; for example, by varying b, the mother wavelet is displaced in time. Figure 4.2 illustrates the effect that changing the scale coefficient, a, has on the wavelet function. The wavelet shown is the Morlet wavelet, which is constructed by modulating a sinusoidal function by a Gaussian function, at scales of 0.5, 1, and 3.

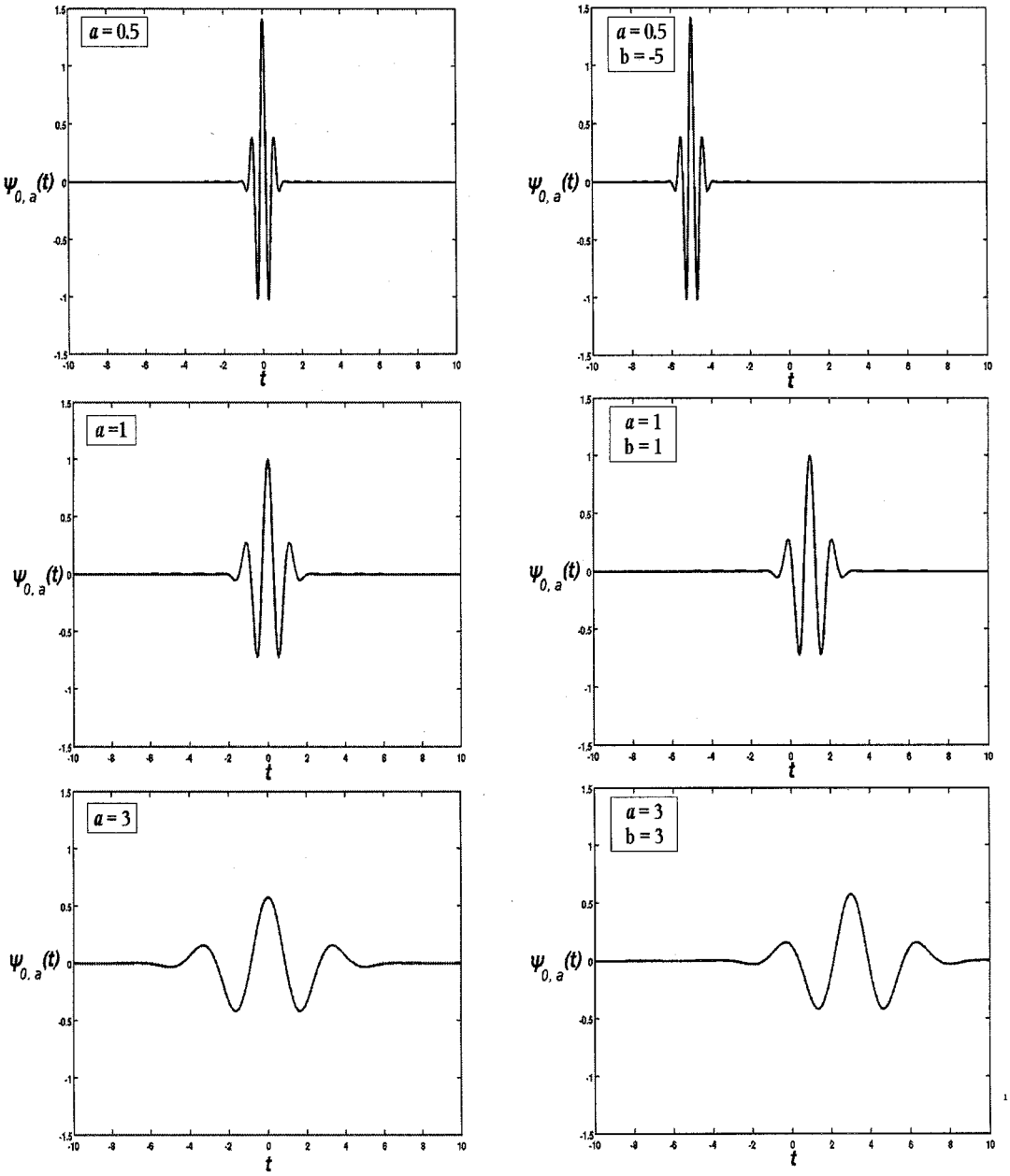

Figure 4.3: Morlet wavelet at different scales (dilations) and translations.

The wavelet functions must satisfy two properties:

$$\int_{-\infty}^{+\infty} \psi(t)\,dt = 0 \tag{4.2}$$

and

$$\int_{-\infty}^{+\infty} |\psi(t)|^2\,dt < \infty \tag{4.3}$$

Equation (4.2) requires that the wavelet is an oscillatory function, meaning a "wave". Equation (4.3) implies that the energy of in $\psi(t)$ if of finite duration. The two properties are easily satisfied by a large number of functions making these two requirements rather unrestrictive.

The continuous wavelet transform of a signal is defined as the correlation between between the signal $x(t)$ and the wavelet $\psi_{b,a}$. The CWT is defined as the following:

$$CWT_x^{\psi}(b,a) = \Psi_x^{\psi}(b,a) = \frac{1}{\sqrt{|a|}} \int x(t)\,\psi'\left(\frac{t-b}{a}\right) dt \tag{4.4}$$

where $'$ denotes the complex conjugate. The result of Equation (4.4) indicates how closely the wavelet function correlates with the signal at scale a. If the signal contains a component of the frequency at the particular scale, then the wavelet basis function at that scale will be similar to the signal at the location where that frequency occurs. These correlations are made with different scales, a, in the wavelet function for all times (translations), b, of a single function. The wavelet transform then gives a translation-scale representation [85,86,87].

Once a mother wavelet is chosen, the computation begins with an initial value of a, typically a=1. The CWT is computed for all values of a that are greater and less than

the initial value. Note that depending on the signal, a complete transform is usually not necessary. For all practical purposes, signals are bandlimited, and therefore, computation for a limited interval of scales is usually adequate.

The wavelet function at scale a and translation b=0 (which is typically the beginning of the signal $x(t)$) is multiplied by the signal and then integrated over all times. The wavelet at scale a is then shifted right by an amount of b to the location t=b. This procedure is repeated until the wavelet reaches the end of the signal. Then, a is increased by a small value, which is controlled by the scale resolution. This procedure is repeated for every value of a. Every computation for a given value of a fills the corresponding single row of the translation-scale plane. When the process is completed for all desired values of a, the CWT of the signal has been calculated [85,86].

4.4.2 THE WAVELET SERIES

Since they are continuous transforms, none of the FT, the STFT, or the CWT can be practically computed by using computers. It is therefore necessary to discretize the transforms. The most intuitive way of doing this for the CWT is by simply sampling the translation-scale plane. However, in the case of the WT, the scale change can be used to reduce the sampling rate. At higher scales (lower frequencies), the sampling rate can be decreased, according to Nyquist's rule. This means that if the translation-scale plane needs to be sampled with a sampling rate of N_1 at scale a_1 , the same plane can be sampled with a sampling rate of $N_2 < N_1$, at scale a_2 , where, $a_1 < a_2$ which correspond to frequencies $f_1 > f_2$. The actual relationship between N_1 and N_2 is given as:

$$N_2=\frac{a_1}{a_2}N_1=\frac{f_2}{f_1}N_1 \tag{4.5}$$

This means that the sampling rate at lower frequencies can be decreased, saving computation time and resources [85,86].

The conventional scheme for discretizing the translation-scale parameters is called the dyadic grid sampling. The scale parameter *a* is discretized first on a logarithmic grid. The translation parameter is then discretized with respect to the scale parameter , meaning a different sampling rate is used for every scale. For this process, time remains continuous but the translation-scale parameters are sampled by choosing $a_j = 2^j$, $b_{j,k} = k2^j$, with $j,k \in Z$ [88]. By inserting these scale and translation parameters, the continuous wavelets are obtained from the mother wavelet as:

$$\psi_{j,k}(t)=2^{-j/2}\psi(2^{-j}t-k) \tag{4.6}$$

For wavelet series, $\psi_{j,k}(t)$ are required to be orthonormal, biorthogonal or frame. For the orthonormal case, shown below, the analysis and synthesis wavelets are the same.

$$\Psi_x^{\psi_{j,k}}=\int x(t)\psi'_{j,k}(t)\,dt \tag{4.7}$$

or

$$x(t)=c_\psi \sum_j \sum_k \Psi_x^{\psi_{j,k}}\psi_{j,k}(t) \tag{4.8}$$

where c_ψ is a constant that depends on the wavelet used and again $'$ denotes the conjugate. If $\psi_{j,k}$ are orthogonal or biorthogonal, the transform is non-redundant [85,86].

4.4.3 THE DISCRETE WAVELET TRANSFORM

Although the wavelet series enables the computation of the CWT by computers, it is still not a true discrete transform, but rather a sampled version of the CWT. The information it

provides is highly redundant for the reconstruction of a signal, and therefore requires a significant amount of computational time and resources.

The discrete wavelet transform (DWT) provides non-redundant information both for analysis (decomposition) and synthesis (reconstruction) of the original signal, with a significant reduction in computational time and resources. The discretization occurs in the scaling and translation variables.

The foundations of the DWT go back to 1976 when Croiser, Esteban, and Galand devised a technique to decompose discrete time signals [89]. Crochiere, Weber, and Flanagan did a similar work on coding of speech signals in the same year [90]. They named their analysis scheme as subband coding. In 1983, Burt defined a technique very similar to subband coding and named it pyramidal coding which is also known as multiresolution analysis [91]. Later in 1989, Vetterli and Le Gall made some improvements to the subband coding scheme, removing the existing redundancy in the pyramidal coding scheme [92]. These techniques, though developed by different people, are essentially identical. The discrete wavelet transform computation involves both multiresolution analysis and subband coding.

4.4.4 MULTIRESOLUTION ANALYSIS

Multiresolution analysis (MRA) is a hierarchical scheme. An MRA involves approximations of functions in a sequence of nested linear vector spaces. The formal definition of an MRA states that it consists of the nested linear vector spaces

$(...\subset V_1 \subset V_0 \subset V_{-1} \subset ...)$ such that

1. The union of subspaces is dense on the space of square integrable functions $L^2(R)$

2. The intersection of these subspaces is one set containing the all-zero function or zero vector.
3. If $f(t) \in V_k$ then $f(2t) \in V_{k-1}$ and vice versa, if $f(t) \in V_{k-1}$ then

$$f(\frac{t}{2}) \in V_k$$

4. There exists a function (scaling function) $\phi(t)$ such that $\{\phi(t-k) : k \text{ integer}\}$ constitute a basis for V_0

The following is an explanation of these properties. First to explain the term *dense* in Property 1, the following example is used: Suppose X and Y are sets of real numbers where $X \subset Y$. X is said to be dense in Y if for every element $y \in Y$ there is an element $x \in X$ that is as close to y as the user determines (The concept of denseness can be found in greater detail in texts on mathematical analysis or topology).

Property 2 states that the only signal common to all vector spaces is the all-zero signal or zero vector. Property 3 introduces dilation by stating that a factor of two dilation of a vector belonging to a subspace at a certain level yields a vector in the next coarser subspace. Note that this can be conversely applied; by dilating by a factor of one half , a function in the next finer subspace can be obtained. Property 4 requires a scaling function such that the set is linearly independent. Also any function $f(t) \in V_0$ can be expressed as

$$f_0(t) = \sum_{n=-\infty}^{\infty} a(0,n)\phi(t-n) \tag{4.09}$$

for a sequence of scalars $a(0,n)$ where $n = \{..., -2, -1, 0, 1,...\}$.

To relate MRA to DWT, a condition is imposed upon the subspaces that states

$V_0 \subset V_{-1}$. This condition requires that all vectors in V_0 also belong to V_{-1}. Property 4 states that $\phi(t)$ is in V_0, so it too must now be in V_{-1}. $\phi(t)$ can be expressed as linear combination of the basis for V_{-1} by $\{\phi(2t-n) : n \text{ integer}\}$. $\phi(t)$ becomes a scaling function. With the addition of the above condition, the resulting property is called the dilation equation, which follows a similar form of that in Equation (4.10):

$$\phi(t)=\sum_{n=-\infty}^{\infty} c(n)\,\phi(2t-n) \tag{4.10}$$

where $c(n)$ is a sequence of scalars for $n = \{..., -2, -1, 0, 1,...\}$.

Equation (4.10) is possible with use of the fact that the basis for V_{-1} is given by translates of $\phi(2t)$ by integer multiples of half-unit intervals. Thus $\phi(t)$ is expressed in terms of its own dyadic dilation and translation, hence it is referred to as a dilation equation or a two-scale difference equation.

The DWT utilizes two sets of functions, a scaling function, $\phi(t)$, and a wavelet function, $\psi(t)$. An interesting property of these functions relates back to the two-scale difference equation in Equation (4.10). Both functions can be obtained as a weighted sum of the scaled (dilated) and shifted versions of the scaling function itself:

$$\phi(t)=\sum_{n} h[n]\,\phi(2t-n) \tag{4.11}$$

and

$$\psi(t)=\sum_{n} g[n]\,\phi(2t-n) \tag{4.12}$$

Conversely, a scaling function or a wavelet function that is discretized at scale j and translation k can be obtained by the original (prototype) function, $\phi(t) = \phi_{0,0}(t)$, or $\psi(t) = \psi_{0,0}(t)$ by:

$$\phi_{j,k}(t)=2^{-j/2}\phi(2^{-j}t-k) \tag{4.13}$$

$$\psi_{j,k}(t)=2^{-j/2}\psi(2^{-j}t-k) \tag{4.14}$$

The wavelet function creates a vector subspace of the detail functions at level zero. Since $\{\phi(2t-n) : n \text{ integer}\}$ is the basis for V_{-1}, the function of the subspace at this level can then be expressed as a linear combination of $\phi(t)$ and $\psi(t)$. This relation can generally be expressed as

$$f_{-1}(t)=\sum_{n=-\infty}^{\infty} a(0,n)\phi(t-n)+\sum_{n=-\infty}^{\infty} b(0,n)\psi(t-n) \tag{4.15}$$

where $a(0,n)$ and $b(0,n)$ are a pair of sequences, which will ultimately be the approximation and details coefficients.

Equation (4.15) displays the true power of the DWT. Using an MRA approach to decompose a signal, the original signal can be obtained by adding the current levels approximation and all the previous levels details. The DWT uses the framework of an MRA but uses the implementation of subband coding, which uses successive high-pass and low-pass filtering to decompose a signal into different time and frequency localizations [85,88].

4.4.5 SUBBAND CODING

The subband coding algorithm is the filter bank implementation used by the discrete wavelet transform (DWT). Subband coding can be thought of as the digital filter implementation of MRA. The procedure starts by passing the signal through a half-band digital low-pass filter with impulse response $h[n]$. Filtering a signal corresponds to the convolution of the signal with the impulse response of the filter. The convolution operation in discrete time is defined by the following:

$$x[n]*h[n]=\sum_{k=-\infty}^{\infty} x[k]\cdot h[n-k] \tag{4.16}$$

After passing the signal through a half band low-pass filter, half of the samples can be eliminated according to the Nyquist's rule, since the signal now has a highest frequency of $\pi/2$ radians instead of π radians. Discarding every other sample will subsample the signal by 2, and render a signal with half the number of points. Referring to Property 3 of an MRA, the scale of the signal is now doubled. Note that low-pass filtering only removes the high frequency information, but leaves the scale unchanged; it is the subsampling process that changes the scale. On the other hand, resolution is related to the amount of information in the signal, and therefore is affected by the filtering operations. Subsampling after filtering does not affect the resolution, since removing half of the spectral components from the signal makes half the number of samples redundant. Therefore, half the samples can be discarded without any loss of information.

The DWT analyzes the signal at different frequency bands with different resolutions by decomposing the signal into a coarse approximation (vector subspaces in MRA) of the original signal and detail information. The DWT uses two sets of functions, scaling functions and wavelet functions, which are associated with the low-pass and high-pass filters of subband coding, respectively.

The decomposition of the signal into different frequency bands is obtained by successive high-pass and low-pass filtering of the time domain signal. The original signal $x[n]$ is first passed through a half-band high-pass filter $g[n]$ and a half-band low-pass filter $h[n]$. As mentioned above, half of the samples can be eliminated after filtering, hence the signal can be subsampled by 2. The results of the filtering operations constitute

one level of decomposition. This process can be expressed mathematically as follows:

$$y_{high}=\sum_{n} x[n]\cdot g[2k-n] \tag{4.17}$$

$$y_{low}=\sum_{n} x[n]\cdot h[2k-n] \tag{4.18}$$

where $y_{high}[k]$ and $y_{low}[k]$ are the outputs of the half-band high-pass and half-band low-pass filters, respectively, after subsampling by 2. Equations (4.17) and (4.18) are the same form of the two-scale equation in Equation (4.10). This relation is what unites MRA, subband coding, and the DWT.

Each level of decomposition reduces the time resolution by half since only half the number of samples now characterizes the entire signal. However, the frequency resolution is now doubled, since the frequency band of the signal now spans only half the previous frequency band. The entire process mentioned above is the subband coding algorithm. It can be repeated successively for as many times as desired until subsampling is no longer possible.

At every level of decomposition, the filtering and subsampling will result in half the number of samples (and half the time resolution) and half the frequency band spanned (and double the frequency resolution), allowing the signal to be analyzed at different frequency ranges with different resolutions. The outputs of the high-pass filters are the detail coefficients and are denoted as d_i, i =1, 2,..., $\log_2 N$, where N is the total number of samples in the signal. The outputs of low-pass filters are the approximation coefficients, a_i, and represent the current resolution levels coarse approximation of the original signal. The subband coding algorithm is illustrated in Figure 4.3.

Here is an example from our analysis. The Daubechies 4 wavelet that is used in analysis has scaling and wavelet function coefficients (each of length 8) which correspond to the low-pass filter $h[n]$ and high-pass filter $g[n]$, respectively. A patient's signal is 257 points long. The output of each level 1 filter is 264 (256+8-1) points long. This reduces to 132 points after subsampling by 2. An approximation signal $A_j(t)$ and a detail signal $D_j(t)$ can be reconstructed from the level j approximation and detail

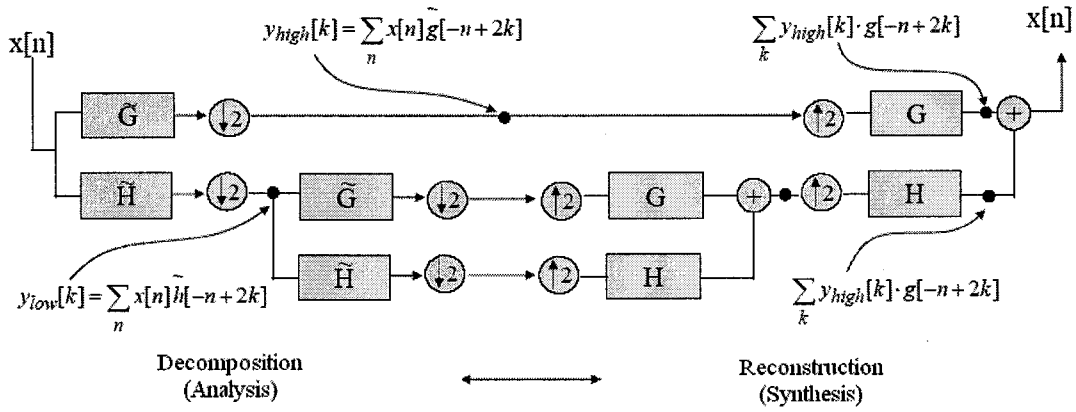

Figure 4.4: Diagram of the subband coding (filter bank) algorithm [85]

coefficients by using substitution in Equations (4.17) and (4.18):

$$A_j(t)=\sum_k a_j[k]\cdot\phi_{j,k}(t) \tag{4.19}$$

$$D_j(t)=\sum_k d_j[k]\cdot\psi_{j,k}(t) \tag{4.20}$$

The original signal $x(t)$ can be reconstructed from the approximation signal $A_j(t)$ at any level j and the sum of all detail signals from levels up to and including level j. This can be expressed as:

$$x(t)=A_j(t)+\sum_{j=-\infty} D_j(t)$$
$$=\sum_k a_j[k]\cdot\phi_{j,k}(t)+\sum_{i=-\infty}^{j}\sum_k d_i[k]\cdot\psi_{i,k}(t) \quad (4.21)$$

By using the properties introduced by an MRA and the subband coding algorithm, the DWT is implemented by using the relationship of the scale and wavelet equations through the two-scale equation.

4.4.6 WAVELET CHOICE

The type of wavelet used for any application is usually chosen according to the similarity of the wavelet to the signal to be analyzed. This similarity better localizes the structures of interest within the signal and reduces the amount of noise in the analysis of the subband structure. The wavelet chosen for this study has been used in different studies for analyzing ERPs, the Daubechies 4 wavelet.

4.4.6a DAUBECHIES 4 WAVELET

Ingrid Daubechies invented the so-called compactly supported orthonormal wavelets, which made discrete wavelet analysis practical. Compact support is given by the size of the window varying throughout the signal so that the window is narrow for high frequencies and wide for low frequencies . The result is good time resolution at high frequencies and good frequency resolution at lower frequencies [22,85,86]. The Daubechies family wavelets are denoted as db*N*, where *N* is the order, and db the "surname" of the wavelet. The first wavelet, dbl, is the Haar wavelet. Figure 4.4 shows the wavelet functions of the next nine members of the family, namely, db2 through db10.

The Daubechies 4 wavelet has been used in several studies for analyzing ERPs in general, as well as for the detection of AD [22,30]. The Daubechies mother wavelet has a 'fractal structure' and has good localizing properties in both time and frequency domains [72].

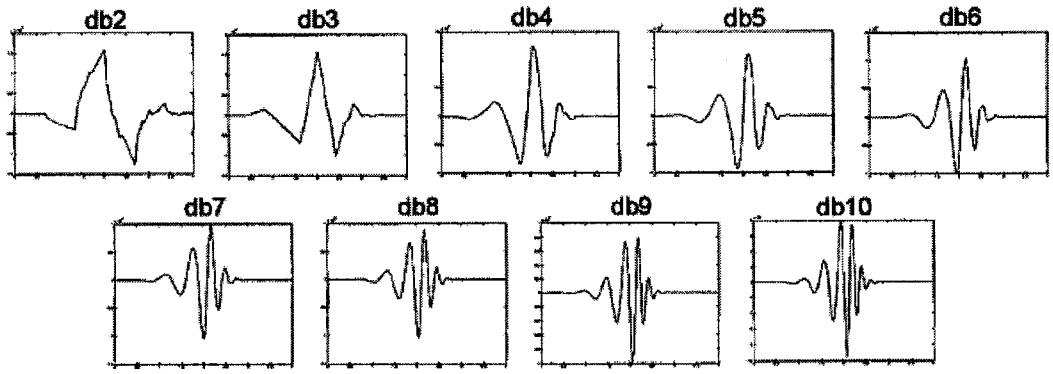

Figure 4.5: Daubechies family function [22].

The high-pass, $h[n]$, and low-pass filter, $g[n]$, coefficients for the Daubechies 4 wavelet are given in Table 4.2, respectively and the wavelet and scale functions are shown in Figures 4.5 and 4.6, respectively.

Table 4.2: Daubechies filter coefficients

$h[n]$	$g[n]$
-0.2304	-0.0106
0.7148	0.0329
-0.6309	0.0308
-0.0280	-0.1870
0.1870	-0.0280
0.0308	0.6309
-0.0329	0.7148
-0.0106	0.2304

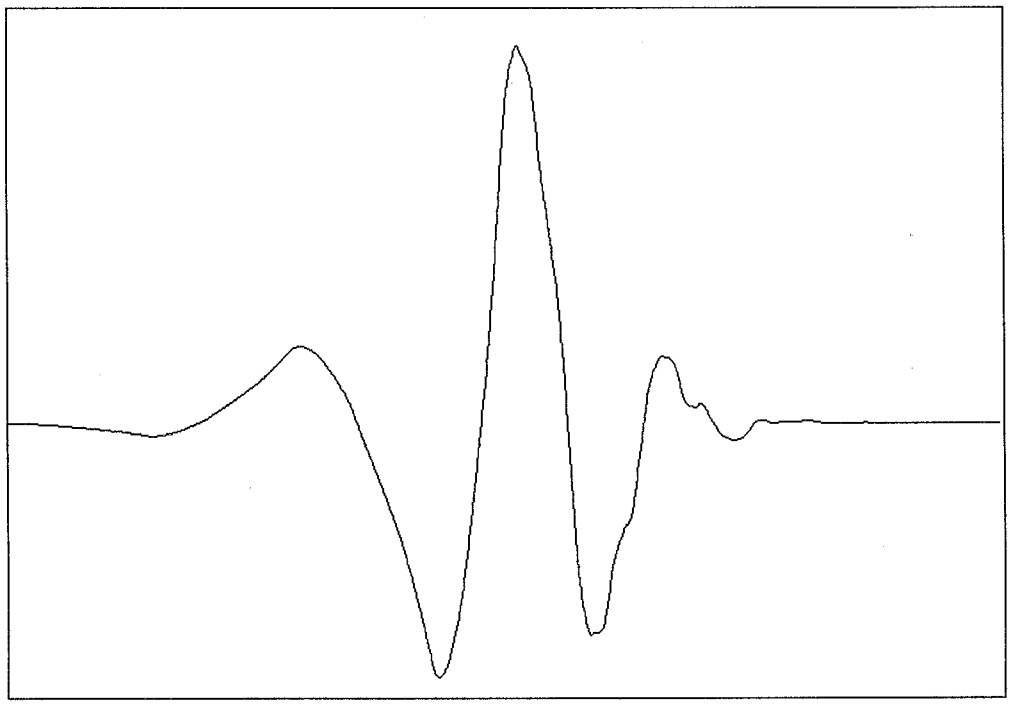

Figure 4.6: Daubechies 4 wavelet function

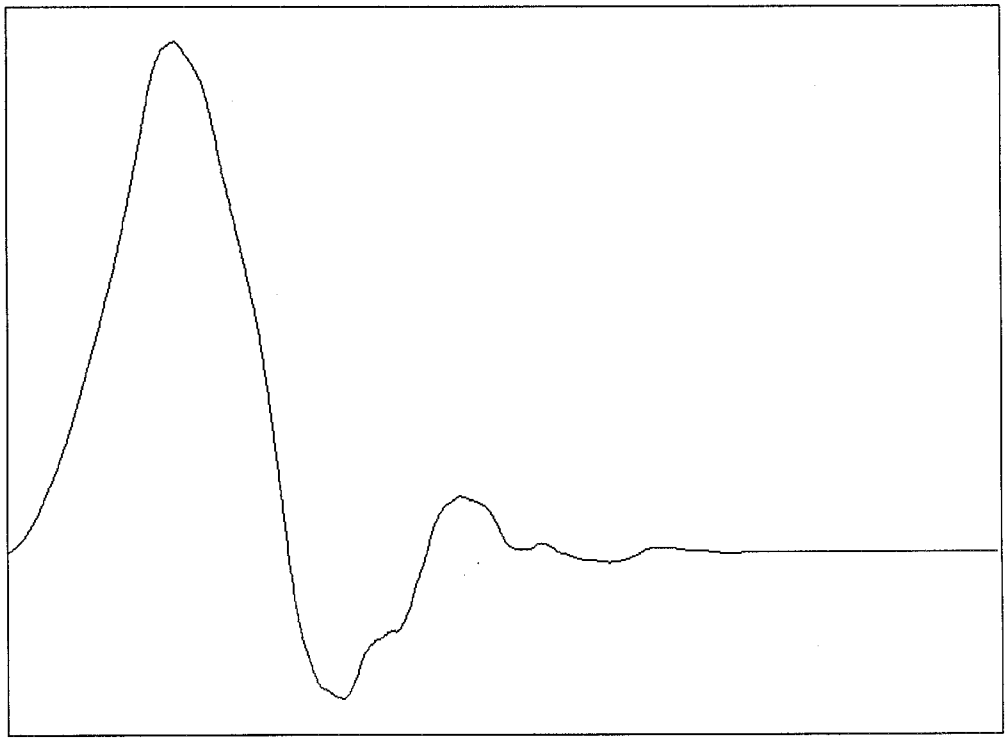

Figure 4.7: Daubechies 4 scaling function

4.5 FEATURES AND CLASSIFICATION

The signals analyzed in this study consist of the preprocessed data from all 19 electrodes. Figure 4.7 illustrates the name and location of the electrodes included. Using the DWT and the db4 wavelet, decomposition of the signals was carried out for 7 levels resulting in the following frequency bands: d_1: 64~128Hz, d_2: 32~64Hz, d_3: 16~32Hz, d_4: 8~16Hz, d_5: 4~8Hz, d_6: 2~4Hz, d_7: 1~2Hz and a7: 0~1Hz. Signal power was generally higher at the higher levels (lower frequencies), hence the 1-2Hz, 2-4Hz, and 4-8Hz subband coefficients were analyzed from all the electrodes during both the novel and target stimuli. The middle coefficients of each subband, corresponding to the spectral features in the 0 – 600ms interval, were analyzed. Subbands were limited to this range to capture any P300 components that may be elicited. Previous analyzes using these selected features yielded diagnostic performances in the mid 60% to low 70% range [79,80,83].

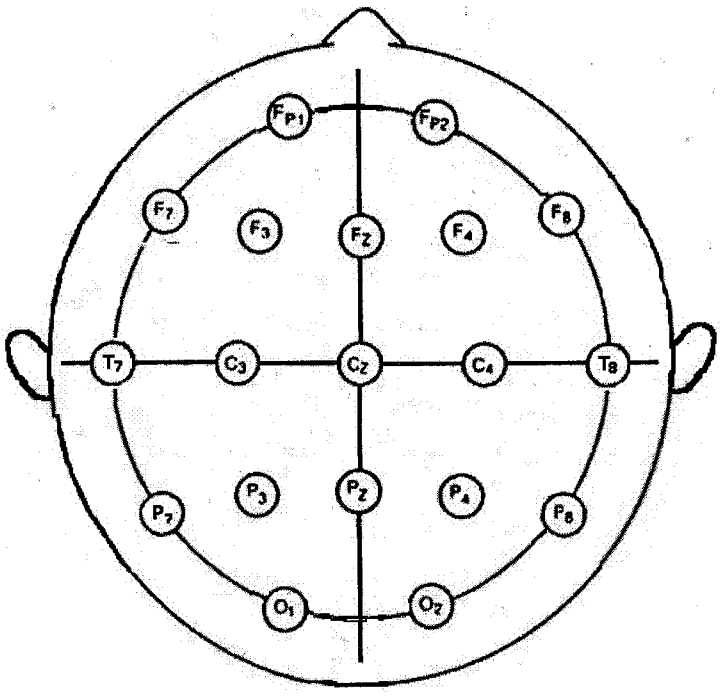

Figure 4.8: The position and names of the 19 electrodes used in our experiments

CHAPTER 5

CLASSIFICATION

The theory involved with the classification aspects of this research is discussed in this chapter. The main topics of each subsection of this chapter are described as follows. First a description of the main classifier used in this study, the multilayer perceptron, and its training algorithm, the back-propagation algorithm. The rest of the chapter discusses data fusion and the two types of data fusion used in this study, feature-level and decision-level fusion. In particular, ensemble of classifiers combination techniques are described along with the decision-level fusion techniques.

5.1 PATTERN RECOGNITION TECHNIQUES

In automated classification applications, distinctive features of the signals to be analyzed are identified and obtained. There are numerous methods available to extract features from the gathered signals. Some examples for feature extraction include filtering, the Fourier transform, multiresolution analysis, the wavelet transform, and statistical measures. Next, a subset of the identified, informative features is placed in a training data set while the remaining data is placed in the testing data set where it is not yet shown to the classifier algorithm. The training data is presented to the classifier's training algorithm for the purpose of setting classifier parameters such as the weights in the multilayer perceptron. The trained classifier system is evaluated on the test data set [93,94].

In an advanced classification system, several classifiers can be combined together. Classifiers trained on features from the same or different data sets for a similar problem is known as an ensemble of classifiers or a multiple classifier system. Through data fusion techniques, the decisions from each classifier in the ensemble can be combined to make a final decision rather than have one classifier make a decision. The main attraction of this method is that combining classifiers has been shown to increase generalization performance (refer to Section 5.3 for further details).

5.2 MULTILAYER PERCEPTRONS

Multilayer feedforward networks consist of a set of sensory units (source nodes) that constitute the input layer, one or more hidden layers of computation nodes, and an output layer of computation nodes. The input signal propagates through the network in a forward direction, on a layer-to-layer basis. The most commonly used example of such neural networks are the multilayer perceptron (MLPs) type networks [93]. MLPs have been applied successfully to solve a variety of difficult and diverse problems by training them in a supervised manner with the highly popular error back-propagation algorithm (see Section 5.2.1) . Error back-propagation learning consists of two passes of data through the different layers of the network: a forward pass and a backward pass. In the forward pass, an activity pattern (input vector) is applied to the sensory nodes of the network, and its effect propagates through the network layer by layer. Finally a set of outputs is produced as the actual response of the network. During the forward pass the synaptic weights of the network are all fixed. During the backward pass, the synaptic weights are all adjusted in accordance with an error-correction rule. Specifically, the actual response

of the network is subtracted from a desired (target) response to produce an error signal. This error signal is then propagated backward through the network. The synaptic weights are adjusted to make the actual response of the network move closer to the desired response in a statistical sense [93].

In pattern recognition involving nonlinearly separable patterns, the neurons in the network are usually nonlinear. This nonlinearity is achieved by using a sigmoid function. The two most commonly used forms are the anti-symmetric logistic function (which is the sigmoid used in our experiments) and the anti-symmetric hyperbolic tangent function. Each neuron is responsible for producing a hyperplane of its own decision space. Through the supervised learning process, the combination of hyperplanes formed by all neurons in the network is iteratively adjusted in order to separate patterns drawn from different classes with the fewest classification errors on average [93].

Figure 5.1 illustrates the structure of an MLP. All nodes are fully interconnected to the nodes of the adjacent layers by a set of weights. The weights connecting the input nodes to the hidden layer nodes are denoted by w_{ij}, where ij is the connection of ith input node to the jth hidden layer node. The weights connecting the hidden layer to the output nodes are denoted by w_{jk},where jk is the connection of jth hidden layer node to the kth output node. The weights are determined through the back-propagation training algorithm described in the next section [93,94]. $\boldsymbol{x}_1$ through $\boldsymbol{x}_i$ are the features of an input vector. $\boldsymbol{y}_1$ through $\boldsymbol{y}_j$ are the activation responses of the respective hidden layer nodes. $\boldsymbol{o}_1$ through $\boldsymbol{o}_k$ are the responses of the respective output nodes. Lastly, $\boldsymbol{d}_1$ through $\boldsymbol{d}_k$ are the target outputs to which $\boldsymbol{o}_1$ through $\boldsymbol{o}_k$ are compared to determine the classifier's accuracy.

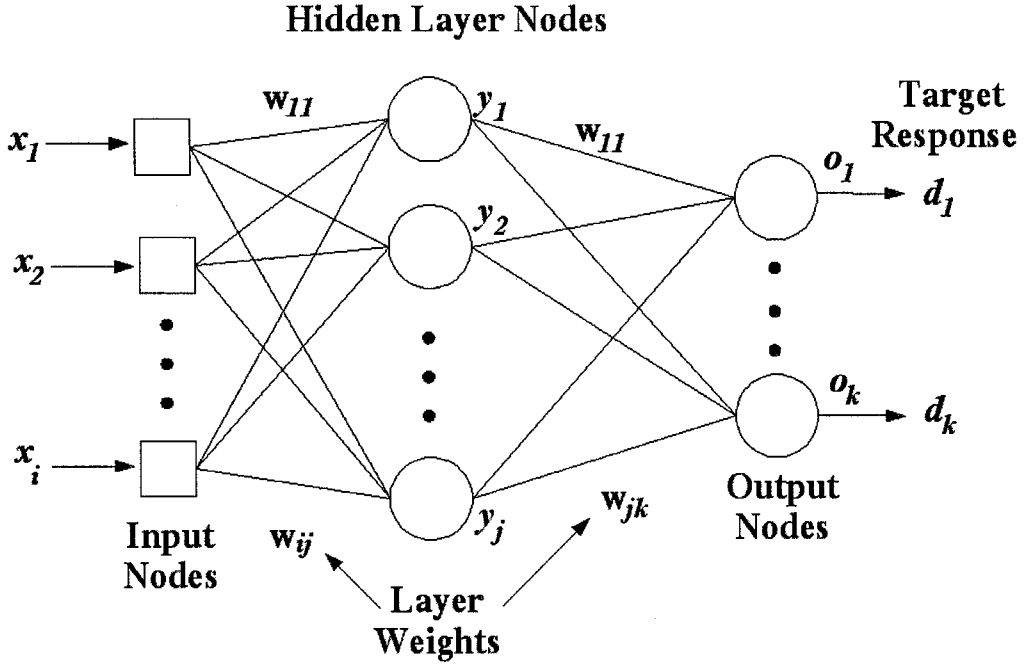

Figure 5.1: MLP network

5.2.1 BACK-PROPAGATION ALGORITHM

Back-propagation learning has emerged as the standard algorithm for training multilayer perceptrons, and against which other learning algorithms are often benchmarked. The back-propagation algorithm derives its name from the fact that the partial derivatives of the cost function (performance measure) with respect to the free parameters (synaptic weights and biases) of the network are determined by back-propagating the error signals (computed by the output neurons) through the network, layer by layer. A full coverage of the back-propagation algorithm is beyond the scope of this thesis. For more details and explanation refer to [93,94].

5.2.1a NOTATION OF THE BACK-PROPAGATION ALGORITHM

The following is an explanation of the notation used in the summary of the back-propagation algorithm in the following section, Section 5.2.1b.

- The indices i, j, and k refer to different layers in the network. These indices refer to the same layers as those illustrated in Figure 5.1.
- Iteration n refers to the nth training data instance being presented to the network.
- The ith element of the input vector for iteration n is $\boldsymbol{x}_i(n)$.
- The kth element of the output vector for iteration n is $\boldsymbol{o}_k(n)$.
- In layer l of an MLP, $l = 0, 1, ..., L$, where L is the depth of the network.
- The synaptic weight connecting the output of neuron i (the input nodes) to the input of neuron j (the hidden layer nodes) for iteration n is given by $\boldsymbol{w}_{ij}(n)$. Conversely, the synaptic weight connecting the output of neuron j (the hidden layer nodes) to the input of neuron k (the output nodes) for iteration n is given by $\boldsymbol{w}_{jk}(n)$.
- The induced local field is the weighted sum of all synaptic input plus the bias of neuron j at iteration n. This actually constitutes the signal being applied to the activation function for neuron j and is denoted by $\boldsymbol{v}_j(n)$.
- The activation function describes the nonlinearity associated with neuron j from the input-output relationship. The activation function is denoted by $\boldsymbol{\varphi}_j(\cdot)$.
- The output of neuron j for the nth iteration is referred to as $\boldsymbol{y}_j(n)$.
- The error signal at the output of neuron j for iteration n is shown as $\boldsymbol{e}_j(n)$.
- The desired response of neuron j is shown $\boldsymbol{d}_j(n)$. This desired response is used to compute $\boldsymbol{e}_j(n)$.

5.2.1b SUMMARY OF THE BACK-PROPAGATION ALGORITHM

The following is a summary of the back-propagation algorithm adapted from [93]:

- ***Initialization*** – Assume that no prior information is available. The synaptic weights are randomly picked from a distribution whose mean is zero, and variance is chosen to make the standard deviation of the induced local fields of the neurons lie at the transition between the linear and saturated parts of the sigmoid activation function. The logarithmic sigmoid was used in this research and is shown in Figure 5.2. The logarithmic sigmoid is defined by:

$$\varphi(n)=\frac{1}{(1+e^{-n})} \tag{5.1}$$

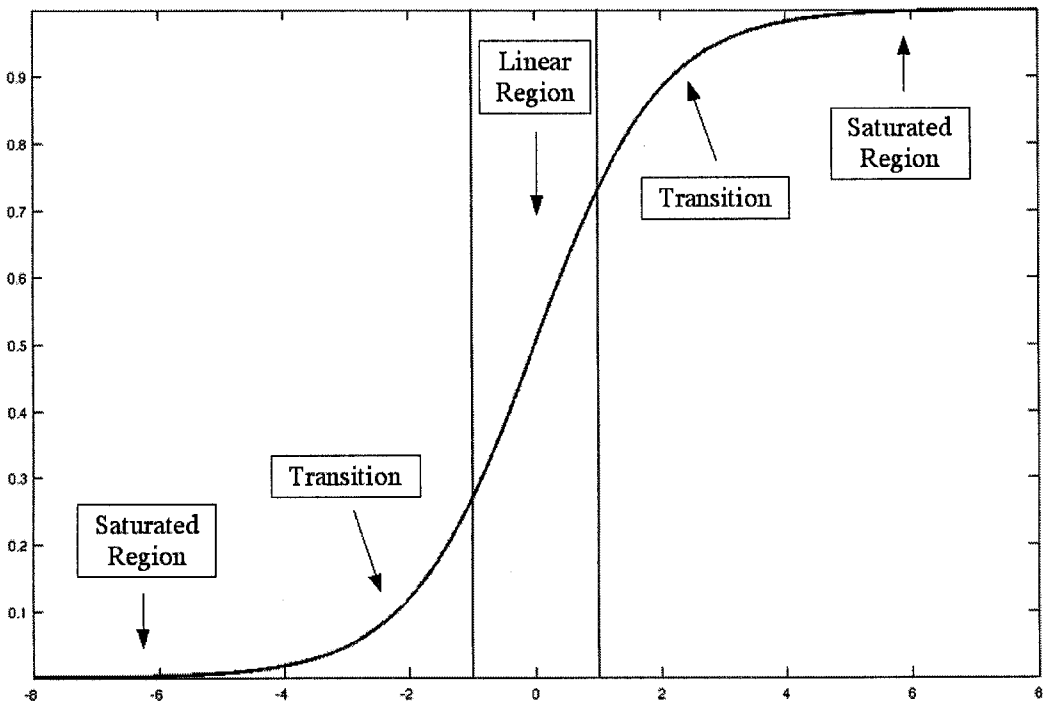

Figure 5.2: The logarithmic sigmoid function.

- ***Presentation of Training Data*** – An epoch of training data is presented to the network. The sequence of forward and backward computations is then performed for each example in the training data set.
- ***Forward Computation*** - Let the training data instance in the epoch be denoted by $(\boldsymbol{x}(n),\boldsymbol{d}(n))$, with the input vector $\boldsymbol{x}$ for iteration n applied to the input layer of sensory nodes and the desired response vector $\boldsymbol{d}$ for iteration n presented to the output layer of computation nodes. The induced local fields of the network are computed by proceeding forward through the network, layer by layer. The induced local field $v_j^{(l)}(n)$ for neuron j in layer l is

$$v_j^{(l)}(n)=\sum_{i=0}^{m_l} w_{ij}^{(l)}(n)\, y_i^{(l-1)}(n) \tag{5.2}$$

where m_l is the size of layer l and ij means from output of neuron i to the input of neuron i. For $i = 0$, we have $y_0^{(l-1)} = 1$ and $w_{0j}^{(l)}(n) = b_j^{(l)}(n)$ is the bias applied to the neuron j in layer l. Assuming a sigmoid function is used for the neuron's activation function, the output signal of neuron j in layer l is

$$y_j^{(l)}(n)=\varphi_j(v_j(n)) \tag{5.3}$$

If neuron j is the output layer, set

$$y_j^{(L)}(n)=o_j(n) \tag{5.4}$$

Then, compute the error signal

$$e_j(n)=d_j(n)-o_j(n) \tag{5.5}$$

- ***Backward Computation*** - The local gradients of the network, $\boldsymbol{\delta}$, are computed, and defined by:

$$\delta_j^{(L)}(n)=e_j^{(L)}(n)\varphi_j'(v_j^{(L)}(n)) \tag{5.6}$$

for neuron j in output layer L, and

$$\delta_j^{(l)}(n)=\varphi_j{}'(v_j^{(L)}(n))\sum_k \delta_k^{l+1}(n)w_{jk}^{(l+1)}(n) \qquad (5.7)$$

for neuron j in hidden layer l. The prime in $\varphi_j'(\cdot)$ denotes differentiation with respect to the argument. The synaptic weights in layer l are adjusted according to the generalized delta rule:

$$w_{ij}^{(l)}(n+1)=w_{ij}^{(l)}(n)+\alpha\left[w_{ij}^{l}(n-1)\right]+\eta\,\delta_j^{(l)}(n)\,y_i^{(l-1)}(n) \qquad (5.8)$$

where η is the learning-rate parameter and α is the momentum constant.

- ***Iteration*** - The forward and backward computations in steps 3 and 4 are iterated by presenting new epochs of training data instances to the network until the stopping criterion is met.

Figure 5.3 illustrates a graphical summary of the signal-flow of back-propagation learning. The flow can be interpreted as follows: The interconnecting weights, $\boldsymbol{w}_{ij}$, are initialized and an input vector $\boldsymbol{x}$ of length three is shown to the input nodes in this example. The induced local field $\boldsymbol{v}$ is calculated for each neuron using Equation (5.2), then shown to the activation function, $\varphi(\cdot)$ and set as the output for each neuron, $\boldsymbol{y}$, as in Equation (5.3). The output from the hidden layer neurons are used to compute the next set of induced fields and again shown to the activation function whose results are set as the output, $\boldsymbol{o}$. The output is compared to the desired response using Equation (5.5) and an error signal is created. The error signal propagates back through the network to create local gradients from Equation (5.6) and (5.7) for the respective layers l. Lastly, the weights are adjusted according to generalized delta rule in Equation (5.8).

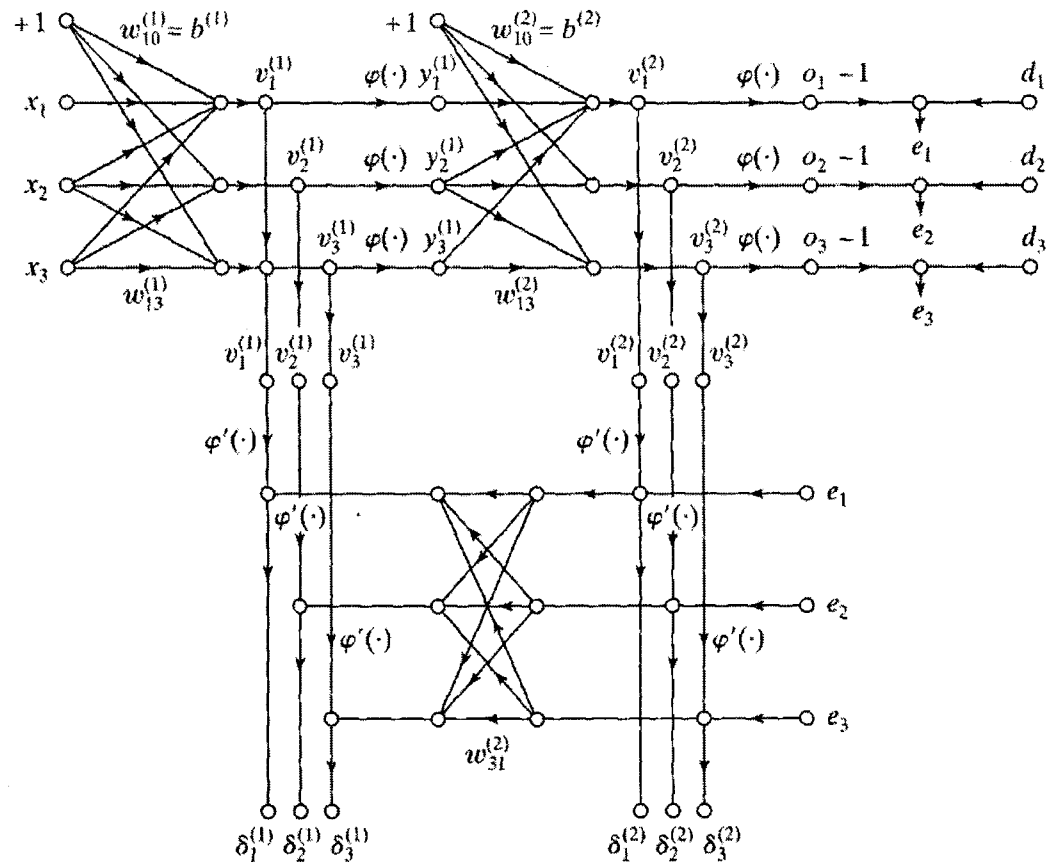

Figure 5.3: Signal-flow of the back-propagation learning algorithm [93]

5.3 DATA FUSION TECHNIQUES

Fusion is the merging of similar or different elements into a union. Within the realm of pattern recognition, fusion can be accomplished in several ways. The two approaches described here are feature-level fusion, which involves the features before applied to any classifier algorithms, and, decision-level or classifier fusion, which combines the decisions of classifiers in an ensemble. The justification behind these techniques is to obtain the most informative features (through feature-level fusion) or the most informative decision (through classifier fusion) for a given problem.

5.3.1 FEATURE-LEVEL FUSION

Feature-level fusion (FLF) involves the combination of different sets of features into one feature vector. Combining features creates a new feature space that will ideally yield a better decision boundary from the classifier. The new feature vectors are then used as the training and testing data sets for a classifier. FLF can be achieved simply by such methods as concatenation, averaging, or summing. The chosen method of combination is defined by the user and varies from premise to premise. In the experiments of this thesis, feature-level fusion was achieved by simply concatenating features and training classifiers of the newly formed input vectors. Figure 5.4 illustrates a conceptual example of feature-level fusion.

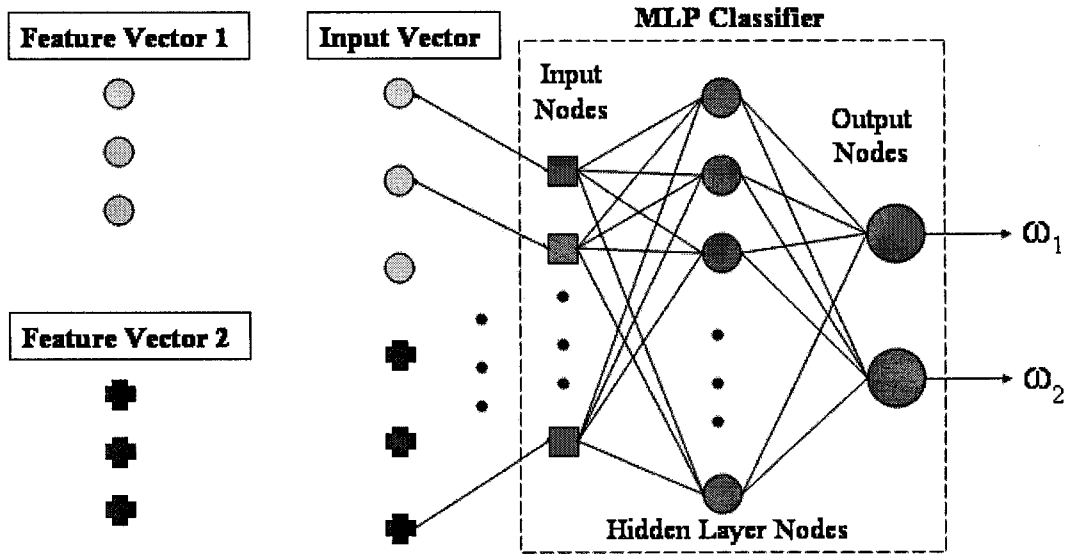

Figure 5.4: Feature-level fusion by concatenation.

5.3.2 CLASSIFIER (DECISION-LEVEL) FUSION

Decision-level fusion is more commonly known as classifier fusion, an ensemble of classifiers combination technique. Unlike feature-level fusion, classifier fusion is a fusion of classifier label outputs. An ensemble based system, also known as a multiple classifier system (MCS), combines several, preferably diverse, classifiers. The diversity in the classifiers is typically achieved by using a different training data set for each classifier but can also be achieved when classifiers learn different regions of the same feature space. Each ensemble member is supposed know well a part of a feature space. Using different feature spaces allows each classifier to generate different decision boundaries. The reasoning and expectation is that each classifier will make different errors. Therefore, the strategic combination of these classifiers can reduce the total error. Figure 5.5 provides a visual example of decision-level fusion.

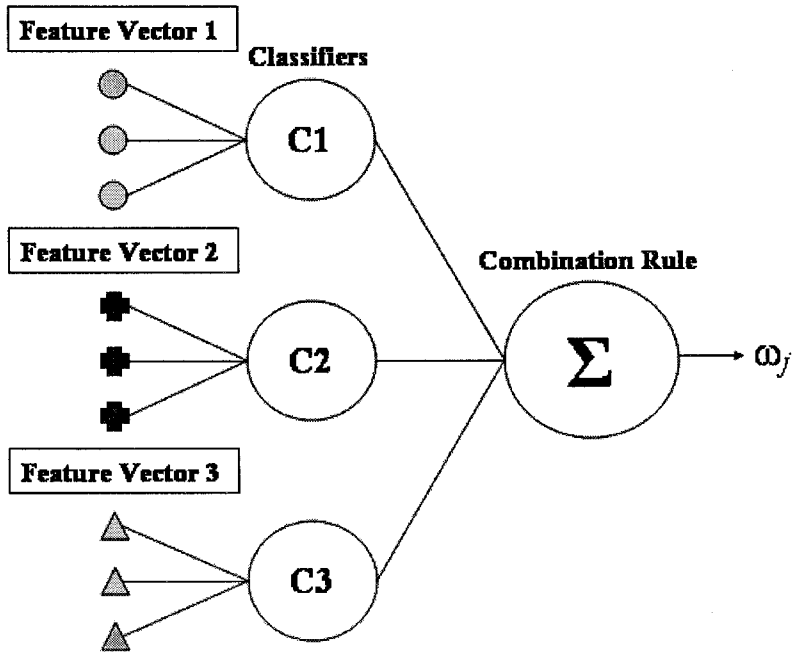

Figure 5.5: A visualization of classifier (decision-level) fusion

5.3.2a COMBINATION RULES

Three combination rules derived in this thesis are weighted majority vote, product rule, and sum rule.

In weighted majority vote, the labels, and the error-based weights are needed from each classifier in the ensemble . The decision of the *i*th classifier is defined as the binary valued $d_{i,j} \in \{0,1\}$, i=1,...,N and j=1,...,c where N is the number of classifiers in an ensemble and c is the number of classes. For a given instance $\boldsymbol{x}$, if the *i*th classifier T_i chooses class j, d_{ij} = 1, and zero otherwise. The voting weight for each classifier is defined as

$$W(T_i)=\log\left(\frac{1}{\beta_{T_i}}\right) \tag{5.9}$$

where β_T is the normalized training error of classifier T_i.

For product rule and sum rule, the continuous outputs of the classifiers, $d_{i,j} \in [0,1]$, which represents the degree of support given by classifier T_i to class j. For any given classifier, these supports are normalized to add up to 1 over different classes by the softmax transformation.

$$d_{i,j}(x)=\frac{\exp(d_{i,j}(x))}{\sum_{j=1}^{c}\exp(d_{i,j}(x))} \tag{5.10}$$

For each rule, the final support, μ_j, given to class j is calculated as

$$\mu_j(x)=\sum_{j=1}^{N} W(T_i)d_{i,j}(x), \quad d_{i,j}(x)\in\{0,1\} \tag{5.11}$$

$$\mu_j(x)=\sum_{j=1}^{N} d_{i,j}(x), \quad d_{i,j}(x)\in[0,1] \tag{5.12}$$

$$\mu_j(x)=\frac{1}{N}\prod_{j=1}^{N} d_{i,j}(x), \quad d_{i,j}(x)\in[0,1] \tag{5.13}$$

for weight majority vote, sum rule, and product rule, respectively [85,86]. Denoting the class labels as $\Omega=\{\omega_1,\omega_2,...,\omega_C\}$, and the ensemble decision for instance $\boldsymbol{x}$ as $\boldsymbol{E}(\mathrm{x})$, then the ensemble decision is ω_m, for which the support $\mu_j(\mathbf{x}), j=1,...,c$ is maximum:

$$E(x)=\omega_m | m=\underset{j}{argmax}(\mu_j(x)) \tag{5.14}$$

5.4 OTHER COMBINATION METHODS

The following methods describe other possible combination techniques. These techniques have been used for the early diagnosis of Alzheimer's disease in our previous studies [79-83].

5.4.1 DECISION TEMPLATES

The decision template DT_j for any class j is defined using the decision profiles $DP(\boldsymbol{x})$ for the given instance $\boldsymbol{x}$. The decision profile is a matrix that summarizes the outputs from all N classifiers in an ensemble for the given $\boldsymbol{x}$. Each classifier T_i in the ensemble $T = \{T_1,\ldots, T_N\}$ outputs c degrees of support for each $\boldsymbol{x}$. The outputs of the N classifiers for a particular $\boldsymbol{x}$ are then organized into a decision profile as shown in Figure 5.5. The jth column with $d_{1,j}$ to $d_{N,j}$ are the supports from classifiers T_1 to T_N to class ω_j, and the ith row with $d_{i,1}$ to $d_{i,c}$ is the support from classifier $T_i(\boldsymbol{x})$ to classes ω_1 through ω_c.

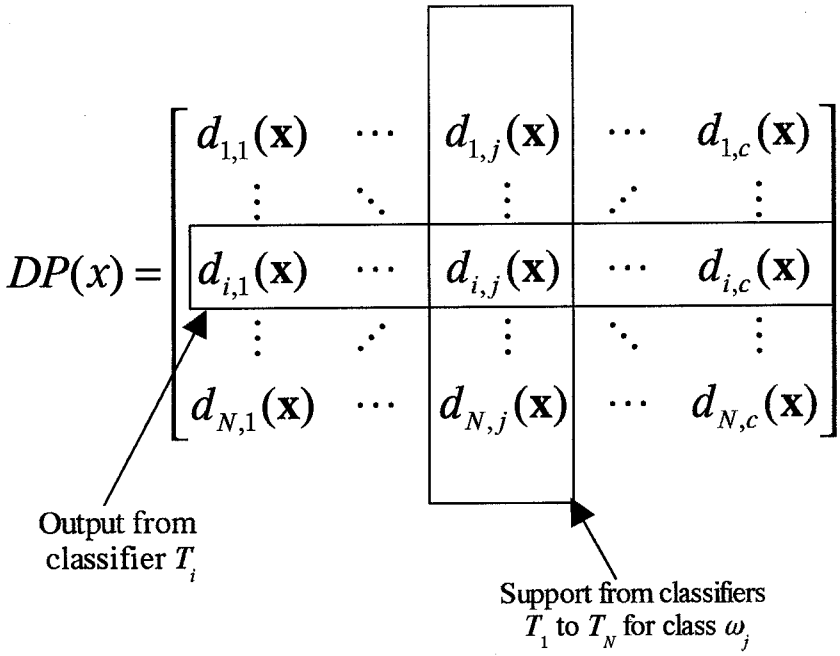

Figure 5.6: Decision Profile[79, 80, 95]

The decision template combiner is based upon the most typical decision profile for each class ω_j. It is calculated as the average of decision profiles of all training instances of class ω_j

$$DT_j = \frac{1}{N_j} \sum_{x \in X_j} DP(x) \tag{5.15}$$

where $\boldsymbol{X}_j$ indicates the set of class ω_j instances, and N_j is the cardinality of this set. For classification of an instance $\boldsymbol{x}$, the decision profile for $\boldsymbol{x}$ is compared to the decision templates of all classes using a similarity measure S. The class whose decision template provides the closest measure (the class that has the highest support) becomes the label of $\boldsymbol{x}$. The similarity measure that is often used is the squared Euclidean distance. Using this measure, the ensemble support for ω_j is then

$$\mu_j(x)=1-\frac{1}{N_c}\sum_{i=1}^{N}\sum_{j=1}^{c}[DT_j(i,j)-d_{i,j}(x)]^2 \tag{5.16}$$

where $DT_j(i,j)$ is the $(i,j)^{th}$ entry in the decision template. [79,80,96]

5.4.2 COMPETENCE WEIGHTING

Competence was originally intended as a classifier selection technique, where a large number of classifiers are generated and those with the largest competencies are retained for the final ensemble. The competence of a classifier is essentially a metric of how well a classifier knows a particular feature space [96]. In a previous study, the feasibility of using the competence as a weight in a combination scheme was pursued [79].

For the competence weight, a distance-based *k-nn* estimate was used such as the one originally proposed by Giacinto and Roli in [97] for image classification applications. A distance-based *k-nn* estimate calculates the competence of a classifier as the weighted average of the classifier's predictions for the correct labels of the *k*-nearest neighbors of a given instance $\boldsymbol{x}$. Let $P_i(l(\boldsymbol{x}_k)|\boldsymbol{x}_k)$ be the estimated probability of the *i*th classifier T_i in correctly labeling $\boldsymbol{x}_k$, where $l(\boldsymbol{x}_k)$ denotes the true class of $\boldsymbol{x}_k$. These probabilities are weighted by the distances between $\boldsymbol{x}$ and its *k*-nearest neighbors. The competence of T_i, given $\boldsymbol{x}$, is

$$C(T_i|\boldsymbol{x})=\frac{\sum_{l(\boldsymbol{x}_k)=\omega_j:\boldsymbol{x}_k\in\omega_j} P_i(l(\boldsymbol{x}_k)|\boldsymbol{x}_k)(1/d(\boldsymbol{x},\boldsymbol{x}_k))}{\sum_{l(\boldsymbol{x}_k)=\omega_j:\boldsymbol{x}_k\in\omega_j}(1/d(\boldsymbol{x},\boldsymbol{x}_k))} \tag{5.17}$$

where $d(\mathbf{x},\mathbf{x}_k)$ is the Euclidean distance between $\boldsymbol{x}$ and its *k*-nearest neighbors. Using this definition of competence, the rules for weighted majority vote, and sum rule in Equations (5.11), and (5.12), and were modified to use the competence as a weight in Equation

(5.18) while product rule from Equation (5.13) was modified to Equation (5.19), as follows:

$$\mu_j(\boldsymbol{x})=\sum_{t=1}^{N} C(T_t|\boldsymbol{x})d_{t,j}(\boldsymbol{x}) \tag{5.18}$$

$$\mu_j(\boldsymbol{x})=\prod_{t=1}^{N} C(T_t|\boldsymbol{x})d_{t,j}(\boldsymbol{x}) \tag{5.19}$$

Once again, the ensemble chooses class ω_m for which the support $\mu_j(\mathbf{x}), j=1,\ldots,c$ is maximum as in Equation (5.14).

The decision template rule was also modified by the competence weighting. Each $DP(\boldsymbol{x})$ entry became the support from the classifier times the competence weight of that classifier, CWDP($\boldsymbol{x}$).

$$CWDP(\boldsymbol{x})=\begin{bmatrix} C(T_1|\boldsymbol{x})d_{1,1}(\boldsymbol{x}) & \cdots & C(T_1|\boldsymbol{x})d_{1,j}(\boldsymbol{x}) & \cdots & C(T_1|\boldsymbol{x})d_{1,c}(\boldsymbol{x}) \\ \vdots & \ddots & \vdots & \iddots & \vdots \\ C(T_t|\boldsymbol{x})d_{t,1}(\boldsymbol{x}) & \cdots & C(T_t|\boldsymbol{x})d_{t,j}(\boldsymbol{x}) & \cdots & C(T_t|\boldsymbol{x})d_{t,c}(\boldsymbol{x}) \\ \vdots & \iddots & \vdots & \ddots & \vdots \\ C(T_N|\boldsymbol{x})d_{N,1}(\boldsymbol{x}) & \cdots & C(T_N|\boldsymbol{x})d_{N,j}(\boldsymbol{x}) & \cdots & C(T_N|\boldsymbol{x})d_{N,c}(\boldsymbol{x}) \end{bmatrix} \tag{5.20}$$

The rest of the decision template algorithm remained the same as in Section 5.4.1 [79,96].

CHAPTER 6

RESULTS

6.1 K-FOLD CROSS-VALIDATION

A cross-validation procedure was implemented to estimate the true generalization performance of each of the classifiers and the ensemble of classifiers. Cross-validation can be used to estimate any statistical parameter with a measure of certainty in the original estimate [94,95]. In a *K*-fold cross-validation, the dataset is divided into *K*-blocks as shown in Figure 6.1. The *k*th block is set aside for testing purposes while the network is trained with *K*-1 remaining blocks. This procedure is repeated *K* times so that each block is used in both the training and testing sets but never at the same time. The average of the performance values on each of the test sets is the *K*-fold cross-validation performance for the data set.

In our experiments, a leave-one-out cross-validation is implemented. In this scheme, *k* is equal to the number of instances in the data set. For example, for the 71 patient cohort, 70 patients would be used in training and 1 patient would be used for testing. This would then be repeated 70 more times so that each instance is included in both the testing and training sets. In this scheme, the performance for each test will either be 0 or 1 (0% or 100%), meaning that the test instance is either incorrectly or correctly classified by the classifier trained on the 70 other instances. The final performance for the leave-one-out trial is then the average of these 1s and 0s.

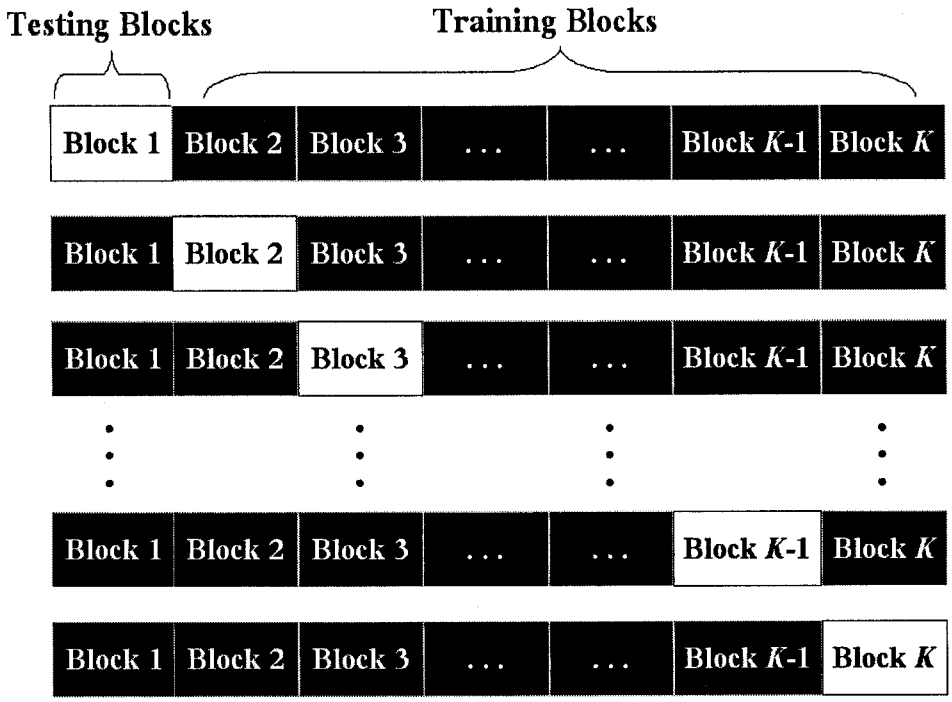

Figure 6.1: *K*-fold cross-validation [95]

6.2 OVERVIEW OF RESULTS

Wavelet analysis was performed on the two designated cohort data sets (one with 71 patients, the other with 66 patients) using the Daubechies 4 wavelet. The detail coefficients from the wavelet analysis were used to train and test MLP neural networks and combined using the fusion rules discussed in Chapter 5. Feature-level fusion was also briefly analyzed for a subset of the detail coefficients and compared to decision-level fusion results of MLPs trained on the same features. Performance figures are provided in tables throughout this chapter.

6.3 WAVELET ANALYSIS RESULTS

The number of coefficients per decomposition level and the corresponding frequency subbands were determined. Table 6.1 outlines the number of coefficients from the decomposition and the corresponding subbands. The coefficients for the levels d7, d6, and d5 were used in the analysis in this work. These coefficients correspond to the 1-2Hz, 2-4Hz, and 4-8Hz subbands for a total of 32 coefficients.

Table 6.1: Number of coefficients and the corresponding frequency subbands.

	a7	***d7***	***d6***	***d5***	***d4***	***d3***	***d2***	***d1***
no. of coefficients	8	8	10	14	22	38	69	132
frequency subbands	0-1Hz	1-2Hz	2-4Hz	4-8Hz	8-16Hz	16-32Hz	32-64Hz	64-128Hz

Figure 6.2 and Figure 6.3 show the decomposition of a signal from a normal subject and a probable AD subject, respectively. Variations in the original signals are obvious when compared visually. However, this is not always the case when using only visual inspection as seen in Figure 2.3 where the AD signal shows characteristics typically found in a normal subject's signal. Wavelet decomposition allows for a better analysis of the frequency components of the signal. It makes the components of each frequency subband more prominent than it otherwise would be in a purely visual analysis.

(a)

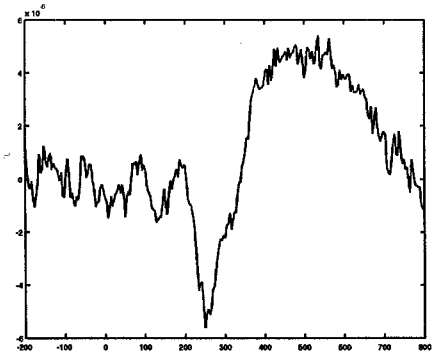

(b)

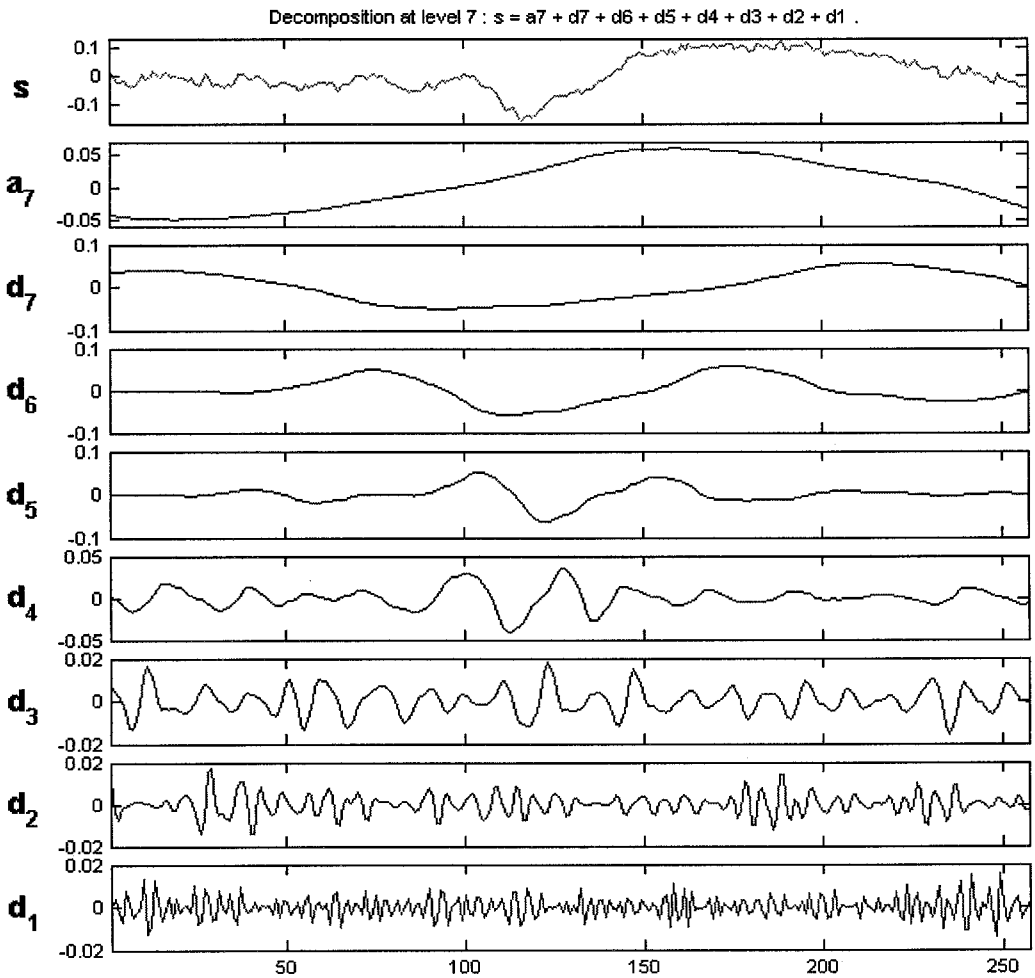

Figure 6.2: Normal subject ERP (a) and its wavelet decomposition (b)

(a)

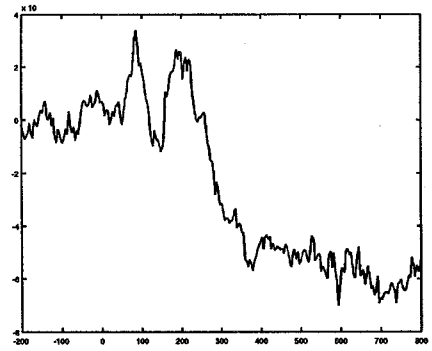

(b)

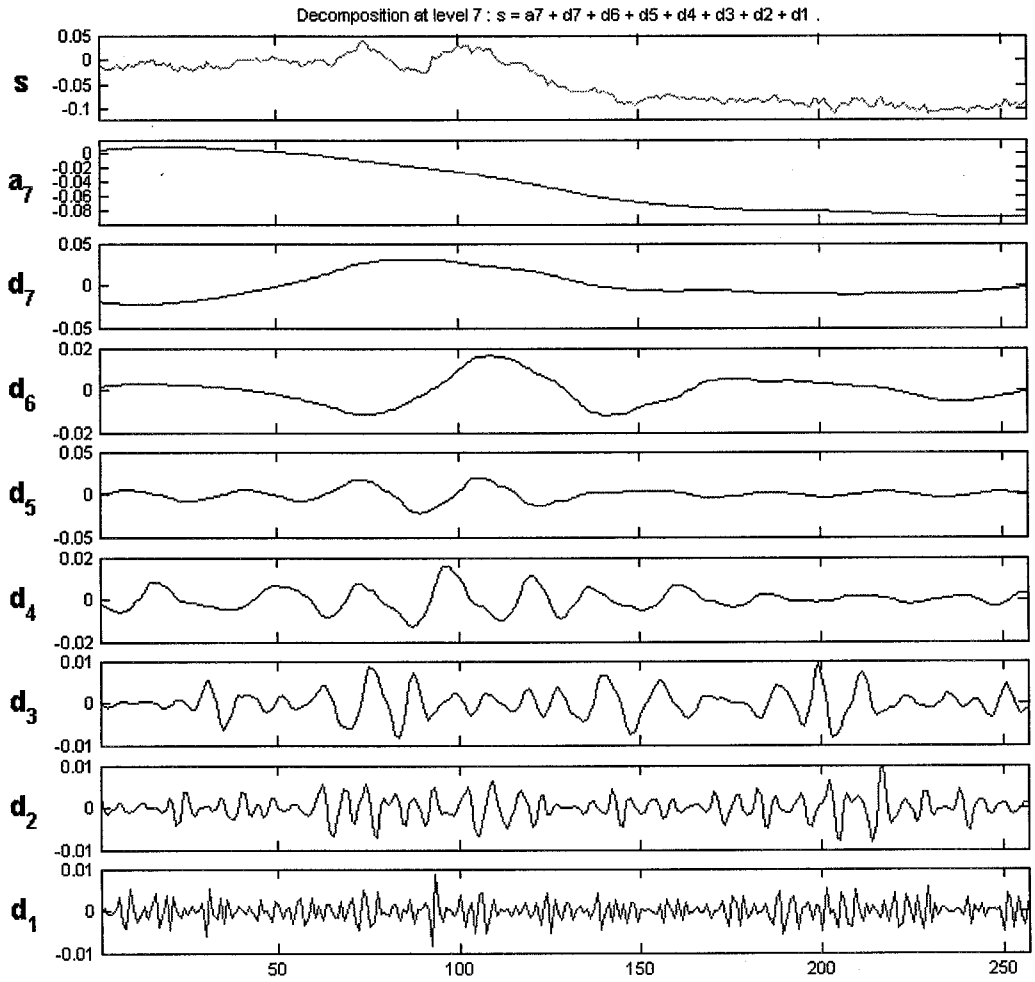

Figure 6.3: AD subject ERP (a) and its wavelet decomposition (b)

6.4 MLP RESULTS FROM ALL ELECTRODES

The following results are single classifier performances from the analysis of target and novel stimuli from all 19 electrodes. Performances were evaluated on both the 71 patient and 66 patient cohorts. Six feature sets were evaluated: 1-2Hz (all features), 1-2Hz (middle-features), 2-4Hz (all features), 2-4Hz (middle features), 4-8Hz (all features) and 4-8Hz (middle features). As mentioned early, these feature sets are based on previously established success [79-83]. The results are organized by classifier and feature set. The average performance of five leave-one-out trials are presented along with the 95% confidence intervals (CI) for each. Average performances of 60% and higher are highlighted.

Table 6.2: Results for the target stimuli recordings from each electrode of the 71 patients cohort at each feature level.

	Feature Level					
Classifier	***1-2Hz(all)***	***1-2Hz(mid)***	***2-4Hz(all)***	***2-4Hz(mid)***	***4-8Hz(all)***	***4-8Hz(mid)***
C4	50.14 ± 4.56%	56.62 ± 6.47%	50.14 ± 1.99%	49.58 ± 4.52%	49.58 ± 6.59%	49.58 ± 4.69%
FP1	55.77 ± 3.83%	***60.28 ± 5.72%***	***60.28 ± 1.46%***	***60.00 ± 4.72%***	46.76 ± 6.47%	43.66 ± 4.63%
O1	43.94 ± 4.35%	44.51 ± 3.63%	48.45 ± 4.56%	56.34 ± 4.79%	43.38 ± 7.56%	43.94 ± 5.01%
P8	54.36 ± 7.78%	53.52 ± 3.91%	53.52 ± 4.46%	57.75 ± 4.79%	44.51 ± 10.9%	37.75 ± 7.25%
P4	***61.97 ± 4.46%***	59.72 ± 4.02%	***63.66 ± 4.18%***	***61.97 ± 3.27%***	41.13 ± 5.30%	37.75 ± 3.79%
P7	***61.13 ± 6.13%***	51.83 ± 5.30%	***60.56 ± 4.10%***	53.52 ± 2.77%	***62.25 ± 4.85%***	58.59 ± 3.41%
F4	***60.84 ± 4.18%***	***60.84 ± 2.88%***	47.60 ± 6.81%	44.22 ± 4.88%	51.55 ± 6.37%	51.55 ± 3.83%
FZ	56.62 ± 3.13%	***60.00 ± 5.33%***	50.14 ± 6.38%	52.39 ± 6.47%	49.58 ± 4.53%	50.42 ± 4.17%
PZ	***62.53 ± 5.88%***	52.96 ± 2.00%	***60.00 ± 1.57%***	59.43 ± 3.58%	47.33 ± 2.93%	49.86 ± 4.39%
P3	57.46 ± 4.35%	56.62 ± 5.30%	***60.84 ± 3.36%***	***63.38 ± 5.67%***	59.44 ± 5.58%	50.14 ± 7.27%
F7	51.27 ± 2.92%	51.83 ± 7.25%	49.29 ± 3.27%	47.60 ± 4.52%	46.48 ± 6.67%	51.27 ± 2.65%
T8	57.75 ± 3.91%	58.87 ± 3.99%	48.45 ± 2.92%	59.44 ± 2.28%	41.13 ± 6.11%	47.04 ± 6.84%
CZ	46.48 ± 6.89%	49.30 ± 3.27%	51.27 ± 2.65%	55.77 ± 3.41%	47.32 ± 4.39%	44.51 ± 2.65%
F3	42.25 ± 6.89%	47.61 ± 4.85%	49.58 ± 5.30%	52.11 ± 1.27%	50.70 ± 6.18%	51.27 ± 4.02%
O2	***60.00 ± 3.18%***	55.49 ± 3.18%	46.76 ± 5.30%	49.02 ± 5.01%	50.99 ± 3.99%	50.14 ± 3.62%
FP2	***61.97 ± 5.93%***	***63.66 ± 4.17%***	50.42 ± 6.93%	49.86 ± 5.04%	52.68 ± 8.88%	42.25 ± 7.32%
F8	56.34 ± 3.91%	***63.94 ± 6.73%***	48.45 ± 3.62%	54.65 ± 8.87%	53.80 ± 5.31%	53.80 ± 4.18%
C3	49.30 ± 6.43%	44.23 ± 4.03%	52.39 ± 10.3%	59.15 ± 7.00%	49.02 ± 7.86%	43.10 ± 4.56%
T7	49.58 ± 4.53%	53.80 ± 5.30%	52.68 ± 3.83%	56.06 ± 5.16%	58.31 ± 3.62%	63.66 ± 4.35%

Table 6.3: Results for the novel stimuli recordings from each electrode of the 71 patients cohort at each feature level.

	Feature Level					
Classifier	***1-2Hz(all)***	***1-2Hz(mid)***	***2-4Hz(all)***	***2-4Hz(mid)***	***4-8Hz(all)***	***4-8Hz(mid)***
C4	51.83 ± 4.85%	56.05 ± 4.52%	***60.28 ± 5.72%***	57.75 ± 5.93%	42.82 ± 5.19%	53.24 ± 6.23%
FP1	***64.79 ± 6.54%***	***62.53 ± 2.35%***	***60.84 ± 8.69%***	***62.25 ± 4.36%***	46.48 ± 3.91%	52.40 ± 5.45%
O1	53.24 ± 6.47%	55.49 ± 1.57%	50.71 ± 4.94%	55.49 ± 5.18%	41.97 ± 8.86%	46.20 ± 3.13%
P8	***61.41 ± 4.39%***	***61.41 ± 5.04%***	***62.54 ± 4.03%***	***64.51 ± 7.56%***	***61.41 ± 2.65%***	55.21 ± 6.11%
P4	***62.82 ± 3.41%***	***62.53 ± 4.03%***	***65.92 ± 6.35%***	***62.53 ± 2.00%***	51.27 ± 5.33%	59.15 ± 3.71%
P7	58.59 ± 7.78%	54.65 ± 6.35%	***64.51 ± 3.99%***	***61.41 ± 5.74%***	53.80 ± 7.14%	58.03 ± 7.15%
F4	59.72 ± 4.56%	56.90 ± 5.33%	50.14 ± 3.62%	54.65 ± 5.30%	50.70 ± 5.10%	46.84 ± 5.53%
FZ	45.92 ± 2.65%	52.11 ± 3.50%	52.96 ± 4.56%	55.21 ± 5.30%	53.24 ± 7.04%	42.82 ± 2.65%
PZ	***61.41 ± 8.62%***	***65.92 ± 1.46%***	***69.01 ± 1.74%***	***71.55 ± 5.58%***	58.59 ± 4.72%	***68.45 ± 4.39%***
P3	***65.63 ± 4.73%***	57.46 ± 3.13%	***66.76 ± 7.59%***	***65.63 ± 7.88%***	59.72 ± 3.41%	63.10 ± 4.18%
F7	54.65 ± 7.46%	53.52 ± 2.77%	51.83 ± 5.71%	51.83 ± 6.35%	41.97 ± 5.85%	45.35 ± 6.93%
T8	***60.28 ± 3.79%***	***61.69 ± 6.35%***	54.65 ± 3.13%	54.93 ± 5.10%	38.03 ± 9.00%	53.24 ± 4.18%
CZ	52.39 ± 4.53%	53.24 ± 3.13%	56.90 ± 3.18%	***63.38 ± 2.14%***	50.42 ± 3.79%	54.37 ± 7.68%
F3	48.45 ± 8.35%	55.49 ± 0.96%	54.08 ± 3.18%	50.14 ± 3.62%	49.30 ± 5.93%	41.97 ± 3.99%
O2	***63.94 ± 3.41%***	***64.79 ± 3.27%***	56.90 ± 3.17%	59.43 ± 2.59%	45.64 ± 5.61%	46.20 ± 5.00%
FP2	59.72 ± 2.34%	58.03 ± 2.59%	54.93 ± 4.11%	***60.28 ± 6.10%***	45.92 ± 3.18%	45.20 ± 8.17%
F8	***62.25 ± 1.92%***	***62.83 ± 3.18%***	49.86 ± 1.99%	57.18 ± 4.39%	42.53 ± 6.35%	44.79 ± 3.79%
C3	52.39 ± 4.18%	56.90 ± 2.65%	***61.41 ± 3.41%***	***65.07 ± 5.98%***	51.55 ± 5.75%	57.18 ± 5.87%
T7	51.83 ± 4.85%	43.38 ± 4.52%	48.73 ± 5.19%	44.23 ± 4.03%	51.55 ± 5.33%	43.10 ± 4.72%

Table 6.4: Results for the target stimuli recordings from each electrode of the 66 patients cohort at each feature level.

	Feature Level					
Classifier	***1-2Hz(all)***	***1-2Hz(mid)***	***2-4Hz(all)***	***2-4Hz(mid)***	***4-8Hz(all)***	***4-8Hz(mid)***
C4	51.82 ± 6.44%	54.24 ± 3.36%	53.64 ± 5.89%	53.64 ± 5.89 %	48.48 ± 5.49%	50.30 ± 5.71%
FP1	58.18 ± 4.72%	***63.03 ± 5.08%***	59.40 ± 6.96%	57.27 ± 3.62 %	49.39 ± 3.90%	39.39 ± 3.76%
O1	43.63 ± 4.49%	47.58 ± 4.33%	54.85 ± 3.09%	56.67 ± 7.24 %	38.18 ± 7.09%	47.88 ± 8.58%
P8	59.40 ± 3.62%	53.03 ± 3.26%	53.94 ± 4.33%	59.70 ± 9.83 %	43.64 ± 6.97%	40.30 ± 2.14%
P4	***63.64 ± 5.48%***	***63.34 ± 0.84%***	***69.39 ± 9.35%***	***70.00 ± 5.22 %***	36.06 ± 6.70%	38.79 ± 7.71%
P7	***60.61 ± 2.97%***	57.27 ± 3.62%	53.64 ± 3.90%	56.67 ± 8.05 %	59.09 ± 6.10%	***60.30 ± 3.62%***
F4	***67.58 ± 5.08%***	***66.97 ± 4.87%***	48.18 ± 11.5%	50.61 ± 5.89 %	***60.00 ± 2.14%***	48.48 ± 5.95%
FZ	56.06 ± 3.26%	56.97 ± 3.90%	56.36 ± 4.29%	***63.33 ± 9.72 %***	54.55 ± 4.41%	48.18 ± 4.87%
PZ	***68.18 ± 4.79%***	58.79 ± 4.08%	***67.88 ± 0.84%***	***70.61 ± 4.90 %***	44.54 ± 3.41%	47.88 ± 3.42%
P3	***65.46 ± 4.87%***	***66.67 ± 3.26%***	***62.73 ± 4.33%***	***63.33 ± 3.09 %***	53.03 ± 7.16%	47.57 ± 4.53%
F7	50.91 ± 7.83%	50.91 ± 6.18%	46.67 ± 6.16%	52.12 ± 9.08 %	48.49 ± 7.17%	47.88 ± 5.08%
T8	59.40 ± 3.62%	56.06 ± 3.52%	49.09 ± 5.89%	54.25 ± 3.36 %	45.75 ± 4.68%	43.94 ± 4.41%
CZ	52.42 ± 6.86%	57.28 ± 3.36%	***61.21 ± 3.90%***	***61.52 ± 2.85 %***	44.24 ± 1.57%	46.67 ± 9.90%
F3	49.09 ± 4.12%	53.64 ± 2.85%	56.06 ± 7.87%	53.64 ± 4.53 %	53.94 ± 6.86%	50.61 ± 6.33%
O2	***62.12 ± 7.17%***	***60.91 ± 2.06%***	48.48 ± 7.41%	51.21 ± 7.45 %	46.66 ± 4.08%	48.18 ± 4.29%
FP2	***66.36 ± 2.06%***	***63.64 ± 2.30%***	44.54 ± 1.68%	50.91 ± 9.65 %	53.64 ± 8.68%	47.27 ± 4.29%
F8	58.49 ± 3.15%	***62.42 ± 8.86%***	45.15 ± 3.36%	48.79 ± 8.46 %	53.03 ± 3.52%	52.12 ± 2.15%
C3	56.06 ± 5.95%	52.12 ± 2.53%	56.67 ± 4.91%	***62.73 ± 7.11 %***	46.36 ± 4.91%	50.61 ± 6.18%
T7	51.21 ± 6.84%	51.52 ± 1.88%	55.15 ± 2.15%	51.82 ± 8.35 %	55.76 ± 4.08%	55.45 ± 4.12%

Table 6.5: Results for the novel stimuli recordings from each electrode of the 66 patients cohort at each feature level.

	Feature Level					
Classifier	***1-2Hz(all)***	***1-2Hz(mid)***	***2-4Hz(all)***	***2-4Hz(mid)***	***4-8Hz(all)***	***4-8Hz(mid)***
C4	***60.61 ± 3.76%***	***60.00 ± 3.67%***	***65.46 ± 3.09%***	55.46 ± 3.66%	***60.61 ± 7.60%***	56.36 ± 8.24%
FP1	***66.36 ± 4.29%***	***62.12 ± 3.99%***	***60.91 ± 5.22%***	56.67 ± 5.42%	***66.36 ± 6.33%***	57.27 ± 7.69%
O1	56.67 ± 2.14%	54.84 ± 3.36%	50.61 ± 4.90%	53.03 ± 4.41%	56.67 ± 5.05%	46.67 ± 6.97%
P8	***68.18 ± 2.30%***	***68.49 ± 2.06%***	***67.88 ± 4.07%***	***71.82 ± 2.85%***	***68.18 ± 4.08%***	53.94 ± 5.74%
P4	***66.67 ± 4.98%***	***67.27 ± 1.68%***	***69.39 ± 4.87%***	***66.67 ± 3.76%***	***66.67 ± 4.33%***	***62.12 ± 4.41%***
P7	58.79 ± 4.87%	53.64 ± 5.25%	***62.12 ± 6.52%***	***60.91 ± 6.29%***	58.79 ± 8.96%	58.18 ± 7.60%
F4	56.67 ± 3.42%	54.55 ± 4.80%	52.73 ± 4.29%	51.21 ± 3.62%	56.67 ± 6.04%	44.54 ± 6.86%
FZ	46.06 ± 2.14%	49.70 ± 4.08%	52.42 ± 3.90%	56.37 ± 5.55%	46.06 ± 4.29%	45.76 ± 6.44%
PZ	***66.67 ± 5.80%***	***73.64 ± 2.855***	***67.58 ± 4.33%***	***74.85 ± 5.25%***	***66.67 ± 5.15%***	***71.52 ± 5.55%***
P3	***65.15 ± 1.88%***	***60.31 ± 4.29%***	***61.52 ± 5.08%***	***64.85 ± 3.09%***	***65.15 ± 7.16%***	57.88 ± 8.46%
F7	50.31 ± 2.46%	50.61 ± 2.15%	58.79 ± 2.79%	55.15 ± 3.90%	50.31 ± 5.08%	35.15 ± 5.86%
T8	56.06 ± 5.95%	57.27 ± 5.22%	***61.52 ± 2.15%***	58.70 ± 4.90%	56.06 ± 6.01%	49.09 ± 5.42%
CZ	55.76 ± 6.16%	***60.00 ± 2.52%***	***63.03 ± 3.42%***	***66.06 ± 3.15%***	55.76 ± 3.15%	52.73 ± 6.01%
F3	53.64 ± 3.15%	54.55 ± 2.97%	47.58 ± 6.86%	50.00 ± 5.95%	53.64 ± 2.06%	37.57 ± 4.08%
O2	***70.61 ± 6.32%***	***65.15 ± 2.30%***	57.58 ± 2.97%	56.67 ± 7.48%	***70.61 ± 3.99%***	47.57 ± 2.15%
FP2	***62.73 ± 5.42%***	59.70 ± 6.03%	58.79 ± 5.86%	***61.22 ± 3.15%***	***62.73 ± 2.45%***	46.97 ± 5.65%
F8	***60.61 ± 5.32%***	***60.30 ± 5.55%***	47.88 ± 5.74%	55.15 ± 7.12%	***60.61 ± 2.15%***	41.51 ± 6.32%
C3	54.85 ± 7.69%	56.97 ± 6.60%	***62.43 ± 7.45%***	***63.34 ± 4.68%***	54.85 ± 4.53%	54.85 ± 6.30%
T7	50.00 ± 3.99%	45.15 ± 5.70%	44.55 ± 9.37%	45.76 ± 5.39%	50.00 ± 3.90%	53.33 ± 3.36%

Table 6.2 through Table 6.5 show varying degrees of success with different stimuli/electrode/feature set combinations. The most promising results yield performances between the mid-60% to low 70% range and several of these results come from the parietal (P3, P4, P7, P8, and PZ) and occipital electrodes (O1 and O2). In our previous work [79-83], only the PZ, FZ, and CZ electrodes were analyzed but the above results show that complimentary information may rest within the recordings obtained from other electrodes. Therefore, the next logical step is to try to improve upon these performance figures by using advanced pattern recognition techniques. Ensembles of classifiers trained on features from the best performing stimuli/parietal/feature set and stimuli/parietal-occipital/feature set combinations are explored in Section 6.6. Feature-level fusion is first used on features previously found to perform well from [79,80].

6.5 RESULTS FROM FEATURE-LEVEL FUSION

Results from a feature-level fusion experiment for both cohorts are presented in this section. The fusion method chosen was simple concatenation. The features evaluated were Novel PZ (middle 1-2Hz), Target PZ (middle 2-4Hz), and Target CZ (middle 2-4Hz). As mentioned in the previous section, these stimuli/electrode/features were previously shown to yield good performances during the analysis of the PZ, CZ, and FZ electrodes [79-83]. For comparison purposes, individual classifiers were also trained on each of the feature sets and combined at the decision-level.

In Table 6.6, "*Fusion*" means feature-level fusion. NPZ means Novel PZ, TPZ means Target PZ, and TCZ means Target CZ. For example, "*1 2 3* MV" means the classifiers 1, 2, and 3 (i.e. classifier 1 is trained on the Novel PZ features, etc.) combined by weighted majority vote. Table 6.7 shows the best 5 performances of this experiment.

Table 6.6: Results from feature-level fusion compared with classifier fusion using the 71 patient cohort (a) and the 66 patient cohort (b).

(a)	
Fusion NPZ,TPZ,TCZ	66.90 ± 1.19 %
Fusion NPZ,TPZ	62.25 ± 2.55 %
Fusion NPZ,TCZ	67.75 ± 2.25 %
Fusion TPZ, TCZ	70.28 ± 2.20 %
1.) NPZ	66.48 ± 2.36 %
2.) TPZ	62.25 ± 3.03 %
3.) TCZ	56.76 ± 2.56 %
1 2 3 MV	65.07 ± 1.49 %
1 2 MV	67.89 ± 2.55 %
1 3 MV	60.84 ± 2.76 %
2 3 MV	58.73 ± 2.28 %
1 2 3 PROD	68.59 ± 2.93 %
1 2 PROD	71.13 ± 2.19 %
1 3 PROD	64.23 ± 2.70 %
2 3 PROD	61.13 ± 3.37 %
1 2 3 SUM	67.89 ± 2.17 %
1 2 SUM	71.27 ± 2.34 %
1 3 SUM	64.37 ± 2.47 %
2 3 SUM	60.99 ± 3.36 %

(b)	
Fusion NPZ,TPZ,TCZ	78.48 ± 1.68 %
Fusion NPZ,TPZ	72.42 ± 1.52 %
Fusion NPZ,TCZ	73.49 ± 2.62 %
Fusion TPZ, TCZ	75.76 ± 1.45 %
1.) NPZ	75.30 ± 1.98 %
2.) TPZ	69.40 ± 3.38 %
3.) TCZ	62.12 ± 4.57 %
1 2 3 MV	73.79 ± 3.61 %
1 2 MV	71.52 ± 2.22 %
1 3 MV	68.79 ± 2.46 %
2 3 MV	68.94 ± 4.16 %
1 2 3 PROD	77.73 ± 1.45 %
1 2 PROD	80.76 ± 2.23 %
1 3 PROD	73.49 ± 2.24 %
2 3 PROD	71.52 ± 3.18 %
1 2 3 SUM	74.70 ± 3.07 %
1 2 SUM	80.61 ± 2.21 %
1 3 SUM	73.49 ± 2.24 %
2 3 SUM	71.37 ± 3.04 %

Table 6.7: Best five results from feature-level fusion compared with decision-level fusion using the 71 patient cohort (a) and the 66 patient cohort (b).

(a)

Combination	Performance	Sensitivity	Specificity	Positive Predictive Value
Fusion TPZ, TCZ	76.06 ± 8.50%	73.53%	78.38%	75.76%
NPZ, TCZ PROD	74.65 ± 8.67%	79.41%	70.27%	71.05%
NPZ, TPZ PROD	74.65 ± 8.67%	73.53%	73.53%	73.53%
NPZ, TPZ, TCZ PROD	73.24 ± 8.82%	73.53%	72.97%	71.43%
NPZ, TPZ PROD	73.24 ± 8.82%	73.53%	72.97%	71.43%

(b)

Combination	Performance	Sensitivity	Specificity	Positive Predictive Value
Fusion NPZ, TPZ, TCZ	83.33 ± 7.71%	80.00%	86.11%	82.76%
NPZ, TPZ PROD	83.33 ± 7.71%	83.33%	83.33%	80.65%
NPZ, TPZ PROD	83.33 ± 7.71%	76.67%	88.89%	85.19%
NPZ, TPZ SUM	83.33 ± 7.71%	80.00%	86.11%	82.76%
NPZ, TPZ PROD	84.85 ± 7.42%	86.67%	83.33%	81.25%

The feature-level fusion technique was more successful when used with the 66 patient cohort. The best feature-level fusion performance for the 71 patient cohort was 76.06% while the best performance for the 66 patient cohort was 83.33%. Although this is a significant difference, the product rule combination of Novel PZ and Target PZ in the 66 patient cohort yielded a performance of almost 85%. It seems that the feature-level fusion method is highly sensitive. This sensitivity may be from redundant or uninformative features. With the effectiveness of this method being inconclusive, the focus of the experiments is turned towards classifier (decision-level) fusion which is a well-established combination method.

6.6 RESULTS FROM CLASSIFIER FUSION

Two comprehensive experiments are performed using classifier fusion. First, classifier fusion was used to combine the ensembles of classifiers trained on features from parietal electrodes, PZ, P3, P4, and P7. These parietal electrodes were chosen because of their performance figures shown in Section 6.2, and their consistency for both target and novel

stimuli. AD has been found to first show symptoms in the parietal region, thus making the features obtained from EEG recordings in this region possible key features for the early detection of AD.

Classifiers were trained on the following 6 feature sets for both target and novel stimuli from the respective electrodes: P4 (middle 2-4Hz features), PZ (all 2-4Hz features), P3 (all 2-4Hz features), P4 (all 1-2Hz features), PZ (all 1-2Hz features), and P7 (all 1-2Hz features). Tables 6.8 through 6.15 show the best 5 performance results from five leave-one-out cross-validation trials along with the 95% confidence interval of that trial. In each trial, fusion was achieved by the weighted majority vote, product rule, and sum rule of various combinations of the six classifiers. All combination possibilities from combining all 6 to combining 3 classifiers were exhausted for a total of 42 different combinations (refer to Appendix C for full results of these combinations). The following tables show the best electrode combinations for both stimuli, the combination rule, and the resulting performance and CI, sensitivity, specificity, and positive predictive value.

To clarify the layout of these tables, here is an example. In Table 6.8, the first row should be interpreted as follows: The sum rule was used to combine 4 classifiers. Each classifier was trained on the feature sets, P4 (middle 2-4Hz), P3 (all 2-4Hz), P4 (all 1-2Hz), and P7 (all 1-2Hz), respectively. This ensemble achieved a performance of 74.65%, a sensitivity of 70.59%, a specificity of 72.97% and positive predictive value of 70.59%.

Table 6.8: Results of 1 classifier each from the target/parietal recordings for 71 patients.

Electrodes and Feature Level	*Combination Rule*	*Performance*	*Sensitivity*	*Specificity*	*Positive Predictive Value*
P4 (2-4Hz), P3 (2-4Hz), P4 (1-2Hz), P7 (1-2Hz)	SUM	74.65 ± 10.37%	70.59%	72.97%	70.59%
PZ (2-4Hz), P3(2-4Hz), P4 (1-2Hz), P7(1-2Hz)	SUM	73.24 ± 10.55%	67.57%	67.57%	67.57%
P4 (2-4Hz), PZ (2-4Hz), P7(1-2Hz)	PRODUCT	73.24 ± 10.55%	72.73%	75.68%	72.73%
PZ (2-4Hz), P4 (1-2Hz), P7 (1-2Hz)	PRODUCT	71.83 ± 10.72%	71.88%	75.68%	71.88%
P3 (2-4Hz), PZ (1-2Hz), P7 (1-2Hz)	PRODUCT	71.83 ± 10.72%	69.44%	70.27%	69.44%

Table 6.9: Results of 3 classifiers each from target/parietal recordings for 71 patients.

Electrodes and Feature Level	*Combination Rule*	*Performance*	*Sensitivity*	*Specificity*	*Positive Predictive Value*
P4 (2-4Hz), P4 (1-2Hz), P7(1-2Hz)	WEIGHTED MAJORITY VOTE	76.06 ± 10.17%	70.59%	81.08%	77.42%
P4 (2-4Hz), P3 (2-4Hz), P4 (1-2Hz), P7 (1-2Hz)	WEIGHTED MAJORITY VOTE	74.65 ± 10.37%	67.65%	81.08%	76.67%
P4 (2-4Hz), PZ (1-2Hz), P7(1-2Hz)	WEIGHTED MAJORITY VOTE	74.65 ± 10.37%	70.59%	78.38%	75.00%
PZ (2-4Hz), P4 (1-2Hz), P7 (1-2Hz)	SUM	74.65 ± 10.37%	70.59%	78.38%	75.00%
P4(2-4Hz), PZ (2-4Hz), P4 (1-2Hz), P7 (1-2Hz)	PRODUCT	73.24 ± 10.55%	64.71%	81.08%	75.86%

Table 6.10:Results of 1 classifier each from target/parietal recordings for 66 patients.

Electrodes and Feature Level	*Combination Rule*	*Performance*	*Sensitivity*	*Specificity*	*Positive Predictive Value*
PZ (2-4Hz), P3 (2-4Hz), P7 (1-2Hz)	WEIGHTED MAJORITY VOTE	81.82 ± 9.55%	80.00%	81.08%	80.00%
P4 (2-4Hz), PZ (2-4Hz), P3 (2-4Hz), PZ (1-2Hz)	WEIGHTED MAJORITY VOTE	78.79 ± 10.13%	80.65%	83.78%	80.65%
P4 (2-4Hz), PZ (2-4Hz), P3 (2-4Hz), PZ (1-2Hz)	SUM	78.79 ± 10.13%	80.65%	83.78%	80.65%
P4 (2-4Hz), PZ (2-4Hz), PZ (1-2Hz), P7(1-2Hz)	WEIGHTED MAJORITY VOTE	78.79 ± 10.13%	78.79%	81.08%	78.79%
PZ (2-4Hz), P3 (2-4Hz), P7 (1-2Hz)	PRODUCT	77.27 ± 10.38%	76.47%	78.38%	76.47%

Table 6.11: Results of 3 classifiers each from target/parietal recordings for 66 patients.

Electrodes and Feature Level	*Combination Rule*	*Performance*	*Sensitivity*	*Specificity*	*Positive Predictive Value*
P4 (2-4Hz), PZ (2-4Hz), P3 (2-4Hz), P4 (1-2Hz), PZ (1-2Hz)	PRODUCT	80.30 ± 9.85%	76.67%	83.33%	79.31%
P4 (2-4Hz), PZ (2-4Hz), P3 (2-4Hz), P4 (1-2Hz), PZ (1-2Hz)	SUM	80.30 ± 9.85%	80.00%	80.56%	77.42%
PZ (2-4Hz), P4 (24Hz), PZ (1-2Hz), P7(1-2Hz)	WEIGHTED MAJORITY VOTE	80.30 ± 9.85%	80.00%	80.56%	77.42%
P4 (2-4Hz), P4 (1-2Hz), PZ (1-2Hz)	SUM	78.79 ± 10.13%	76.67%	80.56%	76.67%
P4 (2-4Hz), PZ (2-4Hz), P3 (2-4Hz), PZ (1-2Hz), P7 (1-2Hz)	WEIGHTED MAJORITY VOTE	78.79 ± 10.13%	76.67%	80.56%	76.67%

Table 6.12: Results of 1 classifier each from novel/parietal recordings for 71 patients.

Electrodes and Feature Level	*Combination Rule*	*Performance*	*Sensitivity*	*Specificity*	*Positive Predictive Value*
PZ (2-4Hz), P3 (2-4Hz), P7 (1-2Hz)	WEIGHTED MAJORITY VOTE	81.69 ± 9.22%	80.00%	81.08%	80.00%
P4 (2-4Hz), PZ (2-4Hz), P3 (2-4Hz), PZ (1-2Hz)	WEIGHTD MAJORITY VOTE	78.87 ± 9.73%	75.68%	75.68%	75.68%
P4 (2-4Hz), PZ (2-4Hz), P3 (2-4Hz), PZ (1-2Hz)	SUM	78.87 ± 9.73%	80.65%	83.79%	80.65%
P4 (2-4Hz), PZ (2-4Hz), PZ (1-2Hz), P7 (1-2Hz)	WEIGHTED MAJORITY VOTE	78.87 ± 9.73%	78.79%	81.08%	78.79%
P4 (2-4Hz), PZ (2-4Hz), P3 (2-4Hz)	PRODUCT	77.46 ± 9.96%	76.47%	78.38%	76.47%

Table 6.13: Results of 3 classifiers each from novel/parietal recordings for 71 patients.

Electrodes and Feature Level	*Combination Rule*	*Performance*	*Sensitivity*	*Specificity*	*Positive Predictive Value*
PZ (2-4Hz), P3 (2-4Hz), P7 (1-2Hz)	PRODUCT	80.28 ± 9.48%	76.47%	83.78%	81.25%
PZ (2-4Hz), P3 (2-4Hz), P7 (1-2Hz)	WEIGHTED MAJORITY VOTE	80.28 ± 9.48%	76.47%	83.78%	81.25%
P4 (2-4Hz), PZ (2-4Hz), P3 (2-4Hz), P7 (1-2Hz)	WEIGHTED MAJORITY VOTE	78.87 ± 9.73%	76.47%	81.08%	78.79%
P3 (2-4Hz), PZ (1-2Hz), P7 (1-2Hz)	WEIGHTED MAJORITY VOTE	77.46 ± 9.96%	79.41%	75.68%	75.00%
P3 (2-4Hz), P4 (1-2Hz), P7 (1-2Hz)	WEIGHTED MAJORITY VOTE	77.46 ± 9.96%	73.53%	81.08%	78.13%

Table 6.14: Results of 1 classifier each from novel/parietal recordings for 66 patients.

Electrodes and Feature Level	*Combination Rule*	*Performance*	*Sensitivity*	*Specificity*	*Positive Predictive Value*
P4 (2-4Hz), PZ (2-4Hz), P4 (1-2Hz), P7 (1-2Hz)	PRODUCT	84.85 ± 8.88%	85.71%	88.89%	85.71%
P4 (2-4Hz), P4 (1-2Hz), P7 (1-2Hz)	PRODUCT	83.33 ± 9.23%	88.00%	91.67%	88.00%
P4 (2-4Hz), P3 (2-4Hz), PZ (1-2Hz)	PRODUCT	81.82 ± 9.55%	82.14%	86.11%	82.14%
P4 (2-4Hz), PZ (2-4Hz), P4 (1-2Hz), PZ (1-2Hz), P7 (1-2Hz)	PRODUCT	81.82 ± 9.55%	82.14%	86.11%	82.14%
P3 (2-4Hz), P4 (1-2Hz), P7 (1-2Hz)	SUM	81.82 ± 9.55%	78.57%	83.33%	78.57%

Table 6.15: Results of 3 classifiers each from novel/parietal recordings for 66 patients.

Electrodes and Feature Level	*Combination Rule*	*Performance*	*Sensitivity*	*Specificity*	*Positive Predictive Value*
P4 (2-4Hz), PZ (2-4Hz), P3 (2-4Hz), P4 (1-2Hz), PZ (1-2Hz)	PRODUCT	81.82 ± 9.55%	80.00%	83.33%	80.00%
P4 (2-4Hz), P3 (2-4Hz), P4 (1-2Hz)	SUM	81.82 ± 9.55%	80.00%	83.33%	80.00%
PZ (2-4Hz), P4 (2-4Hz), PZ (1-2Hz), P7(1-2Hz)	WEIGHTED MAJORITY VOTE	83.33 ± 9.23%	80.00%	86.11%	82.76%
P4 (2-4Hz), PZ (2-4Hz), P4 (1-2Hz), PZ (1-2Hz)	SUM	81.82 ± 9.55%	76.67%	86.11%	82.14%
P4 (2-4Hz), P3 (2-4Hz), P4 (1-2Hz), P7 (1-2Hz)	WEIGHTED MAJORITY VOTE	81.82 ± 9.55%	80.00%	83.33%	80.00%

For the first time in these results, combinations of classifiers for the 71 patient cohort exceed 80% performance, specifically seen in Tables 6.12 and 6.13. To try to compliment these features, a combination of both the target and novel classifiers is tried for the 71 patient cohort. Table 6.16 represents the best 5 performances from five leave-one-out trials with these combinations and the individual trial confidence intervals (refer to Appendix C for full results). Electrode combinations are of one classifier from each stimuli. For example, in Table 6.16, the first entry in the "Electrodes and Feature Level" column says P4 (2-4Hz), PZ (2-4Hz), P3 (2-4Hz), P4 (1-2Hz), and PZ (1-2Hz). This should be interpreted as the combination Target and Novel P4 (2-4Hz), Target and Novel PZ (2-4Hz), etc. at the specified feature levels. Note the subband features do not change for the different stimuli.

Table 6.16: Results from each of the target and novel/parietal classifiers for 71 patients.

Electrodes and Feature Level	***Combination Rule***	***Performance***	***Sensitivity***	***Specificity***	***Positive Predictive Value***
P4 (2-4Hz), P3 (2-4Hz), P7 (1-2Hz)	WEIGHTED MAJORITY VOTE	83.10 ± 8.93%	82.35%	83.78%	82.35%
P4 (2-4Hz), P3 (2-4Hz), PZ (1-2Hz), P7 (1-2Hz)	WEIGHTED MAJORITY VOTE	83.10 ± 8.93%	79.41%	86.49%	84.38%
P4 (2-4Hz), P3 (2-4Hz), P7 (1-2Hz)	SUM	81.69 ± 9.22%	76.47%	86.49%	83.87%
P4 (2-4Hz),PZ (2-4Hz), P3 (2-4Hz), P7 (1-2Hz)	PRODUCT	81.69 ± 9.22%	85.29%	78.38%	78.38%
P4 (2-4Hz), PZ (2-4Hz), P3 (2-4Hz), PZ (1-2Hz), P7 (1-2Hz)	SUM	81.69 ± 9.22%	82.35%	81.08%	80.00%

From the combinations of Target and Novel classifiers for the 71 patient cohort, a performance of 83.10% is obtained through a total of 6 classifiers (Target and Novel P4 (2-4Hz), Target and Novel P3 (2-4Hz), and Target and Novel P7 (1-2Hz)). This result is slightly higher than the 81.69% performance obtained in Table 6.12 when just 3 classifiers (Novel PZ (2-4Hz), Novel P3 (2-4Hz), and Novel P7 (1-2Hz)) were combined through weighted majority vote. Comparatively, the target and novel combination does show improvement in the specificity and positive predictive value.

The last experiments of this thesis involve the parietal and occipital electrode recordings for the 71 patient cohort. The best performing feature set from each electrode was selected. A total of 11 electrode/stimuli combinations were chosen to create the feature sets. Those choices were: Target P4 (all 2-4Hz), Target PZ (middle 2-4Hz), Target P3 (middle 2-4Hz), Novel P8 (middle 2-4Hz), Target O2 (all 1-2Hz), Target P7 (all 1-2Hz), Novel O2 (all 1-2Hz), Novel PZ (middle 2-4Hz), Novel P3 (middle 2-4Hz), Novel P4 (all 1-2Hz), and Novel PZ (1-2Hz). A single classifier was trained on one of these feature sets. All combinations of 3 classifiers (a total of 164) were exhausted and a combination of all 11 classifiers was tried (refer to Appendix C for the full results). As in the previous results, the best 5 resulting combinations from five leave-one-out trials are displayed in Table 6.17 along with the combination rule, sensitivity, specificity, and positive predictive value.. "T" stands for target and "N" stands for novel. For example in the first row and column, TP4 (all 2-4Hz), TP7 (all 1-2Hz), and NPZ (mid 2-4Hz) means that 3 classifiers, each trained on one of the feature sets was combined by weighted majority vote to obtain the reported performance figures.

Table 6.17: Results of 11 classifiers from the parietal and occipital electrodes.

Electrodes and Feature Level	*Combination Rule*	*Performance*	*Sensitivity*	*Specificity*	*Positive Predictive Value*
TP4 (all 2-4Hz), TP7 (all 1-2Hz), NPZ (mid 2-4Hz)	WEIGHTED MAJORITY VOTE	83.10 ± 8.93%	85.29%	81.08%	80.56%
TP4 (all 2-4Hz), NP8 (mid 2-4Hz), NPZ (mid 2-4Hz)	PRODUCT	81.69 ± 9.22%	79.41%	83.78%	81.82%
NP8 (mid 2-4Hz), TO2 (all 1-2Hz), NPZ (mid 2-4Hz)	PRODUCT	81.69 ± 9.22%	79.41%	83.78%	81.82%
TP4 (all 2-4Hz), TP7 (all 1-2Hz), NPZ (mid 2-4Hz)	SUM	80.28 ± 9.48%	76.47%	83.78%	81.25%
NP8 (mid 2-4Hz), TP7 (all 1-2Hz), NPZ (mid 2-4Hz)	PRODUCT	80.28 ± 9.48%	79.41%	81.08%	79.41%

The best performance in the above table is 83.10% and comes from the weighted majority vote combination of 3 feature sets. In the previously mentioned results, 6 classifiers (Target and Novel P4 (2-4Hz), Target and Novel P3 (2-4Hz), and Target and Novel P7 (1-2Hz)) were necessary to obtain 83.10% in Table 6.16. In this scenario with combining Parietal and Occipital features, it takes half the number of classifiers previously stated to obtain the same success.

To further, exhaust combination possibilities, 7 classifiers that yielded the best results from the previous 11, are combined for all possible combinations of 3, 5, and 7 classifiers for a total of 56 combinations. The stimuli and features used to train this ensemble of classifiers were: Target P4 (all 2-4Hz), Target P7 (all 1-2Hz), Novel PZ (middle 2-4Hz), Novel P8 (middle 2-4Hz), Target O2 (all1-2Hz), Novel O2 (all 1-2Hz), and Novel P3 (middle 2-4Hz). Once again, the best 5 combinations from five leave-one-out trials are displayed in Table 6.18.

Table 6.18: Results of 7 classifiers from the parietal and occipital electrodes.

Electrodes and Feature Level	*Combination Rule*	*Performance*	*Sensitivity*	*Specificity*	*Positive Predictive Value*
NP8 (mid 2-4Hz), TP7 (all 1-2Hz), NPZ (mid 2-4Hz)	WEIGHTED MAJORITY VOTE	81.69 ± 7.71%	88.24%	75.68%	76.92%
NP8 (mid 2-4Hz), TP7 (all 1-2Hz), NPZ (mid 2-4Hz)	SUM	80.28 ± 7.93%	85.29%	75.68%	76.32%
TO2 (all 1-2Hz), TP7 (all 1-2Hz), NO2 (all 1-2Hz), NPZ (mid 2-4Hz), NP3 (mid 2-4Hz)	SUM	78.87 ± 8.13%	73.53%	83.78%	80.65%
TP4 (all 1-2Hz), TP7 (all 1-2Hz), NO2 (all 1-2Hz), NPZ (mid 2-4Hz), NP3 (mid 2-4Hz)	WEIGHTED MAJORITY VOTE	78.87 ± 8.13%	79.41%	78.38%	77.14%
NO2 (all 1-2Hz), NPZ (mid 2-4Hz), NP3 (mid 2-4Hz)	PRODUCT	78.87 ± 8.13%	73.53%	83.78%	80.65%

The best performance of the above 7 classifiers is 81.69% and comes from the weighted majority vote combination of 3 feature sets, NP8 (mid 2-4Hz), TP7 (all 1-2Hz), NPZ (mid 2-4Hz). This result is less than the 83% achieved earlier.

For the final test, feature-level fusion is revisited and combined with classifier fusion. In the above tests, only one feature set was used from each electrode except Novel PZ (the 1-2Hz and 2-4Hz features were used). The Target P4 electrode has consistent performance figures for the 2-4Hz feature set (which was used in the above tests) as well as the 1-2Hz feature set. This last experiment incorporates this other feature set of the Target P4 electrode by using feature-level fusion and concatenating it with the 2-4Hz feature set. A classifier was trained on the fused Target P4 features while the other feature sets remained the same (Target P7 (all 1-2Hz), Novel PZ (middle 2-4Hz), Novel

P8 (middle 2-4Hz), Target O2 (all1-2Hz), Novel O2 (all 1-2Hz), and Novel P3 (middle 2-4Hz)). Table 6.19 displays the best 5 performances of this experiment.

Table 6.19: Results of 7 classifiers including the feature-level fused Target P4 from the parietal and occipital electrodes.

Electrodes and Feature Level	***Combination Rule***	***Performance***	***Sensitivity***	***Specificity***	***Positive Predictive Value***
TP4 (all 1-2 + 2-4Hz), TP7 (all 1-2Hz), NO2 (all 1-2Hz), NPZ (mid 2-4Hz), NP3 (mid 2-4Hz)	WEIGHTED MAJORITY VOTE	84.51 ± 8.62%	79.41%	89.19%	87.10%
TP4 (all 1-2 + 2-4Hz), TP7 (all 1-2Hz), NO2 (all 1-2Hz), NPZ (mid 2-4Hz), NP3 (mid 2-4Hz)	SUM	83.10 ± 8.93%	79.41%	86.49%	84.38%
TO2 (all 1-2Hz), NPZ (mid 2-4Hz), NP3 (mid 2-4Hz)	PRODUCT	81.69 ± 9.22%	79.41%	83.78%	81.82%
TP4 (all 1-2 + 2-4Hz), NPZ (mid 2-4Hz), NP3 (mid 2-4Hz)	WEIGHTED MAJORITY VOTE	81.69 ± 9.22%	73.53%	89.19%	86.21%
TO2 (all 1-2Hz), TP7 (all 1-2Hz), NO2 (all 1-2Hz), NPZ (mid 2-4Hz), NP3 (mid 2-4Hz)	WEIGHTED MAJORITY VOTE	80.28 ± 9.48%	76.47%	83.78%	81.25%

The best performance of the above 7 classifiers with the feature-level fused Target P4 was 84.51% and comes from the weighted majority vote combination of 5 electrodes, TP4 (all 1-2 concatenated with 2-4Hz), TP7 (all 1-2Hz), NO2 (all 1-2Hz), NPZ (mid 2-4Hz), and NP3 (mid 2-4Hz). This is the highest performance achieved by the 71 patient cohort and matches the best performance of the 66 patient cohort. This result also reveals that a feature-level and classifier fusion scheme may be able to achieve higher performances than just a single feature-level or classifier fusion scheme.

CHAPTER 7

CONCLUSIONS

7.1 SUMMARY OF ACCOMPLISHMENTS

The approach used in this study involved a multiresolution wavelet analysis of the original time-domain ERP signals for feature extraction. Features from the resulting 1-2Hz, 2-4Hz, and 4-8Hz frequency subbands of the wavelet decomposition were used to train MLP classifiers. Features were combined in feature-level fusion experiments and classifiers trained on these features were combined in classifier fusion experiments. Their performance capabilities were then tested in a leave-one-out cross validation scheme.

This study expands upon our previous studies by performing an analysis on the recordings from all 19 available electrodes. Furthermore, recordings from both the target and novel stimuli were analyzed. This analysis lead to the discovery of other informative features. Of these features, the main focus was on those in the parietal and occipital regions. AD is known to first show symptoms around the hippocampus, hence making these surrounding regions prime candidates for informative features.

It has also been shown in this study that the novel recordings are informative, if not more informative than the target recordings. Classifiers trained on features from the novel recordings generally performed better than those trained on features from target recordings. It was only when the target and novel features were combined that the best performance of almost 85% was achieved.

In experiments prior to those performed in this study, that consisted of examining

only the PZ, CZ, and FZ electrodes, it was thought that certain patients in our cohort were troublesome to our algorithm. These "troublesome" patients had very poor classification rates. The exclusion of these patients from the analysis resulted in higher performances. However within this study, it was shown that it is not necessary to exclude those patients and that our previous conclusions about them were incorrect. A performance equal in success to that of using only 66 patients was achieved with all 71 patients. For this reason, only the 71 patient cohort need be examined in continued efforts.

The metric with which we compared our performance to, was the reported overall diagnostic accuracy of local physicians which was only 75%. Overall, our method has achieved and surpassed this metric in performance. Comparatively, our algorithm's best performance was almost 85%. Although this result was pleasing, the sensitivity (in Table 6.19) was only 79%, whereas it should be higher. On the other hand, the specificity and positive predictive values were high. The positive predictive value (PPV) is the probability that a person who has the disease yields a positive test result, so a high PPV is very satisfactory (refer to Appendix A for formal definitions of positive predictive value, sensitivity, and specificity).

The results achieved in this study are significant. It was shown that a multiresolution wavelet analysis can extract meaningful features from ERP recordings. This is true not only for the target stimuli recordings, but also for the novel stimuli recordings. These features can then be used to train multilayer perceptron classifiers. A combination of classifiers trained on different feature sets improved the generalization performance and yielded the highest performance of this study. The approach used in this study is a novel method that could be made readily available to local healthcare

providers. It is method whose accuracy is comparable to the expertise of a neurophysiologist and would be a valuable tool to have in addition to clinical evaluations.

7.2 SOURCES OF ERROR

The patients recruited for this study were diagnosed using clinical evaluation. As mentioned previously, an evaluation at the local healthcare level has an estimated accuracy of only 75%. The evaluation of the patients used in this study was performed by an expert neurophysiologist. Their clinical evaluation is the current 'gold standard' with an estimated positive predictive value of 90%, but currently there is no way for it to be 100% accurate. Despite this, the classification algorithms of this study were trained as if the patient diagnoses were 100% correct. The original misdiagnoses of a test subject is a potential source of error but less likely to occur because of the expertise of the diagnosis. The only way to obtain a 100% accurate diagnosis is through an autopsy. Inclusion of a postmortem analysis of the test subjects to obtain the true 'gold standard' would prevent this error.

Other errors may lie within the classification algorithms. The free parameters for the MLPs were based on those of our previous work. The error goal for all classifiers was set to 0.01 and the number of hidden layer nodes was either 10 or 20 depending on the number of features. These numbers have not been proved to be the optimal settings despite their success in the past. The assumption of these parameters may also be a potential source of error.

7.3 RECOMMENDATIONS FOR FUTURE WORK

The use of all electrodes should be analyzed further. The extent of the experiments performed in this study open the door to many possibilities. There were electrodes and features combinations other than those of the parietal and occipital regions that performed well. It would be logical and possibly beneficial to further pursue the value of this data.

The Daubechies 4 was the only wavelet used for analysis. Perhaps another wavelet of a different family or even within the same family may be better suited for this type of analysis. For example, Jacques *et al.* in [22] used the Daubechies 4 wavelet, but also used a quadratic b-spline wavelet. The performance obtained in [22] when using the quadratic b-spline wavelet was comparable to that of the Daubechies 4; hence, performing a comparative analysis with a quadratic b-spline or another type of wavelet might be informative.

The combination rules used in the experiments of this study were very basic. Another combination rule such as decision templates, or competence-based classifier selection or weighting as mentioned in Chapter 5, may render better results as more informative features and classifiers are obtained. They have been used with some success in the past and may be worth revisiting.

A multiresolution wavelet analysis has been the main feature extraction technique to this point. Another more strategic feature extraction technique or feature selection method may also be worth pursuing. The features in the 1-8Hz range have shown to be informative. This feature range was analyzed in such a way to focus on the activity of the P300 component. Perhaps analyzing the well-known delta and theta bands which fall in this frequency range along with the alpha, beta, and gamma bands may be complimentary

to our analysis. Maybe a different technique to extract these features such as bandpass filtering may work and save computational resources. Feature selection techniques may allow the most dominant features to be chosen. The performances obtained thus far may be limited by the inclusion of redundant and non-informative features. A genetic algorithm like that mentioned in [74] or an independent component analysis [78] may extract the best features for this problem. These methods may also be a more strategic approach than the trial and error method that has been used in this study and our previous efforts.

REFERENCES

[1] Alzheimer's Disease Fact Sheet, http://www.alz.org/Resources/FactSheets/FSADFacts.pdf, Last accessed: August 14, 2006.

[2] Vellas B.,Fitten L.J., *Research and Practice in Alzheimer 's Disease*, Vol.3., Springer Publishing Company. New York: 2000. pp. 27-32.

[3] Ferri C. P., *et al.*, "Global prevalence of dementia: a Delphi consensus study," *The Lancet*, 2005, 366:2112-2117.

[4] Lim, A., *et al.*, "Clinico-neuropathological correlation of Alzheimer's disease in a community-based case series," *Journal of the American Geriatrics Society,* 1999, Vol. 47. Issue 5, pp. 564-569.

[5] Forstl H., Kurz A., "Clinical features of Alzheimer's disease," *European Archives of Psychiatry and Clinical Neuroscience*, 1999; 249:288-90.

[6] Bianchetti A., Trabucch M., "Clinical aspects of Alzheimer's disease," *Aging Clinical and Experimental Research*, 2001; 13:221-30.

[7] DeCarli C., "The role of neuroimaging in dementia," *Clinics in Geriatric Medicine,* 2001; 17:255-279.

[8] "Alzheimer's disease overview," http://www.cnn.com/HEALTH/library/DS/00161.html, Last accessed: August 16, 2006.

[9] Shenk, D., *The Forgetting, Alzheimer's: Portrait of an Epidemic*. Doubleday. New York: 2001.

[10] Soukup, J. E., *Alzheimer's Disease: A Guide to Diagnosis, Treatment, and Management,* Praeger Publishers, Connecticut, 1996, pp. 11-15.

[11] Hansson O., *et al.*, "Association between CSF biomarkers and incipient Alzheimer's disease in patients with mild cognitive impairment: a follow-up study," *The Lancet Neurology*, 2006; 5: 228–34.

[12] Polich J., Kok A., "Cognitive and biological determinants of P300: an integrative review," *Biological Psychology*, 1995, Vol. 41, pp. 103-146.

[13] Jeong J., "EEG dynamics in patients with Alzheimer's disease," *Clinical Neurophysiology*, 2004, Vol. 115, pp. 1490-1505.

[14] Verma N., *et al.*, "Electrophysiologic validation of two categories of dementias – cortical and subcortical, *Clinical Electroencephalograpgy*, 1987; 18:26-33.

[15] Yagneswaran S., Baker M., Petrosian A., "Power Frequency and Wavelet Characteristics in Differentiating Between Normal and Alzheimer EEG," *The Proceedings of the Second Joint EMBS/BMES Conference,* Houston, TX, 2002.

[16] Feinberg I., "Schizophrenia: caused by a fault in programmed synaptic elimination during adolescence," *Journal of Psychiatric Research*, 1982-1983; 17:319–34.

[17] Sutula T., "Experimental models of temporal lobe epilepsy: new insights from the study of kindling and synaptic reorganization," *Epilepsia*, 1990.

[18] Berger H., "Uber das Elektrenkephalogramm des Menschen. Dritte Mitteilung," *Archiv für Psychiatrie und Nervenkrankheiten*, 1931; 94:16-60.

[19] Lopes de Silva F., *Electroencephalography: Basic Principles, Clinical Applications, and Related Fields*, 4th Ed.,. Lippincott, Williams and Wilkins, Philadelphia, 1999.

[20] Berger H., "Uber das Elektrenkephalogramm des Menschen. Funfte Mitteilung," *Archiv für Psychiatrie und Nervenkrankheiten*, 1932; 98:231–54.

[21] Quiroga R. Q., 'Quantitative analysis of EEG signals: Time-frequency methods and Chaos theory,' *Thesis*:Institute of Physiology and Institute of Signal Processing - Medical University Lubeck,1998.

[22] Jacques G., 'Daubechies and Quadratic B-spline Wavelets for automated early diagnosis of Alzheimer's disease,' *Thesis*:Department of Electrical and Computer Engineering – Rowan University, 2004.

[23] Basar E., *et al.*, "Gamma, alpha, delta, and theta oscillations govern cognitive processes," *International Journal of Psychophysiology*, 2001, Vol. 39, pp. 241-248.

[24] Basar E., *et al.*, "Are cognitive processes manifested in event-related gamma, alpha, theta and delta oscillations in the EEG?" *Neuroscience Letters*, 1999, Vol. 259, pp. 165-168.

[25] Basar E., *et al.*, "Event-related oscillations are 'real brain responses'-wavelet analysis and new strategies," *International Journal of Psychophysiology,* 2001, Vol. 39, pp. 91-127.

[26] Maltseva I., *et al.*, "Alpha oscillations as an indicator of dynamic memory operations-anticipation of omitted stimuli," *International Journal of Psychophysiology*, 2000, Vol. 36, pp. 185-197.

[27] Basar-Eroglu, Canan, *et al.*, "Gamma-band responses in the brain: a short review of physiological correlates and functional significance," *International Journal of Psychophysiology*, 1996, Vol. 24, pp.101-112.

[28] Karakas S., Basar E., "Early Gamma response is sensory in origin: a conclusion based on cross-comparison of results from multiple experimental paradigms," *International Journal of Psychophysiology*, 1998, Vol. 31, 1:13-31.

[29] Karakas S., *et al.*, "The genesis of human event-related responses explained through the theory of oscillatory neural assemblies," *Neuroscience Letters,* 2000. Vol. 285, pp. 45-48.

[30] Polikar R., *et al.*, "Multiresolution Wavelet Analysis of ERPs for the Detection of Alzheimer's Disease," *Proceedings 19th International Conference IEEE*, 1997.

[31] Polich, J., "Neurophysiology of P3a and P3b: A theoretical overview," *Advances in Electrophysiology in Clinical Practice and Research*, Kjellberg, Inc., Wheaton, IL., 2002.

[32] Yamaguchi S., *et al.*, "Event-related brain potentials in response to novel sounds in dementia," *Clinical Neurophysiology*, 2000, Vol. 111, pp. 195-203.

[33] Golob E. J., Starr A., "Age-related qualitative differences in auditory cortical responses during short-term memory," *Clinical Neurophysiology*, 2000, Vol. 111, pp. 2234-2244.

[34] Polich J., *et al.*, "P300 Topography of Amplitude/Latency Correlations," *Brain Topography*, 1997, Vol. 9, 4:275-282.

[35] Junichi K., Polich J., "Auditory and visual P300 topography from a 3 stimulus paradigm," *Clinical Neurophysiology*, 1999, Vol. 110, pp. 463-468.

[36] Brenner R.P., *et al.*, "Computerized EEG spectral analysis in elderly normal, demented and depressed subjects," *Electroencephalography and Clinical Neurophysiology*, 1986; 64:483–92.

[37] Coben L.A., *et al.*, "A longitudinal EEG study of mild senile dementia of Alzheimer type: changes at 1 year and at 2.5 years," *Electroencephalography and Clinical Neurophysiology*, 1985; 61:101 –12.

[38] Penntila M., *et al.*, "Quantitative analysis of occipital EEG in different stages of Alzheimer's disease," *Electroencephalography and Clinical Neurophysiology,* 1985; 60:1-6.

[39] Kowalski J.W., *et al.*, "The diagnostic value of EEG in Alzheimer disease: correlation with the severity of mental impairment," Journal of Clinical Neurophysiology, 2001;18:570-575.

[40] Schreiter-Gasser U., *et al.*, "Quantitative EEG analysis in early onset Alzheimer's disease: correlations with severity, clinical characteristics, visual EEG and CCT," *Electroencephalography and Clinical Neurophysiology*, 1994, Vol. 90, pp. 267-272.

[41] Polich J., Hoffman L.D., "Alzheimer's Disease and P300: evaluation of modality and task difficulty," *Brain Topography Today,* 1998, pp. 527-536.

[42] Frodl T., *et al.*, "Value of event-related P300 subcomponents in the clinical diagnosis of mild cognitive impairment and Alzheimer's Disease," *Psychophysiology*, 2002, Vol. 39, pp. 175-181.

[43] Polich, J., " EEG, ERPs, and Aging: Data and Measurement Issues," *Cognitive Changes Due to Aging and Fatigue as Revealed in the Electrical Brain Activity*, Germany, 1999, pp. 146-171.

[44] Demiralp T., *et al.*, "Time-frequency analysis of single-sweep event-related potentials by means of fast wavelet transform," *Brain and Language*, 1999, Vol. 66, 1:129-145.

[45] Demiralp T., *et al.*, "Wavelet Analysis of P3a and P3b," *Brain Topography*, 2001, Vol. 13, 4:251-267

[46] Basar E., *et al.*, "Event-related oscillations are 'real brain responses'--wavelet analysis and new strategies," *International Journal of Psychophysiology*, 2001, 39:91-127.

[47] Demiralp T., *et al.*, "Wavelet analysis of oddball P300," *International Journal of Psychophysiology*, 2001, 39:221-227.

[48] Aviyente S., *et al.*, "Characterization of event related potentials using information theoretic distance measures," *IEEE Transactions on Biomedical Engineering,* 2004,Vol. 51, 5:737- 743

[49] Goodin D.S., Aminoff M.J., "Electrophysiological differences between subtypes of dementia," Brain: A Journal of Neurology, 1986; 109:1103-1113.

[50] Patterson J.V., *et al.*, "Latency variability of the components of auditory event-related potentials of infrequent stimuli in aging, Alzheimer-type dementia, and depression," *Electroencephalography and Clinical Neurophysiology,* 1988; 71:450-460.

[51] Polich J., *et al.,* "P300 latency reflects the degree of cognitive decline in dementing illness," *Electroencephalography and Clinical Neurophysiology,* 1986; 63:138-144.

[52] Neshige R., *et al.,* "Auditory long latency event-related potentials in Alzheimer's disease and multi-infarct *dementia*," *Journal of Neurology, Neurosurgery, and Psychiatry*, 1988; 51:1120-1125.

[53] Polich J. *et al.*, "P300 assessment of early Alzheimer's disease," *Electroencephalography and Clinical Neurophysiology,* 1990; 77:179-189.

[54] Attias J., *et al.,* "Improved detection of auditory P3 abnormality in dementia using a variety of stimuli," *Acta Neurologica Scandinavica,* 1995; 92:96-101.

[55] Yamaguchi S., Knight R.T., "Age effects on the P300 to novel somatosensory stimuli," *Electroencephalography and Clinical Neurophysiology,* 1991; 78:297-301.

[56] Friedman D., *et al., "*Age-related changes in scalp topography to novel and target stimuli," *Psychophysiology,* 1993; 30:383-396.

[57] Friedman D, Simpson G.V., "Amplitude and scalp distribution of target and novel events: effects of temporal order in young, middle-aged and older adults," *Cognitive Brain Research,* 1994; 2:49-63.

[58] Brenner R.P., *et al., "*Diagnostic efficacy of computerized spectral versus visual EEG analysis in elderly normal, demented and depressed subjects," *Electroencephalography and Clinical Neurophysiology,* 1988; 69:110–117.

[59] Liddle D.W., "Investigation of EEG findings in presenile dementia. *Journal of Neurology, Neurosurgery, and Psychiatry,* 1958; 21:173-1766.

[60] Rae-Grant A., *et al.,* "The electroencephalogram in Alzheimer-type dementia. A sequential study correlating the electroencephalogram with psychometric and quantitative pathologic data," *Archives of Neurology,* 1987;44:50-54.

[61] Soininen H., *et al.*, "EEG findings in senile dementia and normal aging," *Acta Neurologica Scandinavica,* 1982; 65:59–70.

[62] Gordon E.B., Sim M., "The EEG in presenile dementia," *Journal of Neurology, Neurosurgery, and Psychiatry,* 1967; 30:285 –291.

[63] Letemendia F., Pampiglione G., "Clinical and electroencephalographic observations in Alzheimer's disease," *Journal of Neurology, Neurosurgery, and Psychiatry,* 1958; 21:167–172.

[64] Wiener H., Schuster D.B., "The electroencephalogram in dementia: some preliminary observations and correlations," *Electroencephalography and Clinical Neurophysiology,* 1956; 8:479-488.

[65] Erkinjuntti T., *et al., "*EEG in the differential diagnosis between Alzheimer's disease and vascular dementia," *Acta Neurologica Scandinavica,* 1988; 77:36-43.

[66] Johannesson G., *et al.,* "EEG and cognitive impairment in presenile dementia," *Acta Neurologica Scandinavica,* 1979; 59:225-240.

[67] Kaszniak A.W., *et al.,* "Cerebral atrophy, EEG slowing age, education, and cognitive functioning in suspected dementia," *Neurology,* 1979; 29:1273-1279.

[68] Merskey H., *et al.,* "Relationships between psychological measurements and cerebral organic changes in Alzheimer's disease," *The Canadian Journal of Neurological Sciences*, 1980; 7:45-49.

[69] Obrist W.D.,*et al.,* "Relation of the electroencephalogram to intellectual function in senescence," Journal of Gerontology, 1962; 17:197-206.

[70] Roberts M.A., *et al.,* "Electroencephalography and computerized tomography in vascular and non-vascular dementia in old age," *Journal of Neurology, Neurosurgery, and Psychiatry,* 1978; 41:903-906.

[71] Petrosian A., *et al.,* "Recurrent Neural Network and Wavelet Transform based Distinction Between Alzheimer's and Control EEG," *The Proceedings of the First Joint BMES/EMBS Conference Serving Humanity, Advancing Technology*, Atlanta, GA, 1999.

[72] Petrosian A., *et al.*, "Recurrent neural network-based approach for early recognition of Alzheimer's disease in EEG," *Clinical Neurophysiology,* 2001, Vol. 112, pp. 378-1387.

[73] de Trad C.H., "Signal Processing Techniques Predict Characteristic frequencies Of The Alzheimer's Disease Beta-Amyloid Protein And It Precursor," *Proceedings of the Second Joint EMBA/BMES Conference*, Houston, TX, 2002.

[74] Cho S.Y., *et al.,* "Automatic Recognition of Alzheimer's Disease with Single Channel EEG Recording," *Proceedings of the 25th Annual International Conference of the IEEE EMBS,* Cancun, Mexico, 2003.

[75] Jacques G., *et al.*, "Multiresolution wavelet analysis for early diagnosis of Alzheimer's Disease," *Proceedings of 26th International Conference of IEEE Engineering in Medical and Biology Society*, San Francisco, CA, 2004.

[76] Park E.H., *et al.*, "Alzheimer's Disease Detection and Analysis Using P3 Component of ERP in Alzheimer Type Dementia," *Proceedings of the 23rd Annual EMBS International Conference,* Istanbul, Turkey, 2001.

[77] Abasolo D., *et al.,* "Electroencephalogram Analysis with Approximate Entropy to Help in the Diagnosis of Alzheimer's Disease," *Proceedings of the 4th Annual IEEE Conference on Information Technology Applications in Biomedicine*, 2003.

[78] Melissant C., *et al.*, "A method for detection of Alzheimer's disease using ICA-enhanced EEG measurements," Artificial Intelligence in Medicine, 2005, 33: 209-222.

[79] Stepenosky N., Kunios J., Clark C., Polikar R., "Ensemble Techniques with Weighted Combination Rules for Early Diagnosis of Alzheimer's Disease," *Proceedings of the 2006 International Joint Conference on Neural Networks*, Vancouver, BC, Canada, July 2006.

[80] Stepenosky N., Green D., Kounios J., Clark C., Polikar R., "Majority Vote and Decision Template Based Ensemble Classifiers Trained on Event Related Potentials for Early Diagnosis of Alzheimer's Disease," *Proceedings of the 31st International Conference on Acoustics, Speech, and Signal Processing*, Toulouse, France, May 2006.

[81] Parikh D., Stepenosky N. , Topalis A., Green D., Kounios J. , Clark C., Polikar R. , "Ensemble based data fusion for early diagnosis of Alzheimer's disease," *Proceedings of the 27th International Conference of IEEE Engineering in Medicine and Biology Society*, Shanghai, China, September 2005.

[82] Stepenosky N., Topalis A., Syed H., Green D., Kounios J. , Clark C., Polikar R., "Boosting based classification of event related potentials for early diagnosis of Alzheimer's disease," *Procedures of the 27th International Conference of IEEE Engineering in Medicine and Biology Society*, Shanghai, China, September 2005.

[83] Stepenosky N., Topalis A., Frymiare J., Clark C., Polikar R., "Comparison of Pz, Fz and Cz Event Related Potentials For The Early Diagnosis of Alzheimer's Disease," ASME Summer Bioengineering Conference, Vail, CO, June 2005.

[84] McKhann G., *et al.,* "Clinical diagnosis of Alzheimer's disease: report of the NINCDS-ADRDA Work Group under the auspices of Department of Health and Human Services Task Force on Alzheimer's Disease," *Neurology*, 1984, 34:939-944.

[85] *Wavelets: Theory and Engineering Applications* class website: http://users.rowan.edu/~polikar/CLASSES/ECE554/, Last accessed: August 17, 2006.

[86] Polikar R., *The Wavelet Tutorial,* http://users.rowan.edu/-polikar/WAVELETS/WTtutorial.html, Last accessed: August 15, 2006.

[87] Chui, C. K., *Wavelet Analysis and Its Applications Volume 1: An Introduction to Wavelets.* Academic Press, San Diego, CA, 1992.

[88] Rao R.M., Bopardikar A.S., *Wavelet Transforms, Introduction to Theory and Applications*, Addison Wesley Longman, Inc., Reading, MA, 1998.

[89] Croiser A., Esteban D., Galand C., "Perfect channel splitting by use of interpolation/decimation/tree decomposition techniques", *Int. Symp. Info., Circuits, Systems*, Patras Greece, 1976.

[90] Crochiere R., Webber S., Flanagan J., "Digital coding of speech in sub-bands," *Proc. ICASSP*, 1976, Vol. 1, pp. 233-236.

[91] Burt P., Adelson E., "The Laplacian Pyramid as a Compact Image Code," *IEEE Trans. on Communications*, 1983, Vol. COM-31, No. 4.

[92] Vetterli M., le Gall D., "Perfect reconstruction filter banks: Some properties and factorizations," *IEEE Transactions on Acoustics, Speech, and Signal Processing*, 1989, Vol. 37, pp. 1057-1071.

[93] Haykin S., *Neural Networks, A Comprehensive Foundation*, 2nd Ed., Prentice-Hall, Inc., Upper Saddle, NJ, 1999.

[94] Duda R. O., Hart P.E., Stork D.G., *Pattern Classification*, 2nd Ed., John Wiley and Sons, Inc., New York, NY, 2001.

[95] Kuncheva L., *Combining Pattern Classifiers: Methods and Algorithms*, John Wiley and Sons, Inc., Hoboken, NJ, 2005

[96] *Advanced Topics In Pattern Recognition* class website, http://users.rowan.edu/~polikar/CLASSES/ECE555/, Last accessed: August 13, 2006.

[97] Giacinto G., Roli F., "Design of effective neural network ensembles for image classification processes," *Image Vision and Computing Journal*, 2001.

APPENDIX A

SENSITIVITY, SPECIFICITY, AND POSITIVE PREDICTIVE VALUE

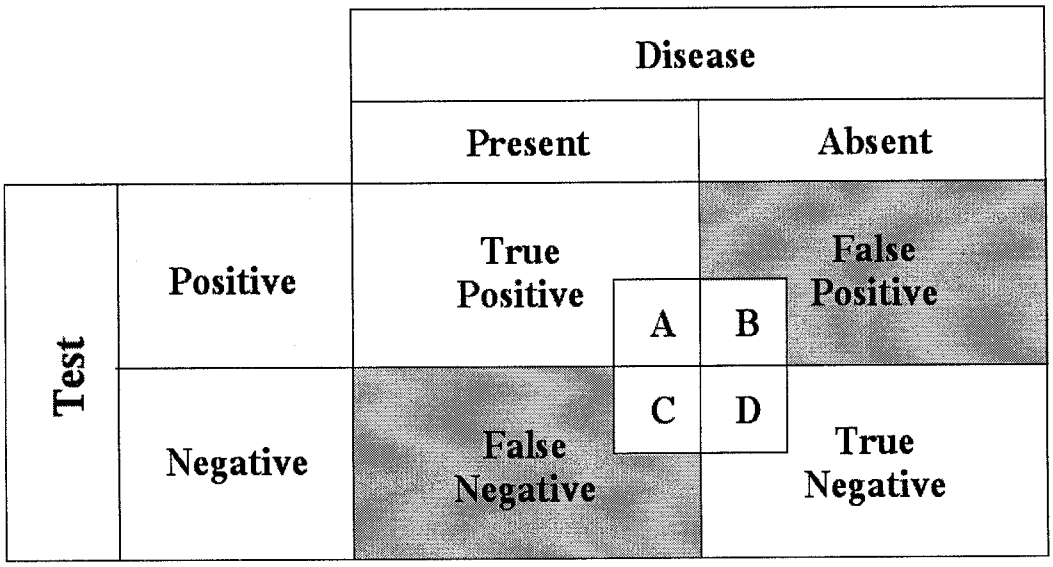

Sensitivity - the probability that a symptom is present given that the person has the disease.

$$Sensitivity = \frac{A}{A+C}$$

Specificity - the probability that a symptom is not present given that the person does not have the disease.

$$Specificity = \frac{D}{B+D}$$

Positive Predictive Value - the probability that a person has the disease given a positive test result.

$$PPV = \frac{A}{A+B}$$

APPENDIX B

ERP GRAPHS

The graphs included in this appendix are the overall average ERP for the probable AD and cognitively normal cohorts from each electrode and from both target and novel stimuli. In each figure, the top graph is from the target recordings and the bottom graph is from the novel recordings. ERPs are often inverted when displayed. This usually makes it easier to visualize the differences between the AD and normal signals.

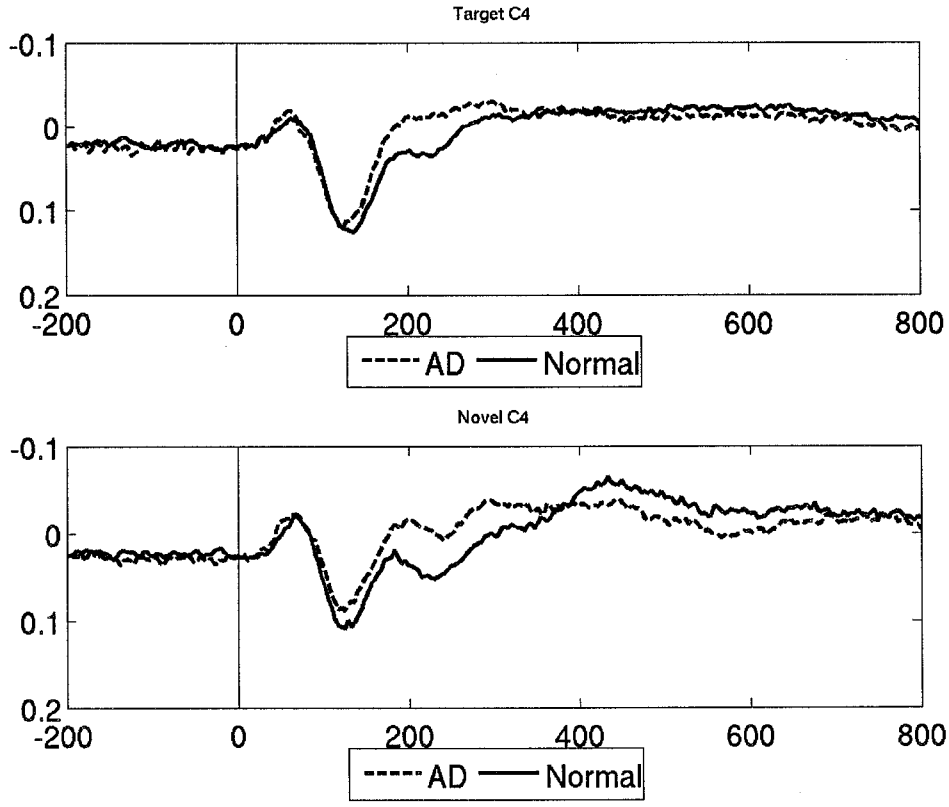

Figure B.1: Overall average ERPs from target (top) and novel (bottom) stimuli from the C4 electrode.

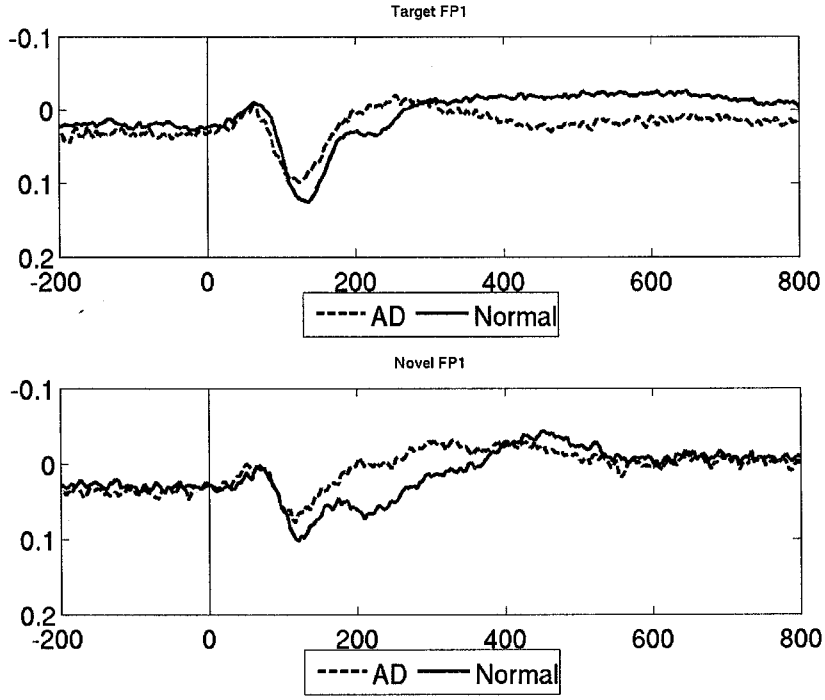

Figure B.2: Overall average ERPs from target (top) and novel (bottom) stimuli from the FP1 electrode.

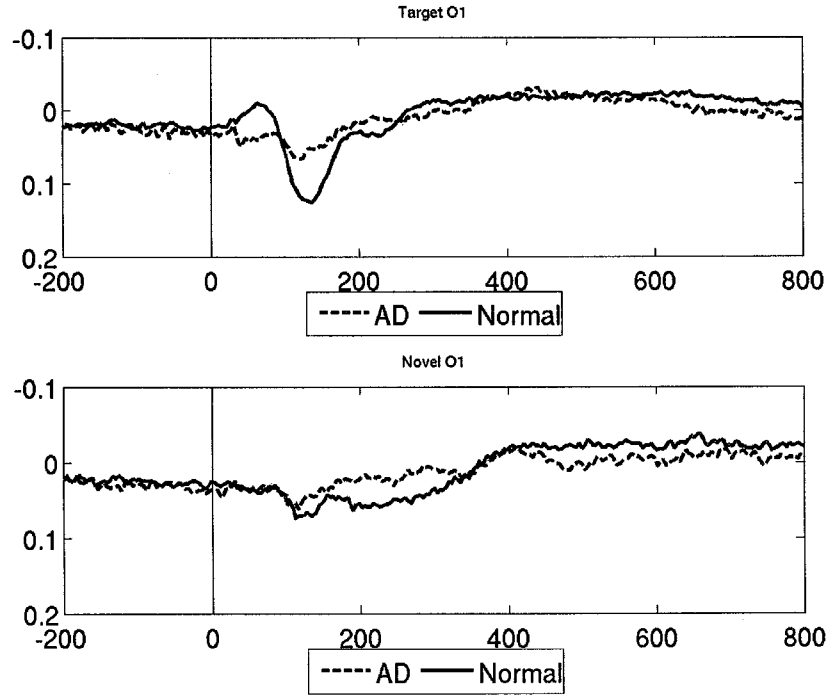

Figure B.3: Overall average ERPs from target (top) and novel (bottom) stimuli from the O1 electrode.

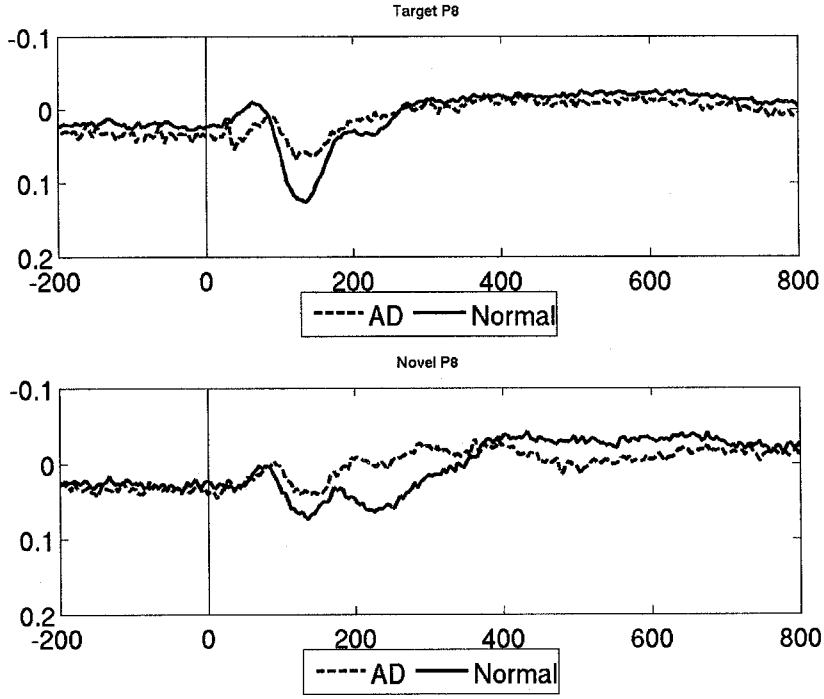

Figure B.4: Overall average ERPs from target (top) and novel (bottom) stimuli from the P8 electrode.

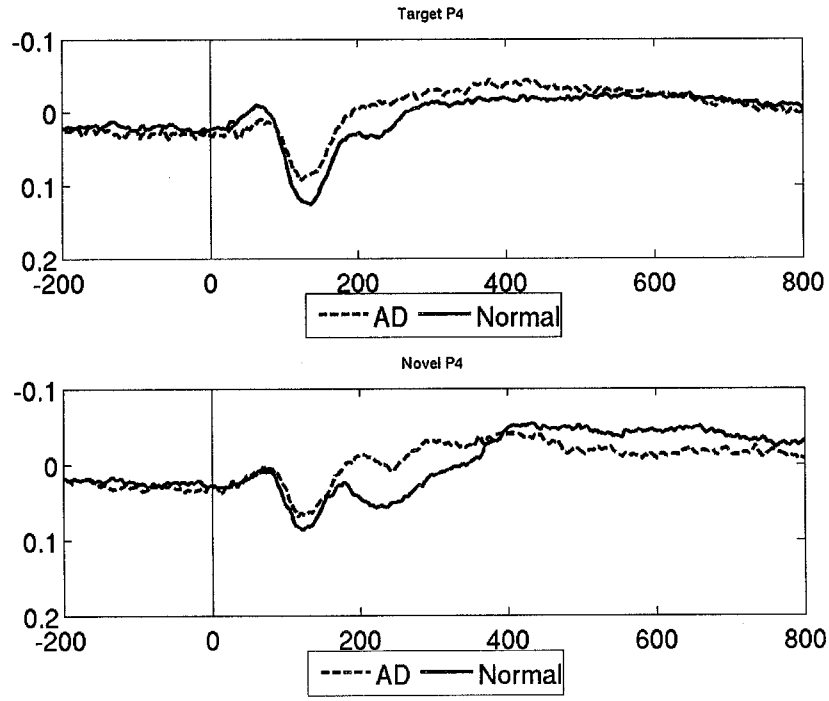

Figure B.5: Overall average ERPs from target (top) and novel (bottom) stimuli from the P4 electrode.

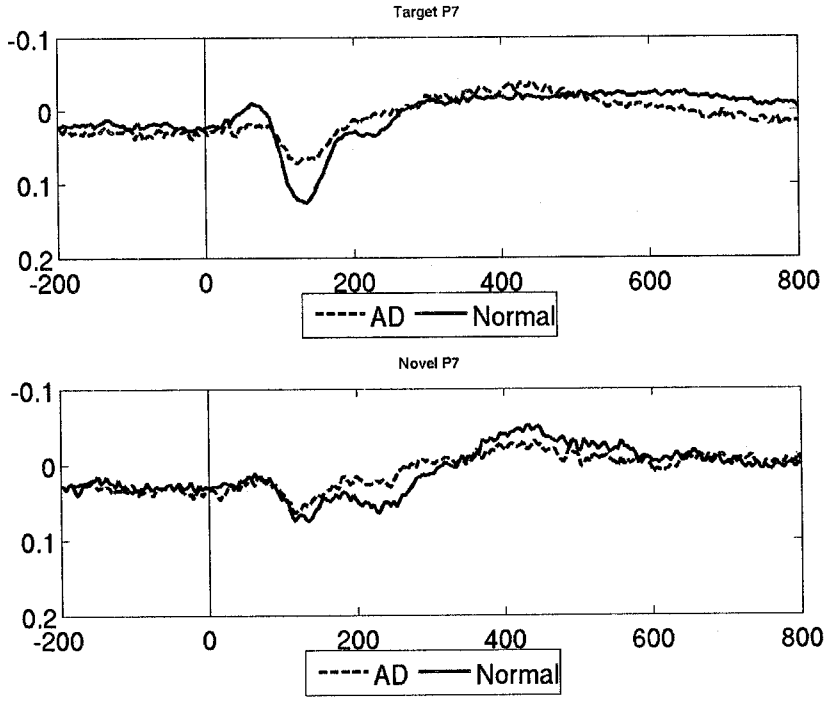

Figure B.6: Overall average ERPs from target (top) and novel (bottom) stimuli from the P7 electrode.

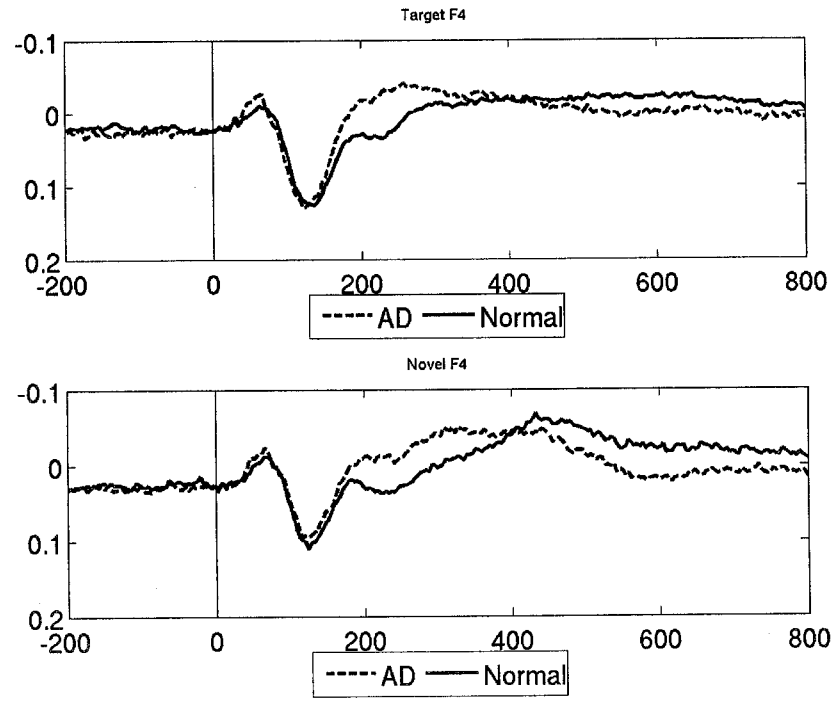

Figure B.7: Overall average ERPs from target (top) and novel (bottom) stimuli from the F4 electrode.

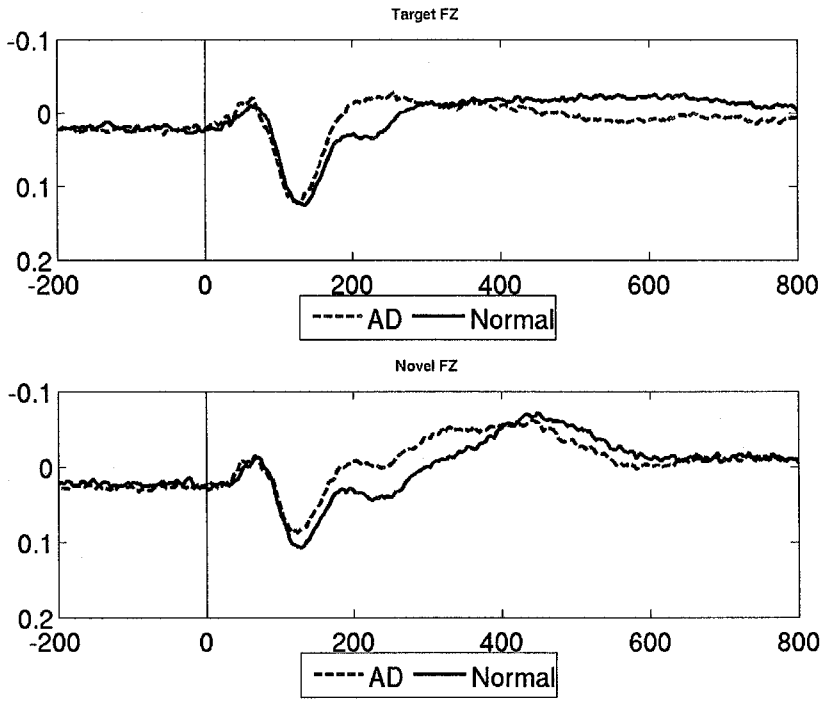

Figure B.8: Overall average ERPs from target (top) and novel (bottom) stimuli from the FZ electrode.

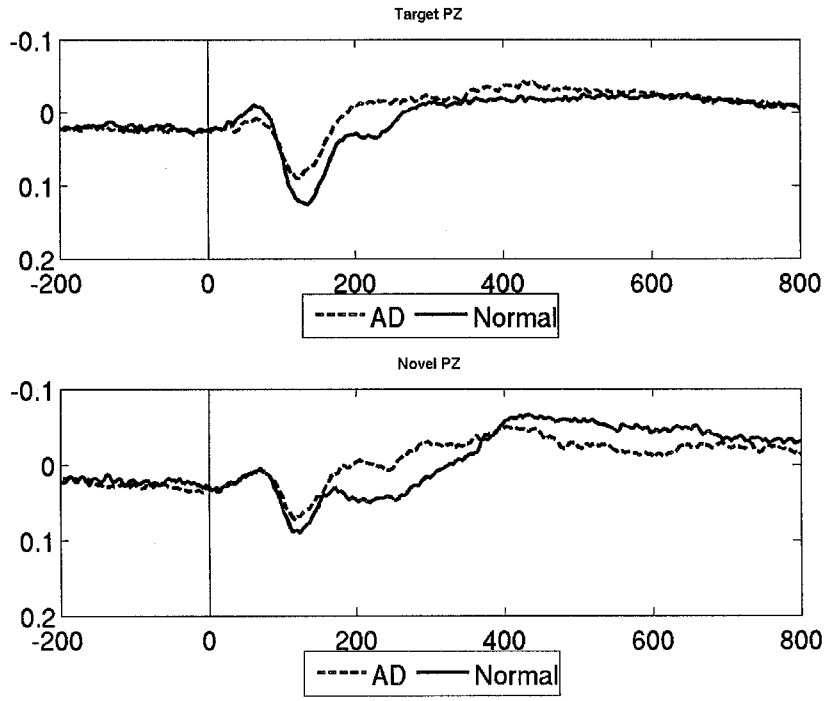

Figure B.9: Overall average ERPs from target (top) and novel (bottom) stimuli from the PZ electrode.

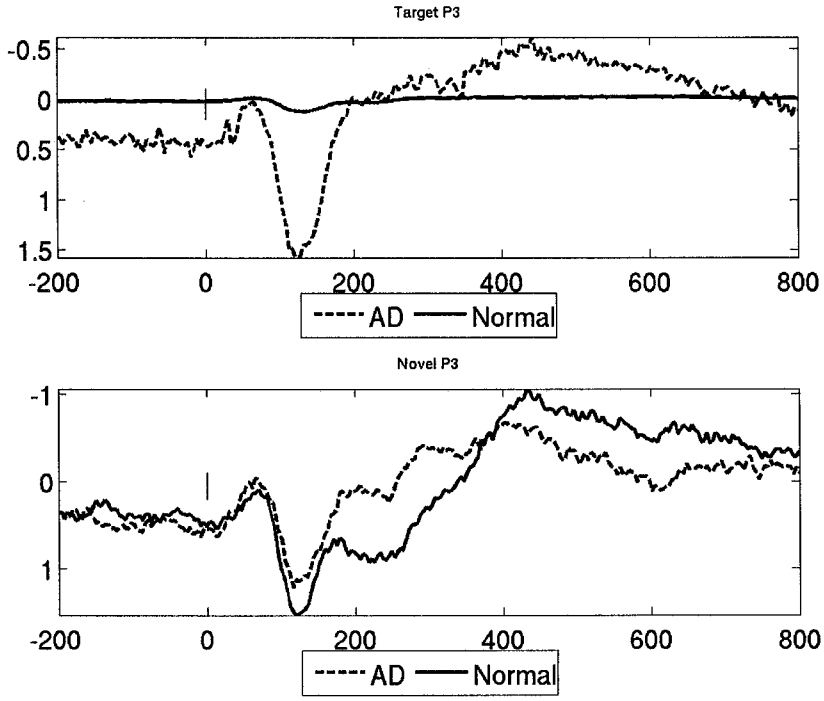

Figure B.10: Overall average ERPs from target (top) and novel (bottom) stimuli from the P3 electrode.

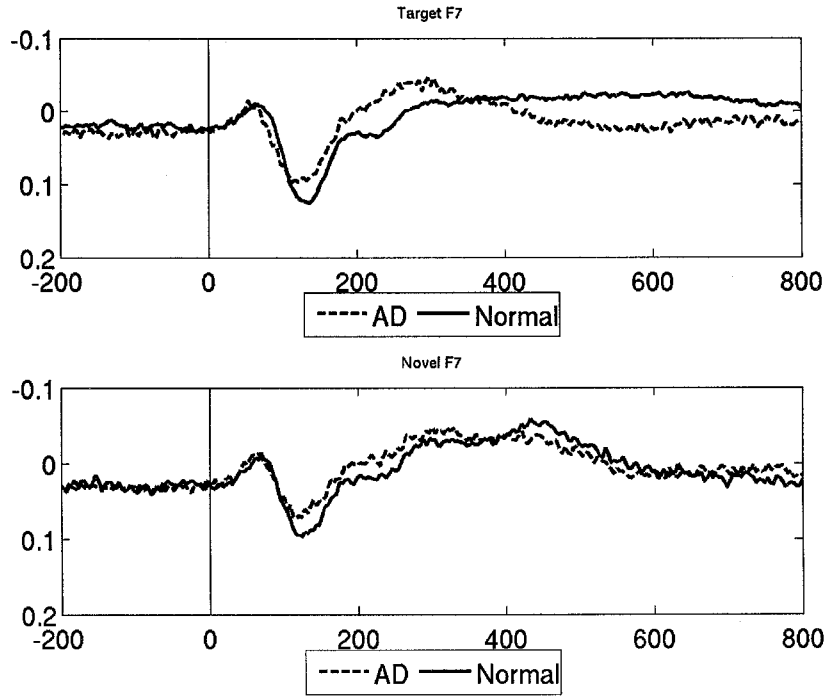

Figure B.11: Overall average ERPs from target (top) and novel (bottom) stimuli from the F7 electrode.

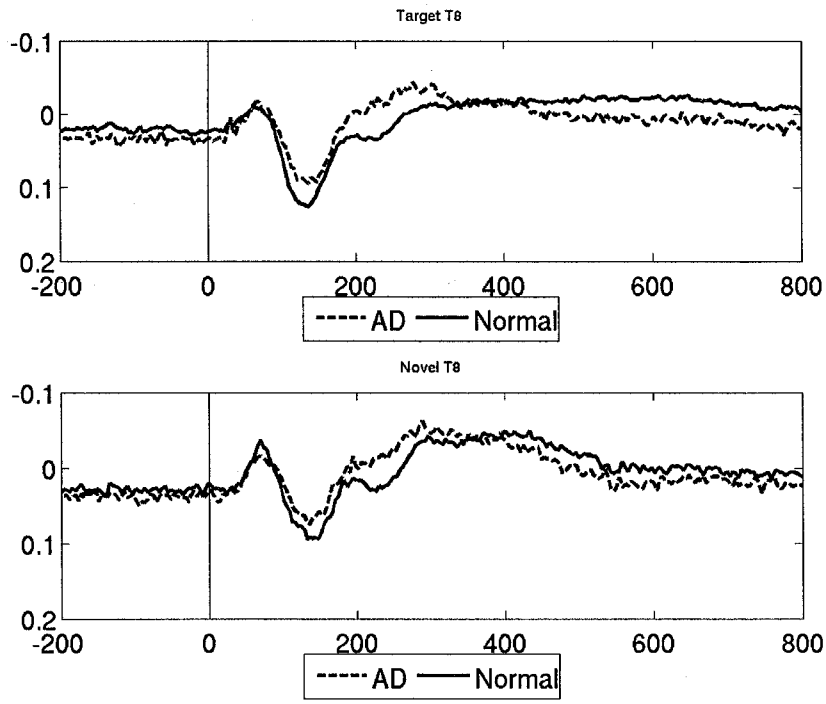

Figure B.12: Overall average ERPs from target (top) and novel (bottom) stimuli from the T8 electrode.

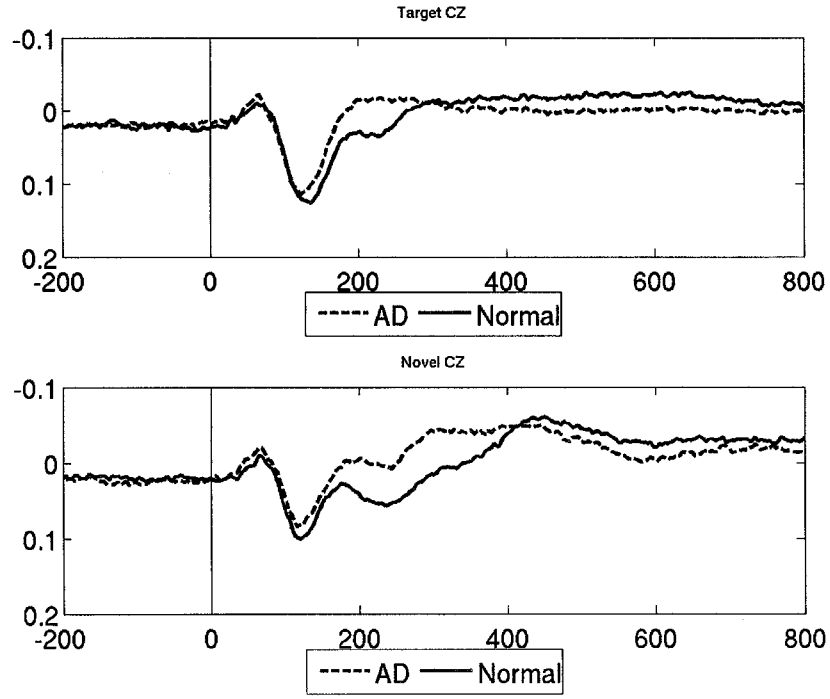

Figure B.13: Overall average ERPs from target (top) and novel (bottom) stimuli from the CZ electrode.

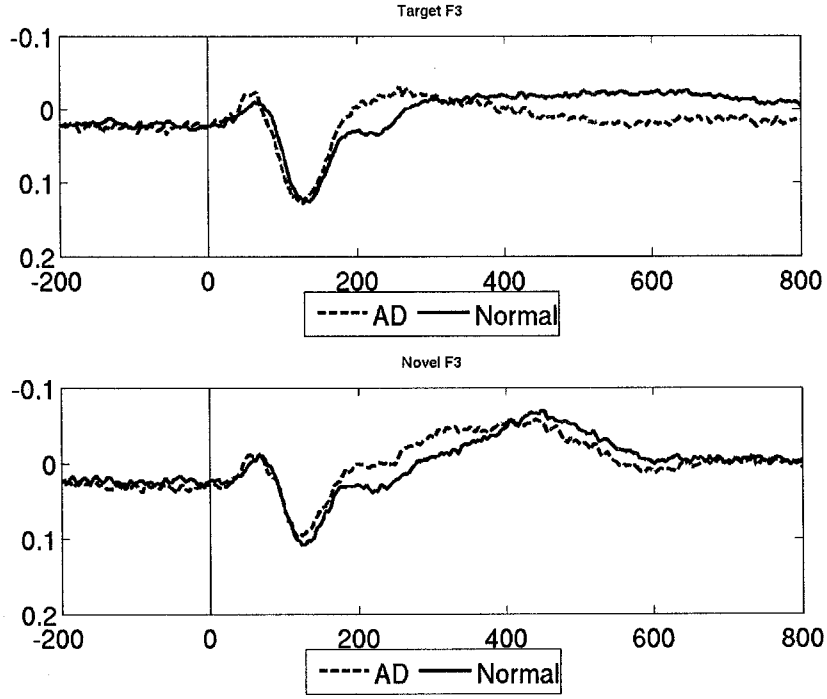

Figure B.14: Overall average ERPs from target (top) and novel (bottom) stimuli from the F3 electrode.

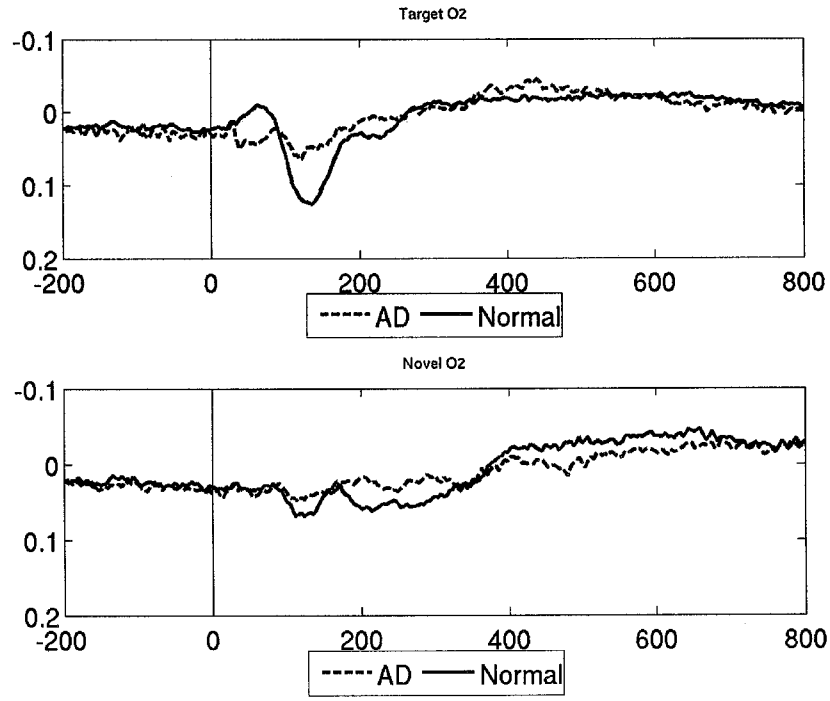

Figure B.15: Overall average ERPs from target (top) and novel (bottom) stimuli from the O2 electrode.

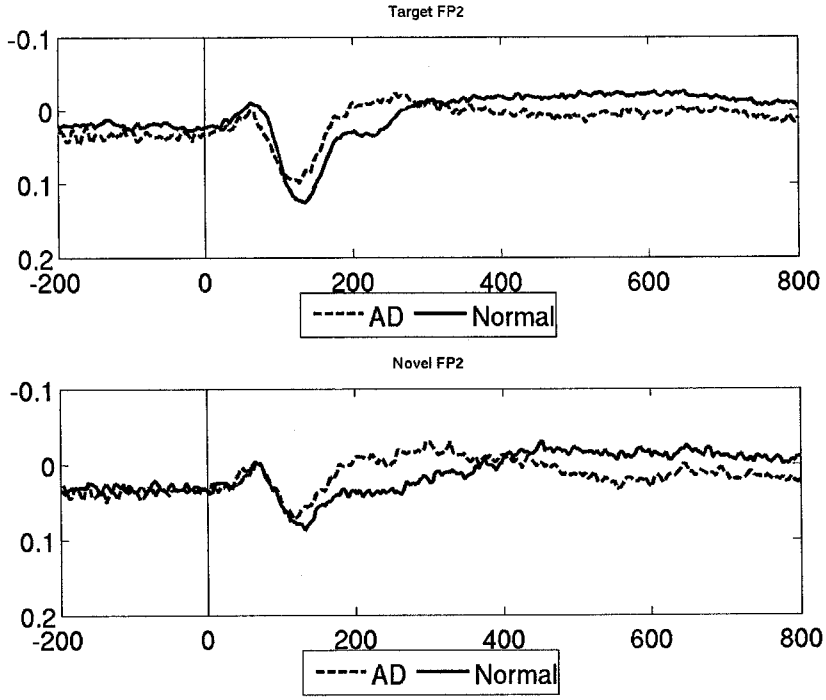

Figure B.16: Overall average ERPs from target (top) and novel (bottom) stimuli from the FP2 electrode.

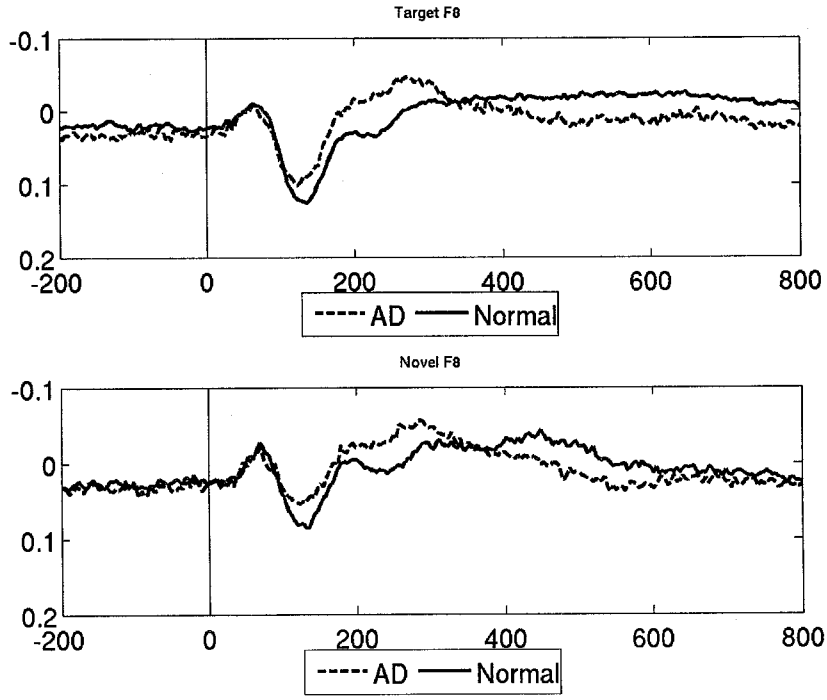

Figure B.17: Overall average ERPs from target (top) and novel (bottom) stimuli from the F8 electrode.

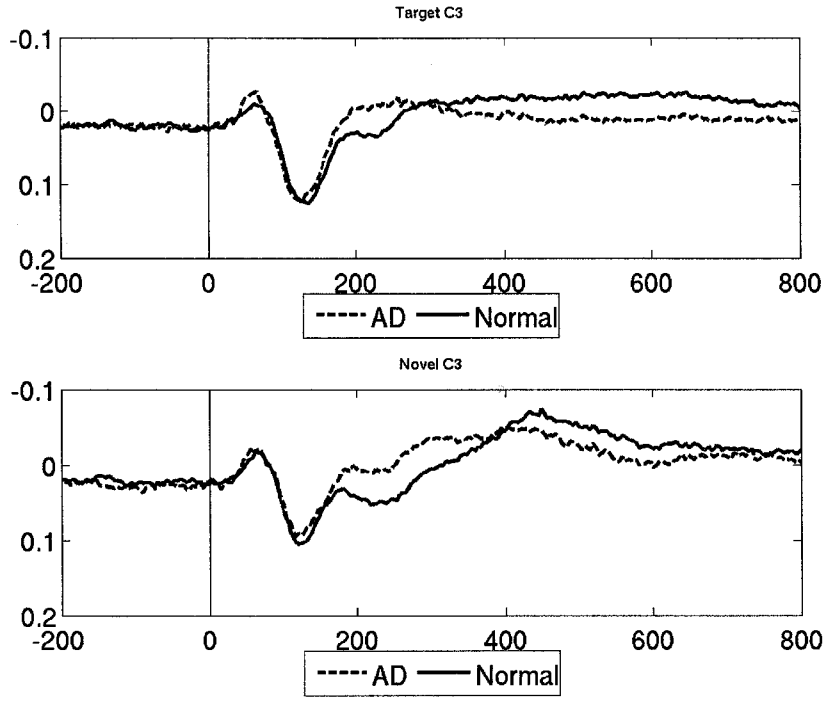

Figure B.18: Overall average ERPs from target (top) and novel (bottom) stimuli from the C3 electrode.

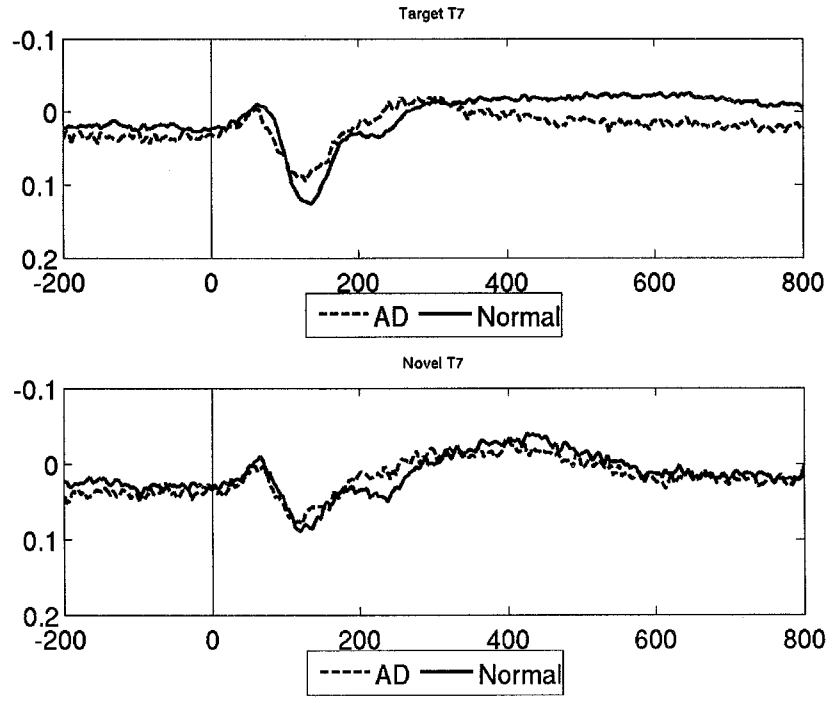

Figure B.19: Overall average ERPs from target (top) and novel (bottom) stimuli from the T7 electrode.

APPENDIX C

EXTENDED RESULTS

The tables of results included in this appendix are the average of five leave-one-out trials and the 95% confidence intervals from the classifier fusion experiments. The include all combinations of the classifiers in the various experiments. Averages over 70% are **bold**.

Table C.1: Averages of 1 classifier each from the target/parietal recordings for 71 patients (refer to Table 6.8).

Single Classifiers	
1.) P4 2-4Hz	61.41 ± 3.83%
2.) PZ 2-4Hz	62.25 ± 2.88%
3.) P3 2-4Hz	61.41 ± 4.56%
4.) P4 1-2Hz	60.28 ± 4.53%
5.) PZ 1-2Hz	60.28 ± 3.36%
6.) P7 1-2Hz	62.25 ± 4.53%

Combinations	
1.) 1 2 3 4 5 6 MV	65.35 ± 3.18%
PROD	64.22 ± 5.33%
SUM	65.35 ± 4.21%
2.) 1 2 3 4 5 MV	63.38 ± 6.06%
PROD	65.07 ± 2.28%
SUM	65.63 ± 4.56%
3.) 1 2 3 4 6 MV	64.51 ± 3.79%
PROD	64.79 ± 4.79%
SUM	65.35 ± 2.00%
4.) 1 3 4 5 6 MV	64.22 ± 4.73%
PROD	64.51 ± 3.99%
SUM	66.76 ± 5.04%
5.) 2 3 4 5 6 MV	63.66 ± 4.69%
PROD	61.97 ± 2.77%
SUM	66.48 ± 3.13%
6.) 1 2 4 5 6 MV	65.92 ± 3.36%
PROD	66.48 ± 2.59%
SUM	68.17 ± 3.62%
7.) 1 2 3 5 6 MV	63.94 ± 3.41%
PROD	64.79 ± 5.93%
SUM	65.92 ± 3.13%
8.) 1 2 3 4 MV	61.41 ± 5.04%
PROD	65.07 ± 4.53%
SUM	63.66 ± 3.37%
9.) 1 2 3 5 MV	62.82 ± 4.22%
PROD	64.51 ± 5.30%
SUM	63.66 ± 4.86%
10.) 1 2 3 6 MV	63.94 ± 2.93%
PROD	64.79 ± 3.27%
SUM	64.23 ± 5.04%
11.) 1 2 4 5 MV	64.79 ± 4.46%
PROD	67.04 ± 1.99%
SUM	68.17 ± 2.92%
12.) 1 2 4 6 MV	66.48 ± 3.79%
PROD	66.20 ± 4.46%
SUM	69.01 ± 2.47%

Combinations	
13.) 1 2 5 6 MV	64.51 ± 2.28%
PROD	66.76 ± 3.62%
SUM	65.92 ± 3.79%
14.) 1 3 4 5 MV	63.10 ± 5.45%
PROD	62.82 ± 2.00%
SUM	64.22 ± 4.72%
15.) 1 3 4 6 MV	65.63 ± 4.39%
PROD	64.23 ± 6.38%
SUM	67.89 ± 6.35%
16.) 1 3 5 6 MV	66.76 ± 2.65%
PROD	65.92 ± 4.17%
SUM	66.48 ± 3.13%
17.) 1 4 5 6 MV	63.38 ± 2.48%
PROD	66.48 ± 1.46%
SUM	65.35 ± 1.57%
18.) 2 3 4 5 MV	61.41 ± 6.61%
PROD	61.13 ± 5.75%
SUM	63.10 ± 5.45%
19.) 2 3 4 6 MV	64.51 ± 5.45%
PROD	63.10 ± 4.85%
SUM	65.92 ± 6.47%
20.) 2 4 5 6 MV	64.79 ± 3.91%
PROD	65.64 ± 2.00%
SUM	66.20 ± 1.75%
21.) 3 4 5 6 MV	63.66 ± 1.46%
PROD	62.81 ± 5.61%
SUM	64.51 ± 2.28%
22.) 2 3 5 6 MV	65.35 ± 4.88%
PROD	63.94 ± 3.63%
SUM	63.94 ± 2.93%
23.) 1 2 3 MV	61.41 ± 3.18%
PROD	64.79 ± 5.39%
SUM	61.97 ± 2.77%
24.) 1 2 4 MV	64.51 ± 1.46%
PROD	65.35 ± 2.92%
SUM	66.48 ± 2.59%
25.) 1 2 5 MV	63.38 ± 3.50%
PROD	65.64 ± 2.00%
SUM	64.51 ± 3.36%
26.) 1 2 6 MV	65.63 ± 4.72%
PROD	65.63 ± 6.13%
SUM	65.35 ± 4.39%
27.) 1 3 4 MV	63.10 ± 1.46%
PROD	60.84 ± 6.82%
SUM	62.82 ± 2.65%

Combinations	
28.) 1 3 5 MV	62.25 ± 3.36%
PROD	64.51 ± 5.85%
SUM	62.82 ± 3.84%
29.) 1 3 6 MV	66.20 ± 2.47%
PROD	65.07 ± 3.99%
SUM	66.48 ± 1.46%
30.) 1 4 5 MV	65.07 ± 1.92%
PROD	66.20 ± 2.76%
SUM	67.05 ± 0.96%
31.) 1 4 6 MV	63.10 ± 3.79%
PROD	64.79 ± 2.48%
SUM	64.51 ± 2.88%
32.) 1 5 6 MV	63.94 ± 5.75%
PROD	64.22 ± 3.62%
SUM	63.38 ± 5.39%
33.) 2 3 4 MV	61.13 ± 5.33%
PROD	62.82 ± 5.33%
SUM	64.22 ± 5.47%
34.) 2 3 5 MV	60.56 ± 7.00%
PROD	62.82 ± 6.84%
SUM	61.69 ± 5.45%
35.) 2 3 6 MV	62.82 ± 5.74%
PROD	63.66 ± 3.99%
SUM	64.51 ± 3.79%
36.) 2 4 5 MV	65.63 ± 5.04%
PROD	65.92 ± 3.36%
SUM	66.76 ± 2.65%
37.) 2 4 6 MV	64.51 ± 4.85%
PROD	65.35 ± 6.14%
SUM	65.07 ± 3.37%
38.) 2 5 6 MV	64.79 ± 3.71%
PROD	65.63 ± 3.18%
SUM	64.51 ± 3.59%
39.) 3 4 5 MV	60.56 ± 4.28%
PROD	60.00 ± 6.95%
SUM	61.41 ± 7.48%
40.) 3 4 6 MV	60.28 ± 5.30%
PROD	60.56 ± 5.93%
SUM	63.94 ± 2.00%
41.) 3 5 6 MV	60.28 ± 4.53%
PROD	65.35 ± 6.26%
SUM	67.33 ± 2.59%
42.) 4 5 6 MV	64.79 ± 2.14%
PROD	62.81 ± 5.47%
SUM	64.51 ± 3.13%

Table C.2: Averages of 3 classifier each from the target/parietal recordings for 71 patients (refer to Table 6.9).

Single Classifiers	
1.) P4 2-4Hz	61.13 ± 2.92 %
2.) PZ 2-4Hz	57.46 ± 3.79 %
3.) P3 2-4Hz	58.59 ± 5.04 %
4.) P4 1-2Hz	62.82 ± 4.22 %
5.) PZ 1-2Hz	62.25 ± 2.88 %
6.) P7 1-2Hz	63.10 ± 4.36 %
11.) P4 2-4Hz	63.94 ± 6.73 %
12.) PZ 2-4Hz	60.28 ± 2.87 %
13.) P3 2-4Hz	63.38 ± 2.77 %
14.) P4 1-2Hz	60.84 ± 4.18 %
15.) PZ 1-2Hz	63.10 ± 7.25 %
16.) P7 1-2Hz	60.84 ± 3.79 %
21.) P4 2-4Hz	61.97 ± 5.39 %
22.) PZ 2-4Hz	59.44 ± 4.53 %
23.) P3 2-4Hz	58.59 ± 5.88 %
24.) P4 1-2Hz	60.85 ± 4.85 %
25.) PZ 1-2Hz	68.17 ± 3.62 %
26.) P7 1-2Hz	63.66 ± 2.88 %

Combinations	
1.) 1 2 3 4 5 6 MV	66.76 ± 4.21 %
PROD	67.33 ± 1.91 %
SUM	68.45 ± 3.17 %
2.) 1 2 3 4 5 MV	66.48 ± 3.99 %
PROD	66.76 ± 3.17 %
SUM	67.61 ± 1.74 %
3.) 1 2 3 4 6 MV	69.58 ± 3.62 %
PROD	67.89 ± 1.46 %
SUM	69.01 ± 1.74 %
4.) 1 3 4 5 6 MV	67.32 ± 2.87 %
PROD	65.64 ± 2.65 %
SUM	68.45 ± 1.99 %
5.) 2 3 4 5 6 MV	66.20 ± 1.75 %
PROD	66.48 ± 2.59 %
SUM	66.76 ± 2.65 %
6.) 1 2 4 5 6 MV	68.17 ± 3.17 %
PROD	69.01 ± 2.14 %
SUM	69.01 ± 2.76 %
7.) 1 2 3 5 6 MV	65.63 ± 3.63 %
PROD	69.30 ± 2.87 %
SUM	68.45 ± 3.83 %
8.) 1 2 3 4 MV	67.32 ± 2.28 %
PROD	64.79 ± 2.77 %
SUM	64.79 ± 3.50 %
9.) 1 2 3 5 MV	66.48 ± 2.28 %
PROD	65.64 ± 1.57 %
SUM	64.79 ± 2.77 %
10.) 1 2 3 6 MV	68.45 ± 3.62 %
PROD	66.76 ± 1.99 %
SUM	69.01 ± 2.47 %

Combinations	
11.) 1 2 4 5 MV	66.20 ± 2.47 %
PROD	68.45 ± 1.56 %
SUM	68.17 ± 2.92 %
12.) 1 2 4 6 MV	67.89 ± 1.46 %
PROD	69.30 ± 4.17 %
SUM	69.29 ± 1.46 %
13.) 1 2 5 6 MV	65.64 ± 2.65 %
PROD	69.01 ± 1.23 %
SUM	68.73 ± 1.91 %
14.) 1 3 4 5 MV	66.76 ± 4.56 %
PROD	65.07 ± 1.92 %
SUM	65.64 ± 3.41 %
15.) 1 3 4 6 MV	69.02 ± 5.67 %
PROD	65.63 ± 3.18 %
SUM	68.45 ± 5.04 %
16.) 1 3 5 6 MV	69.30 ± 4.52 %
PROD	69.01 ± 2.76 %
SUM	69.01 ± 4.10 %
17.) 1 4 5 6 MV	67.61 ± 3.03 %
PROD	69.01 ± 2.14 %
SUM	69.29 ± 1.46 %
18.) 2 3 4 5 MV	66.20 ± 2.14 %
PROD	64.23 ± 3.63 %
SUM	65.35 ± 2.00 %
19.) 2 3 4 6 MV	67.61 ± 4.79 %
PROD	65.92 ± 2.59 %
SUM	67.33 ± 3.36 %
20.) 2 4 5 6 MV	68.17 ± 2.92 %
PROD	68.17 ± 0.95 %
SUM	69.58 ± 3.62 %
21.) 3 4 5 6 MV	68.45 ± 3.83 %
PROD	65.64 ± 2.65 %
SUM	67.61 ± 2.14 %
22.) 2 3 5 6 MV	66.48 ± 4.53 %
PROD	67.33 ± 4.35 %
SUM	66.20 ± 3.27 %
23.) 1 2 3 MV	65.35 ± 3.18 %
PROD	66.48 ± 3.13 %
SUM	66.20 ± 2.14 %
24.) 1 2 4 MV	63.10 ± 3.37 %
PROD	65.92 ± 2.87 %
SUM	64.22 ± 4.21 %
25.) 1 2 5 MV	65.07 ± 3.99 %
PROD	68.45 ± 3.62 %
SUM	66.48 ± 3.79 %
26.) 1 2 6 MV	65.92 ± 5.16 %
PROD	66.76 ± 3.41 %
SUM	68.45 ± 2.92 %

Combinations	
27.) 1 3 4 MV	66.20 ± 2.76 %
PROD	64.51 ± 4.36 %
SUM	66.20 ± 2.14 %
28.) 1 3 5 MV	67.04 ± 4.72 %
PROD	66.48 ± 2.28 %
SUM	67.89 ± 2.87 %
29.) 1 3 6 MV	68.17 ± 1.56 %
PROD	66.20 ± 1.75 %
SUM	69.58 ± 2.34 %
30.) 1 4 5 MV	68.17 ± 3.41 %
PROD	68.45 ± 1.56 %
SUM	68.17 ± 4.02 %
31.) 1 4 6 MV	69.02 ± 5.10 %
PROD	69.86 ± 3.41 %
SUM	68.73 ± 2.28 %
32.) 1 5 6 MV	68.45 ± 5.88 %
PROD	**71.27 ± 0.96 %**
SUM	69.30 ± 2.28 %
33.) 2 3 4 MV	64.79 ± 3.91 %
PROD	64.22 ± 3.41 %
SUM	66.20 ± 4.79 %
34.) 2 3 5 MV	66.48 ± 4.35 %
PROD	64.51 ± 2.88 %
SUM	65.63 ± 2.92 %
35.) 2 3 6 MV	65.92 ± 4.53 %
PROD	66.76 ± 3.83 %
SUM	65.63 ± 3.41 %
36.) 2 4 5 MV	65.63 ± 3.18 %
PROD	64.51 ± 3.13 %
SUM	64.51 ± 3.99 %
37.) 2 4 6 MV	65.35 ± 6.25 %
PROD	69.01 ± 2.14 %
SUM	69.86 ± 3.63 %
38.) 2 5 6 MV	67.89 ± 3.13 %
PROD	**70.42 ± 1.75 %**
SUM	68.45 ± 3.62 %
39.) 3 4 5 MV	63.38 ± 4.79 %
PROD	63.38 ± 3.27 %
SUM	63.38 ± 3.27 %
40.) 3 4 6 MV	65.63 ± 4.21 %
PROD	65.92 ± 4.18 %
SUM	66.48 ± 3.79 %
41.) 3 5 6 MV	67.61 ± 5.67 %
PROD	66.48 ± 2.59 %
SUM	68.17 ± 3.83 %
42.) 4 5 6 MV	68.73 ± 3.99 %
PROD	66.20 ± 3.27 %
SUM	67.61 ± 1.74 %

Table C.3: Averages of 1 classifier each from the target/parietal recordings for 66 patients (refer to Table 6.10).

Single Classifiers	
1.) P4 2-4Hz	65.63 ± 4.37 %
2.) PZ 2-4Hz	**72.68 ± 1.99 %**
3.) P3 2-4Hz	65.63 ± 8.14 %
4.) P4 1-2Hz	61.69 ± 4.84 %
5.) PZ 1-2Hz	62.82 ± 4.87 %
6.) P7 1-2Hz	60.00 ± 0.96 %

Combinations	
1.) 1 2 3 4 5 6 MV	**72.68 ± 3.17 %**
PROD	**70.99 ± 2.91 %**
SUM	**73.52 ± 3.35 %**
2.) 1 2 3 4 5 MV	**72.39 ± 1.99 %**
PROD	**71.83 ± 1.74 %**
SUM	**72.68 ± 2.65 %**
3.) 1 2 3 4 6 MV	**73.52 ± 2.27 %**
PROD	**72.11 ± 3.78 %**
SUM	**72.68 ± 2.92 %**
4.) 1 3 4 5 6 MV	**72.11 ± 3.12 %**
PROD	69.58 ± 1.98 %
SUM	**72.68 ± 1.56 %**
5.) 2 3 4 5 6 MV	**71.27 ± 1.99 %**
PROD	69.58 ± 4.37 %
SUM	**70.14 ± 2.27 %**
6.) 1 2 4 5 6 MV	**72.96 ± 2.59 %**
PROD	**72.11 ± 1.46 %**
SUM	**73.24 ± 2.76 %**
7.) 1 2 3 5 6 MV	**74.08 ± 3.81 %**
PROD	**72.68 ± 3.17 %**
SUM	**72.40 ± 4.54 %**
8.) 1 2 3 4 MV	**72.68 ± 3.17 %**
PROD	**72.96 ± 2.87 %**
SUM	**73.52 ± 2.27 %**
9.) 1 2 3 5 MV	**74.93 ± 5.14 %**
PROD	**72.96 ± 4.16 %**
SUM	**72.96 ± 5.56 %**
10.) 1 2 3 6 MV	**74.08 ± 4.01 %**
PROD	**72.67 ± 4.01 %**
SUM	**73.24 ± 4.09 %**
11.) 1 2 4 5 MV	**72.68 ± 2.92 %**
PROD	**72.39 ± 3.82 %**
SUM	**73.52 ± 4.34 %**
12.) 1 2 4 6 MV	**70.99 ± 4.01 %**
PROD	**70.99 ± 2.64 %**
SUM	**72.11 ± 1.46 %**

Combinations	
13.) 1 2 5 6 MV	69.58 ± 6.59 %
PROD	**72.67 ± 4.54 %**
SUM	**70.70 ± 3.97 %**
14.) 1 3 4 5 MV	**70.70 ± 2.86 %**
PROD	69.86 ± 3.40 %
SUM	**72.68 ± 4.02 %**
15.) 1 3 4 6 MV	**70.70 ± 4.16 %**
PROD	67.89 ± 3.97 %
SUM	**70.70 ± 4.51 %**
16.) 1 3 5 6 MV	69.86 ± 6.59 %
PROD	69.30 ± 4.67 %
SUM	**71.55 ± 4.34 %**
17.) 1 4 5 6 MV	67.89 ± 3.97 %
PROD	**70.14 ± 2.86 %**
SUM	69.86 ± 1.56 %
18.) 2 3 4 5 MV	**71.27 ± 3.17 %**
PROD	69.86 ± 3.40 %
SUM	**70.42 ± 3.26 %**
19.) 2 3 4 6 MV	**70.99 ± 5.17 %**
PROD	**70.14 ± 4.83 %**
SUM	**70.70 ± 3.57 %**
20.) 2 4 5 6 MV	67.89 ± 3.77 %
PROD	**70.14 ± 4.67 %**
SUM	69.58 ± 2.64 %
21.) 3 4 5 6 MV	67.04 ± 5.17 %
PROD	68.45 ± 4.01 %
SUM	67.32 ± 2.86 %
22.) 2 3 5 6 MV	69.86 ± 6.81 %
PROD	**71.55 ± 6.91 %**
SUM	69.86 ± 4.54 %
23.) 1 2 3 MV	**73.52 ± 4.51 %**
PROD	**73.24 ± 3.26 %**
SUM	**72.96 ± 2.87 %**
24.) 1 2 4 MV	**72.39 ± 2.34 %**
PROD	**71.27 ± 3.61 %**
SUM	**72.39 ± 2.92 %**
25.) 1 2 5 MV	69.02 ± 5.91 %
PROD	**72.68 ± 4.02 %**
SUM	69.02 ± 4.93 %
26.) 1 2 6 MV	68.73 ± 4.51 %
PROD	**71.55 ± 4.83 %**
SUM	69.86 ± 3.16 %
27.) 1 3 4 MV	68.17 ± 6.36 %
PROD	67.89 ± 3.11 %
SUM	69.58 ± 3.82 %

Combinations	
28.) 1 3 5 MV	68.73 ± 4.83 %
PROD	**71.27 ± 5.98 %**
SUM	**70.42 ± 3.48 %**
29.) 1 3 6 MV	68.45 ± 5.73 %
PROD	**70.14 ± 4.83 %**
SUM	**70.71 ± 5.56 %**
30.) 1 4 5 MV	68.45 ± 3.61 %
PROD	67.89 ± 0.77 %
SUM	68.45 ± 1.98 %
31.) 1 4 6 MV	67.89 ± 2.27 %
PROD	67.89 ± 6.09 %
SUM	67.89 ± 6.68 %
32.) 1 5 6 MV	69.58 ± 2.64 %
PROD	69.30 ± 4.67 %
SUM	68.73 ± 2.27 %
33.) 2 3 4 MV	**72.11 ± 3.35 %**
PROD	69.86 ± 3.61 %
SUM	**71.27 ± 1.99 %**
34.) 2 3 5 MV	**71.27 ± 4.19 %**
PROD	**71.55 ± 4.99 %**
SUM	69.86 ± 5.02 %
35.) 2 3 6 MV	69.86 ± 8.23 %
PROD	**72.11 ± 4.99 %**
SUM	**71.55 ± 4.51 %**
36.) 2 4 5 MV	65.64 ± 1.56 %
PROD	69.02 ± 3.48 %
SUM	67.33 ± 1.91 %
37.) 2 4 6 MV	**70.14 ± 3.12 %**
PROD	69.01 ± 1.23 %
SUM	**70.70 ± 3.78 %**
38.) 2 5 6 MV	**72.68 ± 2.65 %**
PROD	**71.83 ± 3.70 %**
SUM	**72.96 ± 3.97 %**
39.) 3 4 5 MV	65.92 ± 3.35 %
PROD	66.20 ± 4.09 %
SUM	66.20 ± 3.69 %
40.) 3 4 6 MV	66.20 ± 7.49 %
PROD	62.82 ± 4.37 %
SUM	66.48 ± 4.16 %
41.) 3 5 6 MV	65.35 ± 6.71 %
PROD	67.89 ± 7.23 %
SUM	67.32 ± 5.96 %
42.) 4 5 6 MV	65.64 ± 1.99 %
PROD	63.66 ± 2.27 %
SUM	64.51 ± 1.46 %

Table C.4: Averages of 3 classifier each from the target/parietal recordings for 66 patients (refer to Table 6.11).

Single Classifiers	
1.) P4 2-4Hz	66.67 ± 5.79 %
2.) PZ 2-4Hz	**70.00 ± 3.62 %**
3.) P3 2-4Hz	61.21 ± 1.68 %
4.) P4 1-2Hz	68.79 ± 5.89 %
5.) PZ 1-2Hz	66.06 ± 4.33 %
6.) P7 1-2Hz	60.30 ± 8.76 %
11.) P4 2-4Hz	64.55 ± 6.99 %
12.) PZ 2-4Hz	67.58 ± 2.85 %
13.) P3 2-4Hz	63.03 ± 8.78 %
14.) P4 1-2Hz	66.97 ± 6.15 %
15.) PZ 1-2Hz	67.27 ± 3.90 %
16.) P7 1-2Hz	62.43 ± 4.29 %
21.) P4 2-4Hz	68.49 ± 8.96 %
22.) PZ 2-4Hz	66.36 ± 4.87 %
23.) P3 2-4Hz	63.64 ± 5.64 %
24.) P4 1-2Hz	67.27 ± 1.68 %
25.) PZ 1-2Hz	67.58 ± 3.42 %
26.) P7 1-2Hz	64.24 ± 3.66 %

Combinations	
1.) 1 2 3 4 5 6 MV	**73.64 ± 3.90 %**
PROD	**75.46 ± 3.37 %**
SUM	**74.85 ± 2.85 %**
2.) 1 2 3 4 5 MV	**73.33 ± 5.08 %**
PROD	**75.45 ± 5.86 %**
SUM	**75.15 ± 5.58 %**
3.) 1 2 3 4 6 MV	**72.73 ± 3.99 %**
PROD	**75.15 ± 2.14 %**
SUM	**75.76 ± 3.26 %**
4.) 1 3 4 5 6 MV	**73.33 ± 4.53 %**
PROD	**72.42 ± 1.57 %**
SUM	**73.64 ± 2.85 %**
5.) 2 3 4 5 6 MV	**72.73 ± 4.61 %**
PROD	**72.12 ± 2.52 %**
SUM	**74.85 ± 2.85 %**
6.) 1 2 4 5 6 MV	**74.55 ± 2.45 %**
PROD	**75.45 ± 1.57 %**
SUM	**75.46 ± 2.79 %**
7.) 1 2 3 5 6 MV	**73.64 ± 5.89 %**
PROD	**73.03 ± 1.57 %**
SUM	**75.76 ± 2.97 %**
8.) 1 2 3 4 MV	**71.21 ± 2.66 %**
PROD	**71.21 ± 2.97 %**
SUM	**72.42 ± 4.08 %**
9.) 1 2 3 5 MV	69.39 ± 3.62 %
PROD	**71.21 ± 4.61 %**
SUM	69.70 ± 2.97 %
10.) 1 2 3 6 MV	**70.00 ± 3.37 %**
PROD	**70.61 ± 1.68 %**
SUM	**71.51 ± 3.37 %**

Combinations	
11.) 1 2 4 5 MV	**74.55 ± 1.57 %**
PROD	**73.64 ± 1.03 %**
SUM	**74.85 ± 1.03 %**
12.) 1 2 4 6 MV	**72.73 ± 1.88 %**
PROD	**73.03 ± 1.57 %**
SUM	**75.15 ± 1.03 %**
13.) 1 2 5 6 MV	**74.55 ± 3.09 %**
PROD	**75.45 ± 1.57 %**
SUM	**74.55 ± 2.45 %**
14.) 1 3 4 5 MV	**70.91 ± 3.62 %**
PROD	**71.52 ± 3.62 %**
SUM	**73.94 ± 1.57 %**
15.) 1 3 4 6 MV	**71.21 ± 5.15 %**
PROD	**71.82 ± 1.68 %**
SUM	**73.03 ± 2.45 %**
16.) 1 3 5 6 MV	**70.30 ± 2.86 %**
PROD	**73.33 ± 3.42 %**
SUM	**74.24 ± 1.33 %**
17.) 1 4 5 6 MV	**73.94 ± 2.45 %**
PROD	**73.64 ± 2.15 %**
SUM	**73.64 ± 2.15 %**
18.) 2 3 4 5 MV	69.09 ± 3.15 %
PROD	**72.42 ± 3.09 %**
SUM	**72.12 ± 3.42 %**
19.) 2 3 4 6 MV	**70.30 ± 2.15 %**
PROD	**71.21 ± 1.33 %**
SUM	**72.42 ± 3.09 %**
20.) 2 4 5 6 MV	**76.36 ± 3.15 %**
PROD	**72.42 ± 3.62 %**
SUM	**76.06 ± 2.45 %**
21.) 3 4 5 6 MV	**71.51 ± 3.36 %**
PROD	**71.82 ± 2.14 %**
SUM	**73.64 ± 1.03 %**
22.) 2 3 5 6 MV	**71.21 ± 3.76 %**
PROD	**73.64 ± 2.85 %**
SUM	**73.94 ± 1.57 %**
23.) 1 2 3 MV	68.18 ± 2.30 %
PROD	69.70 ± 4.80 %
SUM	68.79 ± 2.85 %
24.) 1 2 4 MV	**73.33 ± 2.52 %**
PROD	**71.21 ± 2.30 %**
SUM	**73.94 ± 2.06 %**
25.) 1 2 5 MV	**73.03 ± 4.49 %**
PROD	**74.55 ± 2.45 %**
SUM	**74.24 ± 2.31 %**
26.) 1 2 6 MV	**74.24 ± 3.52 %**
PROD	**73.33 ± 1.68 %**
SUM	**73.94 ± 2.45 %**

Combinations	
27.) 1 3 4 MV	**70.61 ± 3.66 %**
PROD	68.79 ± 1.68 %
SUM	**71.52 ± 4.87 %**
28.) 1 3 5 MV	**70.91 ± 5.22 %**
PROD	**70.91 ± 5.22 %**
SUM	**70.30 ± 4.72 %**
29.) 1 3 6 MV	**70.00 ± 3.09 %**
PROD	**71.21 ± 2.97 %**
SUM	**70.91 ± 3.09 %**
30.) 1 4 5 MV	**74.24 ± 3.76 %**
PROD	**72.73 ± 3.99 %**
SUM	**73.03 ± 3.86 %**
31.) 1 4 6 MV	**71.82 ± 3.90 %**
PROD	**72.42 ± 3.09 %**
SUM	**72.42 ± 2.45 %**
32.) 1 5 6 MV	**73.03 ± 3.09 %**
PROD	**73.94 ± 2.45 %**
SUM	**71.52 ± 4.87 %**
33.) 2 3 4 MV	69.40 ± 2.79 %
PROD	**71.52 ± 3.62 %**
SUM	**70.30 ± 3.41 %**
34.) 2 3 5 MV	**71.21 ± 4.61 %**
PROD	**72.73 ± 4.80 %**
SUM	**70.91 ± 5.22 %**
35.) 2 3 6 MV	68.79 ± 1.68 %
PROD	**70.30 ± 2.15 %**
SUM	69.09 ± 3.90 %
36.) 2 4 5 MV	**72.73 ± 3.76 %**
PROD	**72.12 ± 2.85 %**
SUM	**72.73 ± 2.66 %**
37.) 2 4 6 MV	**73.64 ± 3.41 %**
PROD	**72.73 ± 3.26 %**
SUM	**73.94 ± 1.57 %**
38.) 2 5 6 MV	**73.33 ± 3.41 %**
PROD	**75.15 ± 2.52 %**
SUM	**74.85 ± 2.85 %**
39.) 3 4 5 MV	**70.00 ± 2.79 %**
PROD	**70.30 ± 4.33 %**
SUM	**70.30 ± 3.66 %**
40.) 3 4 6 MV	66.97 ± 3.09 %
PROD	69.70 ± 1.88 %
SUM	69.40 ± 3.37 %
41.) 3 5 6 MV	68.79 ± 4.33 %
PROD	**72.73 ± 2.66 %**
SUM	**71.82 ± 2.85 %**
42.) 4 5 6 MV	**72.73 ± 2.66 %**
PROD	**72.73 ± 2.30 %**
SUM	**73.94 ± 2.06 %**

Table C.5: Averages of 1 classifier each from the novel/parietal recordings for 71 patients (refer to Table 6.12).

Single Classifiers	
1.) P4 2-4Hz	65.63 ± 4.39 %
2.) PZ 2-4Hz	**72.68 ± 2.00 %**
3.) P3 2-4Hz	65.63 ± 8.17 %
4.) P4 1-2Hz	61.69 ± 4.85 %
5.) PZ 1-2Hz	62.82 ± 4.89 %
6.) P7 1-2Hz	60.00 ± 0.96 %

Combinations	
1.) 1 2 3 4 5 6 MV	**72.68 ± 3.18 %**
PROD	**70.99 ± 2.92 %**
SUM	**73.52 ± 3.36 %**
2.) 1 2 3 4 5 MV	**72.39 ± 2.00 %**
PROD	**71.83 ± 1.75 %**
SUM	**72.68 ± 2.65 %**
3.) 1 2 3 4 6 MV	**73.52 ± 2.28 %**
PROD	**72.11 ± 3.79 %**
SUM	**72.68 ± 2.93 %**
4.) 1 3 4 5 6 MV	**72.11 ± 3.13 %**
PROD	69.58 ± 1.99 %
SUM	**72.68 ± 1.57 %**
5.) 2 3 4 5 6 MV	**71.27 ± 2.00 %**
PROD	69.58 ± 4.39 %
SUM	**70.14 ± 2.28 %**
6.) 1 2 4 5 6 MV	**72.96 ± 2.60 %**
PROD	**72.11 ± 1.46 %**
SUM	**73.24 ± 2.77 %**
7.) 1 2 3 5 6 MV	**74.08 ± 3.83 %**
PROD	**72.68 ± 3.18 %**
SUM	**72.40 ± 4.56 %**
8.) 1 2 3 4 MV	**72.68 ± 3.18 %**
PROD	**72.96 ± 2.88 %**
SUM	**73.52 ± 2.28 %**
9.) 1 2 3 5 MV	**74.93 ± 5.16 %**
PROD	**72.96 ± 4.18 %**
SUM	**72.96 ± 5.58 %**
10.) 1 2 3 6 MV	**74.08 ± 4.03 %**
PROD	**72.67 ± 4.03 %**
SUM	**73.24 ± 4.10 %**
11.) 1 2 4 5 MV	**72.68 ± 2.93 %**
PROD	**72.39 ± 3.84 %**
SUM	**73.52 ± 4.36 %**
12.) 1 2 4 6 MV	**70.99 ± 4.03 %**
PROD	**70.99 ± 2.65 %**
SUM	**72.11 ± 1.46 %**

Combinations	
13.) 1 2 5 6 MV	69.58 ± 6.61 %
PROD	**72.67 ± 4.56 %**
SUM	**70.70 ± 3.99 %**
14.) 1 3 4 5 MV	**70.70 ± 2.87 %**
PROD	69.86 ± 3.41 %
SUM	**72.68 ± 4.03 %**
15.) 1 3 4 6 MV	**70.70 ± 4.18 %**
PROD	67.89 ± 3.99 %
SUM	**70.70 ± 4.53 %**
16.) 1 3 5 6 MV	69.86 ± 6.61 %
PROD	69.30 ± 4.69 %
SUM	**71.55 ± 4.35 %**
17.) 1 4 5 6 MV	67.89 ± 3.99 %
PROD	**70.14 ± 2.87 %**
SUM	69.86 ± 1.57 %
18.) 2 3 4 5 MV	**71.27 ± 3.18 %**
PROD	69.86 ± 3.41 %
SUM	**70.42 ± 3.27 %**
19.) 2 3 4 6 MV	**70.99 ± 5.19 %**
PROD	**70.14 ± 4.85 %**
SUM	**70.70 ± 3.58 %**
20.) 2 4 5 6 MV	67.89 ± 3.79 %
PROD	**70.14 ± 4.69 %**
SUM	69.58 ± 2.65 %
21.) 3 4 5 6 MV	67.04 ± 5.19 %
PROD	68.45 ± 4.02 %
SUM	67.32 ± 2.87 %
22.) 2 3 5 6 MV	69.86 ± 6.84 %
PROD	**71.55 ± 6.93 %**
SUM	69.86 ± 4.56 %
23.) 1 2 3 MV	**73.52 ± 4.53 %**
PROD	**73.24 ± 3.27 %**
SUM	**72.96 ± 2.88 %**
24.) 1 2 4 MV	**72.39 ± 2.35 %**
PROD	**71.27 ± 3.63 %**
SUM	**72.39 ± 2.93 %**
25.) 1 2 5 MV	69.02 ± 5.93 %
PROD	**72.68 ± 4.03 %**
SUM	69.02 ± 4.94 %
26.) 1 2 6 MV	68.73 ± 4.53 %
PROD	**71.55 ± 4.85 %**
SUM	69.86 ± 3.17 %
27.) 1 3 4 MV	68.17 ± 6.38 %
PROD	67.89 ± 3.13 %
SUM	69.58 ± 3.83 %

Combinations	
28.) 1 3 5 MV	68.73 ± 4.85 %
PROD	**71.27 ± 6.01 %**
SUM	**70.42 ± 3.50 %**
29.) 1 3 6 MV	68.45 ± 5.75 %
PROD	**70.14 ± 4.85 %**
SUM	**70.71 ± 5.58 %**
30.) 1 4 5 MV	68.45 ± 3.62 %
PROD	67.89 ± 0.78 %
SUM	68.45 ± 1.99 %
31.) 1 4 6 MV	67.89 ± 2.28 %
PROD	67.89 ± 6.11 %
SUM	67.89 ± 6.71 %
32.) 1 5 6 MV	69.58 ± 2.65 %
PROD	69.30 ± 4.69 %
SUM	68.73 ± 2.28 %
33.) 2 3 4 MV	**72.11 ± 3.36 %**
PROD	69.86 ± 3.63 %
SUM	**71.27 ± 2.00 %**
34.) 2 3 5 MV	**71.27 ± 4.21 %**
PROD	**71.55 ± 5.01 %**
SUM	69.86 ± 5.04 %
35.) 2 3 6 MV	69.86 ± 8.26 %
PROD	**72.11 ± 5.00 %**
SUM	**71.55 ± 4.52 %**
36.) 2 4 5 MV	65.64 ± 1.57 %
PROD	69.02 ± 3.49 %
SUM	67.33 ± 1.91 %
37.) 2 4 6 MV	**70.14 ± 3.13 %**
PROD	69.01 ± 1.23 %
SUM	**70.70 ± 3.79 %**
38.) 2 5 6 MV	**72.68 ± 2.65 %**
PROD	**71.83 ± 3.71 %**
SUM	**72.96 ± 3.99 %**
39.) 3 4 5 MV	65.92 ± 3.36 %
PROD	66.20 ± 4.10 %
SUM	66.20 ± 3.71 %
40.) 3 4 6 MV	66.20 ± 7.52 %
PROD	62.82 ± 4.39 %
SUM	66.48 ± 4.17 %
41.) 3 5 6 MV	65.35 ± 6.73 %
PROD	67.89 ± 7.25 %
SUM	67.32 ± 5.98 %
42.) 4 5 6 MV	65.64 ± 2.00 %
PROD	63.66 ± 2.28 %
SUM	64.51 ± 1.46 %

Table C.6: Averages of 3 classifiers each from the novel/parietal recordings for 71 patients (refer to Table 6.13).

Single Classifiers	
1.) P4 2-4Hz	65.07 ± 6.93 %
2.) PZ 2-4Hz	**70.42 ± 5.93 %**
3.) P3 2-4Hz	67.89 ± 2.28 %
4.) P4 1-2Hz	64.79 ± 6.05 %
5.) PZ 1-2Hz	61.13 ± 5.88 %
6.) P7 1-2Hz	55.49 ± 2.65 %
11.) P4 2-4Hz	67.32 ± 2.87 %
12.) PZ 2-4Hz	**73.52 ± 1.92 %**
13.) P3 2-4Hz	69.58 ± 5.47 %
14.) P4 1-2Hz	61.41 ± 4.21 %
15.) PZ 1-2Hz	59.44 ± 2.28 %
16.) P7 1-2Hz	56.34 ± 6.06 %
21.) P4 2-4Hz	63.38 ± 5.39 %
22.) PZ 2-4Hz	**72.40 ± 4.56 %**
23.) P3 2-4Hz	69.29 ± 3.36 %
24.) P4 1-2Hz	64.79 ± 3.27 %
25.) PZ 1-2Hz	62.82 ± 4.03 %
26.) P7 1-2Hz	58.59 ± 4.21 %

Combinations	
1.) 123456MV	**72.68 ± 2.93 %**
PROD	**72.96 ± 3.36 %**
SUM	**73.52 ± 0.78 %**
2.) 12345MV	**73.24 ± 1.75 %**
PROD	**73.24 ± 3.50 %**
SUM	**74.93 ± 2.28 %**
3.) 12346MV	**72.39 ± 5.04 %**
PROD	**72.67 ± 4.03 %**
SUM	**73.80 ± 3.63 %**
4.) 13456MV	**71.83 ± 3.03 %**
PROD	**70.99 ± 4.73 %**
SUM	**72.68 ± 2.93 %**
5.) 23456MV	**71.83 ± 2.14 %**
PROD	**70.99 ± 3.41 %**
SUM	**71.55 ± 2.28 %**
6.) 12456MV	**71.27 ± 2.00 %**
PROD	**72.11 ± 3.37 %**
SUM	**71.55 ± 2.28 %**
7.) 12356MV	**70.99 ± 3.63 %**
PROD	**72.96 ± 3.79 %**
SUM	**72.11 ± 3.59 %**
8.) 1234MV	**72.68 ± 3.18 %**
PROD	**72.11 ± 3.79 %**
SUM	**72.96 ± 1.92 %**
9.) 1235MV	**72.96 ± 3.13 %**
PROD	**72.68 ± 0.96 %**
SUM	**72.39 ± 3.41 %**
10.) 1236MV	**72.96 ± 4.85 %**
PROD	**73.80 ± 4.39 %**
SUM	**72.96 ± 4.18 %**

Combinations	
11.) 1245MV	**73.24 ± 1.75 %**
PROD	**73.24 ± 2.14 %**
SUM	**73.52 ± 2.28 %**
12.) 1246MV	**70.42 ± 2.47 %**
PROD	**72.11 ± 1.92 %**
SUM	**71.27 ± 2.93 %**
13.) 1256MV	**71.83 ± 2.77 %**
PROD	**71.83 ± 2.48 %**
SUM	**71.83 ± 3.27 %**
14.) 1345MV	**73.52 ± 3.13 %**
PROD	**71.83 ± 2.48 %**
SUM	**72.96 ± 4.35 %**
15.) 1346MV	**71.27 ± 3.63 %**
PROD	**71.55 ± 3.59 %**
SUM	**71.83 ± 3.50 %**
16.) 1356MV	**71.27 ± 5.04 %**
PROD	**70.70 ± 2.28 %**
SUM	**72.11 ± 2.28 %**
17.) 1456MV	**70.70 ± 1.46 %**
PROD	**71.83 ± 1.24 %**
SUM	**71.55 ± 0.78 %**
18.) 2345MV	**70.70 ± 3.36 %**
PROD	**70.14 ± 2.28 %**
SUM	**71.55 ± 2.28 %**
19.) 2346MV	**73.24 ± 2.14 %**
PROD	**74.08 ± 2.65 %**
SUM	**73.52 ± 3.99 %**
20.) 2456MV	**70.14 ± 0.78 %**
PROD	**72.11 ± 2.88 %**
SUM	**70.14 ± 2.28 %**
21.) 3456MV	**70.70 ± 3.36 %**
PROD	**72.39 ± 3.18 %**
SUM	**71.83 ± 1.75 %**
22.) 2356MV	**73.52 ± 3.13 %**
PROD	**74.37 ± 2.59 %**
SUM	**71.83 ± 4.11 %**
23.) 123MV	**73.52 ± 3.13 %**
PROD	**72.68 ± 2.35 %**
SUM	**72.39 ± 2.65 %**
24.) 124MV	**71.83 ± 2.48 %**
PROD	**73.24 ± 2.14 %**
SUM	**73.52 ± 2.88 %**
25.) 125MV	**70.14 ± 2.59 %**
PROD	**71.83 ± 2.77 %**
SUM	**70.99 ± 3.41 %**
26.) 126MV	69.86 ± 0.96 %
PROD	**70.70 ± 1.46 %**
SUM	**70.70 ± 1.46 %**

Combinations	
27.) 134MV	**71.83 ± 1.75 %**
PROD	**70.42 ± 3.27 %**
SUM	**72.39 ± 3.63 %**
28.) 135MV	**71.27 ± 2.92 %**
PROD	**71.55 ± 0.78 %**
SUM	**71.27 ± 3.83 %**
29.) 136MV	**72.11 ± 2.88 %**
PROD	**71.83 ± 3.91 %**
SUM	**70.42 ± 2.76 %**
30.) 145MV	69.58 ± 3.41 %
PROD	**70.42 ± 3.03 %**
SUM	69.01 ± 5.39 %
31.) 146MV	**70.70 ± 1.92 %**
PROD	**72.39 ± 3.63 %**
SUM	**72.11 ± 2.88 %**
32.) 156MV	67.32 ± 2.87 %
PROD	**70.42 ± 2.47 %**
SUM	67.89 ± 2.28 %
33.) 234MV	**74.37 ± 4.18 %**
PROD	**73.52 ± 3.36 %**
SUM	**73.80 ± 4.03 %**
34.) 235MV	**74.65 ± 1.24 %**
PROD	**74.37 ± 2.28 %**
SUM	**72.96 ± 3.59 %**
35.) 236MV	**75.49 ± 4.56 %**
PROD	**76.90 ± 3.41 %**
SUM	**74.65 ± 2.47 %**
36.) 245MV	69.01 ± 1.74 %
PROD	**70.70 ± 1.46 %**
SUM	68.45 ± 2.92 %
37.) 246MV	**73.52 ± 2.28 %**
PROD	**73.80 ± 2.92 %**
SUM	**73.80 ± 2.00 %**
38.) 256MV	**71.83 ± 1.24 %**
PROD	**70.70 ± 1.92 %**
SUM	**71.27 ± 3.18 %**
39.) 345MV	69.58 ± 2.34 %
PROD	**70.99 ± 3.63 %**
SUM	**70.14 ± 3.36 %**
40.) 346MV	**72.67 ± 4.89 %**
PROD	**71.55 ± 3.79 %**
SUM	**71.27 ± 3.83 %**
41.) 356MV	**71.55 ± 6.23 %**
PROD	**70.42 ± 1.24 %**
SUM	68.17 ± 1.99 %
42.) 456MV	67.04 ± 3.18 %
PROD	**70.14 ± 3.99 %**
SUM	67.61 ± 4.28 %

Table C.7: Averages of 1 classifiers each from the novel/parietal recordings for 66 patients (refer to Table 6.14).

Single Classifiers	
1.) P4 2-4Hz	68.18 ± 4.41 %
2.) PZ 2-4Hz	69.70 ± 3.26 %
3.) P3 2-4Hz	65.15 ± 4.97 %
4.) P4 1-2Hz	66.06 ± 5.74 %
5.) PZ 1-2Hz	69.39 ± 1.57 %
6.) P7 1-2Hz	62.12 ± 6.65 %

Combinations	
1.) 1 2 3 4 5 6 MV	**74.85 ± 5.08 %**
PROD	**76.36 ± 3.42 %**
SUM	**76.67 ± 4.33 %**
2.) 1 2 3 4 5 MV	**75.15 ± 4.72 %**
PROD	**76.06 ± 3.62 %**
SUM	**75.76 ± 4.80 %**
3.) 1 2 3 4 6 MV	**73.03 ± 4.69 %**
PROD	**75.76 ± 2.30 %**
SUM	**75.15 ± 3.90 %**
4.) 1 3 4 5 6 MV	**73.94 ± 6.70 %**
PROD	**76.97 ± 3.85 %**
SUM	**74.55 ± 6.96 %**
5.) 2 3 4 5 6 MV	**75.76 ± 4.61 %**
PROD	**76.97 ± 3.36 %**
SUM	**75.76 ± 3.76 %**
6.) 1 2 4 5 6 MV	**75.15 ± 2.85 %**
PROD	**75.76 ± 4.80 %**
SUM	**77.57 ± 2.79 %**
7.) 1 2 3 5 6 MV	**73.03 ± 2.79 %**
PROD	**74.54 ± 3.36 %**
SUM	**73.94 ± 2.45 %**
8.) 1 2 3 4 MV	**72.12 ± 3.67 %**
PROD	**76.06 ± 4.29 %**
SUM	**74.24 ± 1.88 %**
9.) 1 2 3 5 MV	**73.33 ± 3.15 %**
PROD	**76.67 ± 5.73 %**
SUM	**74.54 ± 2.79 %**
10.) 1 2 3 6 MV	**72.42 ± 3.62 %**
PROD	**72.73 ± 1.33 %**
SUM	**73.94 ± 3.62 %**
11.) 1 2 4 5 MV	**76.36 ± 3.15 %**
PROD	**74.85 ± 4.12 %**
SUM	**76.06 ± 3.09 %**
12.) 1 2 4 6 MV	**73.94 ± 3.62 %**
PROD	**74.85 ± 7.48 %**
SUM	**73.94 ± 3.86 %**

Combinations	
13.) 1 2 5 6 MV	**73.33 ± 2.15 %**
PROD	**72.73 ± 2.66 %**
SUM	**73.33 ± 2.85 %**
14.) 1 3 4 5 MV	**72.12 ± 4.72 %**
PROD	**74.85 ± 5.58 %**
SUM	**76.36 ± 4.90 %**
15.) 1 3 4 6 MV	**72.12 ± 3.15 %**
PROD	**73.64 ± 2.15 %**
SUM	**75.76 ± 4.41 %**
16.) 1 3 5 6 MV	**73.33 ± 2.85 %**
PROD	**75.15 ± 3.15 %**
SUM	**75.15 ± 3.15 %**
17.) 1 4 5 6 MV	**76.67 ± 2.85 %**
PROD	**75.45 ± 2.45 %**
SUM	**75.45 ± 3.09 %**
18.) 2 3 4 5 MV	**76.06 ± 3.36 %**
PROD	**75.76 ± 2.97 %**
SUM	**76.06 ± 2.06 %**
19.) 2 3 4 6 MV	**73.33 ± 3.66 %**
PROD	**75.76 ± 1.88 %**
SUM	**74.55 ± 4.87 %**
20.) 2 4 5 6 MV	**72.43 ± 2.06 %**
PROD	**74.24 ± 1.33 %**
SUM	**74.54 ± 0.84 %**
21.) 3 4 5 6 MV	**76.36 ± 5.08 %**
PROD	**76.36 ± 4.33 %**
SUM	**76.06 ± 4.87 %**
22.) 2 3 5 6 MV	**71.82 ± 2.14 %**
PROD	**73.33 ± 4.72 %**
SUM	**72.12 ± 3.90 %**
23.) 1 2 3 MV	**72.42 ± 3.09 %**
PROD	**73.64 ± 2.15 %**
SUM	**72.73 ± 2.31 %**
24.) 1 2 4 MV	**73.33 ± 2.85 %**
PROD	**74.55 ± 4.87 %**
SUM	**74.24 ± 5.15 %**
25.) 1 2 5 MV	**73.94 ± 2.79 %**
PROD	**71.82 ± 4.90 %**
SUM	**73.64 ± 2.15 %**
26.) 1 2 6 MV	**70.60 ± 3.15 %**
PROD	**70.91 ± 4.87 %**
SUM	**71.21 ± 6.24 %**
27.) 1 3 4 MV	**70.00 ± 5.70 %**
PROD	**74.24 ± 2.31 %**
SUM	**71.51 ± 5.05 %**

Combinations	
28.) 1 3 5 MV	**71.21 ± 3.52 %**
PROD	**75.15 ± 6.04 %**
SUM	**71.82 ± 2.14 %**
29.) 1 3 6 MV	**72.12 ± 5.89 %**
PROD	**72.73 ± 2.30 %**
SUM	**72.73 ± 4.61 %**
30.) 1 4 5 MV	**74.24 ± 3.52 %**
PROD	**73.94 ± 1.57 %**
SUM	**74.85 ± 2.85 %**
31.) 1 4 6 MV	69.70 ± 2.97 %
PROD	**74.24 ± 6.91 %**
SUM	**72.73 ± 5.32 %**
32.) 1 5 6 MV	**70.91 ± 2.79 %**
PROD	**72.73 ± 3.52 %**
SUM	**72.12 ± 1.68 %**
33.) 2 3 4 MV	**73.33 ± 4.53 %**
PROD	**76.36 ± 2.85 %**
SUM	**73.33 ± 4.72 %**
34.) 2 3 5 MV	**74.24 ± 3.99 %**
PROD	**75.15 ± 5.08 %**
SUM	**74.24 ± 5.15 %**
35.) 2 3 6 MV	**70.91 ± 4.08 %**
PROD	**73.33 ± 3.66 %**
SUM	**72.12 ± 2.85 %**
36.) 2 4 5 MV	69.70 ± 3.52 %
PROD	**70.91 ± 3.62 %**
SUM	**70.00 ± 3.85 %**
37.) 2 4 6 MV	**72.73 ± 3.26 %**
PROD	**74.24 ± 4.21 %**
SUM	**76.06 ± 2.06 %**
38.) 2 5 6 MV	**74.55 ± 6.15 %**
PROD	**74.24 ± 4.41 %**
SUM	**75.15 ± 5.08 %**
39.) 3 4 5 MV	**71.21 ± 5.64 %**
PROD	**74.55 ± 3.09 %**
SUM	**72.12 ± 5.74 %**
40.) 3 4 6 MV	**72.12 ± 5.58 %**
PROD	**74.24 ± 5.64 %**
SUM	**75.45 ± 5.55 %**
41.) 3 5 6 MV	**70.61 ± 7.48 %**
PROD	**73.33 ± 2.15 %**
SUM	**71.52 ± 5.22 %**
42.) 4 5 6 MV	69.70 ± 4.80 %
PROD	**72.73 ± 5.15 %**
SUM	**71.21 ± 4.61 %**

Table C.8: Averages of 3 classifiers each from the novel/parietal recordings for 66 patients (refer to Table 6.15).

Single Classifiers	
1.) P4 2-4Hz	67.58 ± 3.90 %
2.) PZ 2-4Hz	**72.42 ± 3.62 %**
3.) P3 2-4Hz	64.85 ± 6.83 %
4.) P4 1-2Hz	**70.00 ± 3.37 %**
5.) PZ 1-2Hz	64.85 ± 8.76 %
6.) P7 1-2Hz	63.34 ± 2.06 %
11.) P4 2-4Hz	**71.21 ± 6.65 %**
12.) PZ 2-4Hz	**71.82 ± 5.08 %**
13.) P3 2-4Hz	66.36 ± 3.09 %
14.) P4 1-2Hz	69.39 ± 2.46 %
15.) PZ 1-2Hz	65.76 ± 7.35 %
16.) P7 1-2Hz	63.03 ± 7.48 %
21.) P4 2-4Hz	**70.61 ± 3.42 %**
22.) PZ 2-4Hz	**70.91 ± 3.85 %**
23.) P3 2-4Hz	65.76 ± 3.42 %
24.) P4 1-2Hz	**70.30 ± 2.85 %**
25.) PZ 1-2Hz	65.15 ± 4.80 %
26.) P7 1-2Hz	59.40 ± 7.69 %

Combinations	
1.) 1 2 3 4 5 6 MV	**77.88 ± 2.52 %**
PROD	**77.27 ± 2.66 %**
SUM	**79.09 ± 2.45 %**
2.) 1 2 3 4 5 MV	**76.97 ± 3.09 %**
PROD	**76.67 ± 4.12 %**
SUM	**78.48 ± 1.57 %**
3.) 1 2 3 4 6 MV	**76.67 ± 2.86 %**
PROD	**75.45 ± 2.45 %**
SUM	**76.67 ± 2.15 %**
4.) 1 3 4 5 6 MV	**77.88 ± 3.90 %**
PROD	**77.27 ± 3.52 %**
SUM	**78.49 ± 4.29 %**
5.) 2 3 4 5 6 MV	**75.46 ± 5.05 %**
PROD	**75.76 ± 3.52 %**
SUM	**77.88 ± 5.08 %**
6.) 1 2 4 5 6 MV	**78.79 ± 1.88 %**
PROD	**78.48 ± 1.57 %**
SUM	**79.39 ± 2.53 %**
7.) 1 2 3 5 6 MV	**74.85 ± 2.85 %**
PROD	**73.33 ± 3.42 %**
SUM	**75.15 ± 2.85 %**
8.) 1 2 3 4 MV	**76.36 ± 1.68 %**
PROD	**74.85 ± 4.33 %**
SUM	**75.76 ± 1.88 %**
9.) 1 2 3 5 MV	**73.94 ± 3.36 %**
PROD	**72.42 ± 3.62 %**
SUM	**73.33 ± 1.68 %**
10.) 1 2 3 6 MV	**75.45 ± 3.62 %**
PROD	**73.03 ± 2.45 %**
SUM	**74.85 ± 3.67 %**

Combinations	
11.) 1 2 4 5 MV	**74.55 ± 3.62 %**
PROD	**79.09 ± 2.45 %**
SUM	**78.79 ± 2.97 %**
12.) 1 2 4 6 MV	**76.97 ± 2.45 %**
PROD	**76.06 ± 0.84 %**
SUM	**77.58 ± 1.57 %**
13.) 1 2 5 6 MV	**74.24 ± 3.76 %**
PROD	**75.46 ± 4.29 %**
SUM	**75.76 ± 5.64 %**
14.) 1 3 4 5 MV	**77.27 ± 1.33 %**
PROD	**76.36 ± 3.90 %**
SUM	**78.48 ± 3.36 %**
15.) 1 3 4 6 MV	**78.49 ± 3.37 %**
PROD	**75.15 ± 2.85 %**
SUM	**79.09 ± 1.57 %**
16.) 1 3 5 6 MV	**74.24 ± 4.21 %**
PROD	**73.03 ± 4.29 %**
SUM	**75.45 ± 4.49 %**
17.) 1 4 5 6 MV	**75.15 ± 5.25 %**
PROD	**76.97 ± 2.45 %**
SUM	**75.45 ± 3.09 %**
18.) 2 3 4 5 MV	**76.36 ± 2.15 %**
PROD	**75.45 ± 1.57 %**
SUM	**76.36 ± 1.68 %**
19.) 2 3 4 6 MV	**78.49 ± 0.84 %**
PROD	**76.67 ± 3.41 %**
SUM	**78.79 ± 2.31 %**
20.) 2 4 5 6 MV	**76.36 ± 6.32 %**
PROD	**76.97 ± 2.45 %**
SUM	**77.27 ± 2.30 %**
21.) 3 4 5 6 MV	**73.94 ± 4.87 %**
PROD	**76.06 ± 3.62 %**
SUM	**75.76 ± 5.15 %**
22.) 2 3 5 6 MV	**73.33 ± 5.58 %**
PROD	**72.42 ± 5.22 %**
SUM	**73.94 ± 5.39 %**
23.) 1 2 3 MV	**75.76 ± 3.52 %**
PROD	**73.33 ± 2.53 %**
SUM	**74.54 ± 2.79 %**
24.) 1 2 4 MV	**76.67 ± 2.15 %**
PROD	**77.58 ± 1.57 %**
SUM	**77.27 ± 1.33 %**
25.) 1 2 5 MV	**72.43 ± 2.79 %**
PROD	**73.33 ± 3.90 %**
SUM	**72.42 ± 2.06 %**
26.) 1 2 6 MV	**73.33 ± 4.72 %**
PROD	**71.82 ± 2.14 %**
SUM	**73.94 ± 3.62 %**

Combinations	
27.) 1 3 4 MV	**76.97 ± 1.57 %**
PROD	**76.06 ± 2.79 %**
SUM	**78.79 ± 2.97 %**
28.) 1 3 5 MV	**73.03 ± 2.79 %**
PROD	**72.73 ± 3.76 %**
SUM	**73.94 ± 3.09 %**
29.) 1 3 6 MV	**73.33 ± 4.12 %**
PROD	**73.03 ± 2.45 %**
SUM	**74.85 ± 1.68 %**
30.) 1 4 5 MV	**75.15 ± 2.14 %**
PROD	**74.24 ± 2.66 %**
SUM	**74.55 ± 2.45 %**
31.) 1 4 6 MV	**76.36 ± 3.90 %**
PROD	**76.67 ± 2.86 %**
SUM	**76.36 ± 3.15 %**
32.) 1 5 6 MV	**72.42 ± 4.08 %**
PROD	**72.73 ± 3.76 %**
SUM	**72.73 ± 4.21 %**
33.) 2 3 4 MV	**77.88 ± 2.85 %**
PROD	**76.06 ± 2.45 %**
SUM	**79.09 ± 1.57 %**
34.) 2 3 5 MV	**74.24 ± 4.61 %**
PROD	**73.33 ± 5.42 %**
SUM	**75.15 ± 3.42 %**
35.) 2 3 6 MV	**73.64 ± 1.03 %**
PROD	**73.03 ± 4.29 %**
SUM	**73.33 ± 2.15 %**
36.) 2 4 5 MV	**73.94 ± 3.62 %**
PROD	**73.63 ± 1.68 %**
SUM	**72.42 ± 3.09 %**
37.) 2 4 6 MV	**76.36 ± 3.90 %**
PROD	**78.18 ± 1.03 %**
SUM	**80.00 ± 0.84 %**
38.) 2 5 6 MV	**73.03 ± 2.45 %**
PROD	**74.24 ± 2.66 %**
SUM	**74.85 ± 2.14 %**
39.) 3 4 5 MV	**74.55 ± 3.62 %**
PROD	**74.85 ± 3.15 %**
SUM	**73.94 ± 1.57 %**
40.) 3 4 6 MV	**73.94 ± 4.87 %**
PROD	**75.76 ± 3.99 %**
SUM	**76.67 ± 3.66 %**
41.) 3 5 6 MV	**70.00 ± 4.87 %**
PROD	69.39 ± 4.08 %
SUM	**70.61 ± 4.53 %**
42.) 4 5 6 MV	**73.64 ± 5.25 %**
PROD	**73.63 ± 4.12 %**
SUM	**74.55 ± 5.86 %**

Table C.9: Averages of 1 classifier each from the target and novel/parietal recordings for 71 patients (refer to Table 6.16).

Single Classifiers	
1.) TP4 2-4Hz	63.66 ± 3.59 %
2.) TPZ 2-4Hz	58.03 ± 3.36 %
3.) TP3 2-4Hz	61.41 ± 4.21 %
4.) TP4 1-2Hz	59.16 ± 2.47 %
5.) TPZ 1-2Hz	61.13 ± 6.13 %
6.) TP7 1-2Hz	61.69 ± 4.85 %
11.) NP4 2-4Hz	63.38 ± 6.42 %
12.) NPZ 2-4Hz	**73.80 ± 5.87 %**
13.) NP3 2-4Hz	68.17 ± 5.75 %
14.) NP4 1-2Hz	61.13 ± 6.13 %
15.) NPZ 1-2Hz	60.56 ± 2.76 %
16.) NP7 1-2Hz	58.87 ± 5.01 %

Combinations	
1.) 1 2 3 4 5 6 MV	**71.83 ± 4.46 %**
PROD	**71.55 ± 3.99 %**
SUM	**74.08 ± 4.02 %**
2.) 1 2 3 4 5 MV	**70.99 ± 2.92 %**
PROD	**72.11 ± 3.36 %**
SUM	**71.83 ± 4.79 %**
3.) 1 2 3 4 6 MV	**73.52 ± 3.37 %**
PROD	**72.39 ± 5.19 %**
SUM	**72.11 ± 4.69 %**
4.) 1 3 4 5 6 MV	**71.83 ± 4.79 %**
PROD	**71.27 ± 3.41 %**
SUM	**72.39 ± 4.56 %**
5.) 2 3 4 5 6 MV	**71.27 ± 6.13 %**
PROD	**71.55 ± 4.35 %**
SUM	**73.24 ± 5.09 %**
6.) 1 2 4 5 6 MV	**71.83 ± 2.48 %**
PROD	**71.55 ± 3.79 %**
SUM	**72.96 ± 3.13 %**
7.) 1 2 3 5 6 MV	**73.24 ± 5.39 %**
PROD	**73.52 ± 4.85 %**
SUM	**75.77 ± 5.72 %**
8.) 1 2 3 4 MV	**72.68 ± 1.57 %**
PROD	**72.67 ± 3.62 %**
SUM	**71.83 ± 4.1 %**
9.) 1 2 3 5 MV	**72.96 ± 2.6 %**
PROD	**73.80 ± 5.47 %**
SUM	**72.40 ± 4.03 %**
10.) 1 2 3 6 MV	**73.80 ± 3.63 %**
PROD	**75.21 ± 5.47 %**
SUM	**76.05 ± 6.06 %**
11.) 1 2 4 5 MV	**70.98 ± 2.93 %**
PROD	**71.55 ± 3.13 %**
SUM	**72.39 ± 3.18 %**

Combinations	
12.) 1 2 4 6 MV	**71.27 ± 1.57 %**
PROD	**71.83 ± 1.75 %**
SUM	**72.11 ± 2.28 %**
13.) 1 2 5 6 MV	**72.40 ± 4.03 %**
PROD	**73.24 ± 3.50 %**
SUM	**72.96 ± 2.88 %**
14.) 1 3 4 5 MV	69.86 ± 3.62 %
PROD	**70.14 ± 2.28 %**
SUM	**71.27 ± 3.63 %**
15.) 1 3 4 6 MV	**72.68 ± 5.04 %**
PROD	**71.27 ± 4.03 %**
SUM	**72.39 ± 2.00 %**
16.) 1 3 5 6 MV	**72.39 ± 7.06 %**
PROD	**75.49 ± 4.56 %**
SUM	**76.06 ± 6.06 %**
17.) 1 4 5 6 MV	69.58 ± 4.02 %
PROD	**71.27 ± 2.65 %**
SUM	**72.39 ± 2.65 %**
18.) 2 3 4 5 MV	**70.42 ± 3.50 %**
PROD	**72.40 ± 4.03 %**
SUM	**72.39 ± 4.56 %**
19.) 2 3 4 6 MV	**72.39 ± 6.95 %**
PROD	**72.39 ± 4.03 %**
SUM	**72.96 ± 5.98 %**
20.) 2 4 5 6 MV	69.58 ± 4.56 %
PROD	**71.27 ± 2.93 %**
SUM	**73.24 ± 3.27 %**
21.) 3 4 5 6 MV	68.45 ± 6.95 %
PROD	69.30 ± 3.36 %
SUM	**71.55 ± 5.85 %**
22.) 2 3 5 6 MV	**72.11 ± 5.00 %**
PROD	**72.68 ± 2.00 %**
SUM	**74.36 ± 5.01 %**
23.) 1 2 3 MV	**74.37 ± 5.85 %**
PROD	**74.37 ± 5.16 %**
SUM	**75.78 ± 4.35 %**
24.) 1 2 4 MV	69.29 ± 2.59 %
PROD	**71.55 ± 1.46 %**
SUM	**71.27 ± 2.00 %**
25.) 1 2 5 MV	69.30 ± 3.99 %
PROD	**70.70 ± 2.28 %**
SUM	**71.83 ± 4.95 %**
26.) 1 2 6 MV	69.01 ± 4.79 %
PROD	**70.99 ± 3.18 %**
SUM	**72.11 ± 3.79 %**
27.) 1 3 4 MV	**70.42 ± 5.10 %**
PROD	69.58 ± 2.92 %
SUM	**70.70 ± 4.18 %**

Combinations	
28.) 1 3 5 MV	**70.14 ± 5.30 %**
PROD	**72.96 ± 5.44 %**
SUM	**71.55 ± 4.69 %**
29.) 1 3 6 MV	**75.49 ± 6.95 %**
PROD	**74.08 ± 6.84 %**
SUM	**75.49 ± 7.68 %**
30.) 1 4 5 MV	69.29 ± 2.28 %
PROD	69.30 ± 2.28 %
SUM	69.86 ± 3.62 %
31.) 1 4 6 MV	69.01 ± 4.46 %
PROD	**70.70 ± 0.78 %**
SUM	**72.11 ± 3.13 %**
32.) 1 5 6 MV	68.73 ± 6.93 %
PROD	**72.96 ± 2.28 %**
SUM	**72.39 ± 2.35 %**
33.) 2 3 4 MV	**71.83 ± 5.10 %**
PROD	**71.83 ± 5.39 %**
SUM	**72.68 ± 3.41 %**
34.) 2 3 5 MV	**71.55 ± 5.45 %**
PROD	**72.11 ± 3.79 %**
SUM	**72.11 ± 4.69 %**
35.) 2 3 6 MV	**73.80 ± 5.88 %**
PROD	**72.11 ± 5.15 %**
SUM	**73.52 ± 4.85 %**
36.) 2 4 5 MV	**70.42 ± 3.27 %**
PROD	69.02 ± 3.03 %
SUM	**71.26 ± 4.39 %**
37.) 2 4 6 MV	**71.55 ± 5.30 %**
PROD	**70.98 ± 2.00 %**
SUM	**72.68 ± 3.41 %**
38.) 2 5 6 MV	67.89 ± 6.47 %
PROD	68.17 ± 2.65 %
SUM	69.86 ± 3.63 %
39.) 3 4 5 MV	67.89 ± 4.53 %
PROD	66.48 ± 2.87 %
SUM	67.33 ± 3.79 %
40.) 3 4 6 MV	**70.70 ± 4.69 %**
PROD	69.30 ± 5.16 %
SUM	**72.11 ± 5.00 %**
41.) 3 5 6 MV	**71.55 ± 4.52 %**
PROD	**70.98 ± 2.35 %**
SUM	**72.39 ± 6.95 %**
42.) 4 5 6 MV	67.04 ± 1.99 %
PROD	69.01 ± 5.10 %
SUM	69.86 ± 0.96 %

Table C.10: Averages of 11 classifiers for the parietal and occipital features for 71 patients (refer to Table 6.17).

Single Classifiers	
1.) TP4 2-4Hz	61.13 ± 6.26%
2.) TPZ 2-4Hz	56.90 ± 3.17%
2.) TP3 2-4Hz	59.15 ± 5.93%
4.) NP8 2-4Hz	68.17 ± 3.41%
5.) TO2 1-2Hz	58.31 ± 5.88%
6.) TP7 1-2Hz	65.64 ± 2.00%
7.) NO2 1-2Hz	59.44 ± 3.36%
8.) NPZ 2-4Hz	**71.55 ± 2.88%**
9.) NP3 2-4Hz	66.48 ± 2.59%
10.) NP4 1-2Hz	62.82 ± 3.18%
11.) NPZ 1-2Hz	62.82 ± 5.61%

Combinations	
1,2,3 MV	59.43 ± 4.17%
PROD	62.25 ± 2.28%
SUM	61.13 ± 5.61%
1,2,4 MV	66.48 ± 3.79%
PROD	**70.98 ± 2.00%**
SUM	66.76 ± 5.88%
1,2,5 MV	63.10 ± 6.23%
PROD	66.48 ± 3.79%
SUM	64.22 ± 5.04%
1,2,6 MV	62.82 ± 4.22%
PROD	66.76 ± 5.33%
SUM	65.07 ± 4.69%
1,2,7 MV	62.82 ± 4.89%
PROD	65.07 ± 5.72%
SUM	63.38 ± 6.99%
1,2,8 MV	64.51 ± 6.47%
PROD	68.73 ± 2.87%
SUM	65.63 ± 5.74%
1,2,9 MV	63.66 ± 4.85%
PROD	67.04 ± 4.56%
SUM	66.20 ± 6.42%
1,2,10 MV	62.54 ± 4.73%
PROD	63.66 ± 2.28%
SUM	63.66 ± 5.16%
1,2,11 MV	64.22 ± 7.68%
PROD	65.91 ± 4.53%
SUM	66.48 ± 8.33%
1,3,4 MV	68.17 ± 2.65%
PROD	66.76 ± 2.34%
SUM	68.73 ± 2.28%
1,3,5 MV	62.25 ± 4.18%
PROD	62.82 ± 2.93%
SUM	63.10 ± 3.13%
1,3,6 MV	67.04 ± 4.21%
PROD	64.79 ± 2.14%
SUM	68.17 ± 2.92%
1,3,7 MV	60.84 ± 4.53%
PROD	62.25 ± 2.28%
SUM	60.56 ± 4.46%
1,3,8 MV	67.04 ± 4.03%
PROD	68.17 ± 5.04%
SUM	67.89 ± 4.85%
1,3,9 MV	65.07 ± 1.46%
PROD	67.04 ± 1.99%
SUM	64.51 ± 2.88%
1,3,10 MV	64.23 ± 2.00%
PROD	62.25 ± 2.28%
SUM	64.51 ± 3.13%

Combinations	
1,3,11 MV	64.51 ± 5.45%
PROD	62.82 ± 5.33%
SUM	63.94 ± 4.22%
1,4,5 MV	66.76 ± 5.88%
PROD	**71.27 ± 5.18%**
SUM	67.33 ± 2.59%
1,4,6 MV	**70.70 ± 1.92%**
PROD	**72.11 ± 4.69%**
SUM	**70.99 ± 4.39%**
1,4,7 MV	65.63 ± 3.62%
PROD	**70.70 ± 4.53%**
SUM	67.32 ± 3.36%
1,4,8 MV	**71.83 ± 4.62%**
PROD	**73.80 ± 5.61%**
SUM	**72.67 ± 3.41%**
1,4,9 MV	**70.42 ± 4.79%**
PROD	**73.52 ± 4.69%**
SUM	**71.83 ± 4.11%**
1,4,10 MV	67.89 ± 4.52%
PROD	69.29 ± 3.58%
SUM	67.89 ± 3.13%
1,4,11 MV	69.30 ± 5.16%
PROD	**70.42 ± 4.28%**
SUM	69.58 ± 4.03%
1,5,6 MV	65.07 ± 6.71%
PROD	66.48 ± 9.45%
SUM	67.61 ± 4.46%
1,5,7 MV	62.82 ± 2.93%
PROD	65.63 ± 4.73%
SUM	63.66 ± 2.60%
1,5,8 MV	69.58 ± 4.56%
PROD	**73.24 ± 3.71%**
SUM	**71.27 ± 4.03%**
1,5,9 MV	67.89 ± 4.17%
PROD	70.99 ± 5.04%
SUM	68.45 ± 4.02%
1,5,10 MV	66.76 ± 4.02%
PROD	66.76 ± 3.62%
SUM	68.17 ± 1.99%
1,5,11 MV	65.07 ± 5.85%
PROD	65.07 ± 3.13%
SUM	67.61 ± 2.47%
1,6,7 MV	65.92 ± 1.92%
PROD	67.04 ± 5.47%
SUM	66.48 ± 3.13%
1,6,8 MV	**73.80 ± 7.28%**
PROD	**73.24 ± 4.46%**
SUM	**74.09 ± 5.88%**

Table C.10: Averages of 11 classifiers for the parietal and occipital features for 71 patients (refer to Table 6.17). (continued)

Combinations	
1,6,9 MV	**71.55 ± 2.60%**
PROD	**71.55 ± 6.23%**
SUM	72.96 ± 5.44%
1,6,10 MV	66.76 ± 6.26%
PROD	67.04 ± 6.01%
SUM	68.73 ± 6.93%
1,6,11 MV	67.32 ± 6.82%
PROD	68.45 ± 4.56%
SUM	69.86 ± 2.92%
1,7,8 MV	**70.14 ± 2.87%**
PROD	**70.71 ± 4.53%**
SUM	**70.14 ± 3.79%**
1,7,9 MV	68.73 ± 4.17%
PROD	**70.14 ± 3.36%**
SUM	69.86 ± 4.03%
1,7,10 MV	63.38 ± 2.77%
PROD	66.19 ± 7.52%
SUM	64.51 ± 3.99%
1,7,11 MV	63.38 ± 4.46%
PROD	65.07 ± 3.37%
SUM	64.51 ± 3.59%
1,8,9 MV	**73.80 ± 2.92%**
PROD	**72.96 ± 3.58%**
SUM	**72.96 ± 3.13%**
1,8,10 MV	69.58 ± 5.88%
PROD	68.73 ± 5.72%
SUM	69.58 ± 4.72%
1,8,11 MV	69.58 ± 4.88%
PROD	68.73 ± 3.36%
SUM	69.01 ± 4.95%
1,9,10 MV	67.89 ± 6.59%
PROD	67.61 ± 2.47%
SUM	69.01 ± 4.94%
1,9,11 MV	65.92 ± 6.47%
PROD	69.58 ± 3.41%
SUM	68.17 ± 3.62%
1,10,11 MV	63.66 ± 3.99%
PROD	65.35 ± 3.41%
SUM	65.92 ± 4.18%
2,3,4 MV	63.10 ± 2.28%
PROD	65.92 ± 3.13%
SUM	63.38 ± 3.03%
2,3,5 MV	59.72 ± 7.06%
PROD	63.66 ± 6.23%
SUM	63.10 ± 4.17%
2,3,6 MV	61.13 ± 4.39%
PROD	65.63 ± 5.04%
SUM	66.48 ± 4.53%

Combinations	
2,3,7 MV	60.56 ± 2.76%
PROD	61.13 ± 3.83%
SUM	61.41 ± 2.35%
2,3,8 MV	65.91 ± 5.45%
PROD	67.89 ± 1.91%
SUM	66.20 ± 3.91%
2,3,9 MV	61.97 ± 5.10%
PROD	64.51 ± 2.28%
SUM	62.54 ± 5.19%
2,3,10 MV	61.41 ± 5.33%
PROD	63.10 ± 3.37%
SUM	64.51 ± 3.13%
2,3,11 MV	59.15 ± 8.11%
PROD	62.82 ± 3.83%
SUM	61.97 ± 5.10%
2,4,5 MV	69.58 ± 4.02%
PROD	**71.83 ± 5.09%**
SUM	69.58 ± 2.92%
2,4,6 MV	**72.11 ± 5.85%**
PROD	**73.24 ± 2.77%**
SUM	**73.52 ± 4.69%**
2,4,7 MV	69.01 ± 4.79%
PROD	**71.27 ± 5.33%**
SUM	68.73 ± 4.85%
2,4,8 MV	**71.83 ± 3.50%**
PROD	**74.09 ± 2.65%**
SUM	**71.83 ± 4.79%**
2,4,9 MV	67.32 ± 2.87%
PROD	**72.39 ± 2.93%**
SUM	**70.42 ± 2.76%**
2,4,10 MV	68.17 ± 1.56%
PROD	**70.99 ± 4.73%**
SUM	**70.14 ± 3.99%**
2,4,11 MV	**70.14 ± 2.59%**
PROD	**72.11 ± 2.60%**
SUM	**71.55 ± 3.37%**
2,5,6 MV	66.76 ± 2.65%
PROD	69.30 ± 3.58%
SUM	68.73 ± 4.52%
2,5,7 MV	61.41 ± 2.92%
PROD	63.66 ± 4.17%
SUM	62.82 ± 2.65%
2,5,8 MV	67.61 ± 2.14%
PROD	69.01 ± 2.76%
SUM	67.89 ± 3.13%
2,5,9 MV	66.48 ± 3.58%
PROD	69.86 ± 6.01%
SUM	68.45 ± 4.02%

Combinations	
2,5,10 MV	66.20 ± 1.75%
PROD	65.07 ± 2.28%
SUM	66.48 ± 2.59%
2,5,11 MV	65.07 ± 5.72%
PROD	64.51 ± 3.37%
SUM	67.04 ± 2.34%
2,6,7 MV	64.51 ± 1.92%
PROD	69.01 ± 6.88%
SUM	67.60 ± 3.49%
2,6,8 MV	**73.24 ± 2.14%**
PROD	**73.80 ± 2.35%**
SUM	**72.96 ± 3.79%**
2,6,9 MV	67.89 ± 2.28%
PROD	67.61 ± 4.94%
SUM	**70.42 ± 2.76%**
2,6,10 MV	67.04 ± 2.92%
PROD	69.01 ± 5.25%
SUM	68.17 ± 3.62%
2,6,11 MV	68.45 ± 1.99%
PROD	**70.42 ± 2.14%**
SUM	69.86 ± 2.35%
2,7,8 MV	69.58 ± 4.21%
PROD	68.73 ± 3.13%
SUM	68.73 ± 3.13%
2,7,9 MV	66.48 ± 5.72%
PROD	67.04 ± 6.38%
SUM	66.48 ± 2.59%
2,7,10 MV	63.10 ± 2.28%
PROD	63.94 ± 3.62%
SUM	65.07 ± 1.92%
2,7,11 MV	64.51 ± 4.17%
PROD	66.76 ± 2.65%
SUM	67.32 ± 3.13%
2,8,9 MV	**70.70 ± 4.18%**
PROD	**72.68 ± 5.04%**
SUM	**71.55 ± 6.23%**
2,8,10 MV	68.45 ± 5.04%
PROD	65.63 ± 2.65%
SUM	66.76 ± 3.62%
2,8,11 MV	68.45 ± 5.04%
PROD	67.04 ± 3.41%
SUM	67.61 ± 3.91%
2,9,10 MV	64.51 ± 2.88%
PROD	66.76 ± 7.88%
SUM	66.48 ± 4.85%
2,9,11 MV	65.35 ± 3.63%
PROD	67.89 ± 4.52%
SUM	67.89 ± 3.58%

Table C.10: Averages of 11 classifiers for the parietal and occipital features for 71 patients (refer to Table 6.17). (continued)

Combinations	
2,10,11 MV	61.97 ± 3.91%
PROD	64.51 ± 3.37%
SUM	63.10 ± 3.13%
3,4,5 MV	67.61 ± 7.62%
PROD	69.58 ± 4.56%
SUM	69.30 ± 4.85%
3,4,6 MV	**70.99 ± 5.04%**
PROD	**70.70 ± 2.88%**
SUM	**70.99 ± 4.56%**
3,4,7 MV	67.61 ± 4.10%
PROD	68.73 ± 3.13%
SUM	68.45 ± 4.56%
3,4,8 MV	**71.27 ± 4.56%**
PROD	**72.96 ± 4.85%**
SUM	**70.99 ± 3.63%**
3,4,9 MV	69.58 ± 3.41%
PROD	**71.83 ± 1.75%**
SUM	69.30 ± 2.87%
3,4,10 MV	69.01 ± 3.03%
PROD	68.45 ± 4.39%
SUM	69.01 ± 2.76%
3,4,11 MV	66.76 ± 4.72%
PROD	67.89 ± 3.36%
SUM	66.76 ± 3.17%
3,5,7 MV	61.69 ± 3.37%
PROD	61.12 ± 3.41%
SUM	61.97 ± 3.50%
3,5,8 MV	66.20 ± 7.42%
PROD	68.73 ± 6.71%
SUM	67.89 ± 7.86%
3,5,9 MV	64.79 ± 6.66%
PROD	66.48 ± 3.13%
SUM	65.35 ± 3.18%
3,5,10 MV	63.38 ± 5.39%
PROD	60.28 ± 3.99%
SUM	64.22 ± 4.21%
3,5,11 MV	62.82 ± 6.84%
PROD	61.69 ± 7.96%
SUM	63.66 ± 6.93%
3,6,7 MV	65.35 ± 5.75%
PROD	64.79 ± 5.53%
SUM	65.35 ± 4.03%
3,6,8 MV	**70.14 ± 1.91%**
PROD	68.17 ± 6.73%
SUM	**70.42 ± 2.47%**
3,6,9 MV	69.30 ± 5.01%
PROD	64.51 ± 1.46%
SUM	68.45 ± 4.02%

Combinations	
3,6,10 MV	64.79 ± 8.65%
PROD	62.54 ± 4.72%
SUM	66.20 ± 5.10%
3,6,11 MV	60.00 ± 6.38%
PROD	61.13 ± 5.19%
SUM	65.35 ± 4.72%
3,7,8 MV	**70.70 ± 4.69%**
PROD	68.73 ± 5.58%
SUM	**70.42 ± 4.46%**
3,7,9 MV	67.89 ± 5.85%
PROD	65.07 ± 5.31%
SUM	67.89 ± 5.85%
3,7,10 MV	62.25 ± 5.15%
PROD	61.69 ± 6.35%
SUM	63.94 ± 4.22%
3,7,11 MV	63.10 ± 5.01%
PROD	62.53 ± 4.88%
SUM	64.79 ± 3.27%
3,8,9 MV	66.48 ± 2.28%
PROD	68.17 ± 3.62%
SUM	67.04 ± 1.99%
3,8,10 MV	69.86 ± 3.17%
PROD	66.76 ± 7.88%
SUM	68.17 ± 2.92%
3,8,11 MV	68.45 ± 3.41%
PROD	68.17 ± 7.68%
SUM	67.32 ± 4.52%
3,9,10 MV	67.61 ± 5.10%
PROD	63.66 ± 3.37%
SUM	67.32 ± 6.47%
3,9,11 MV	66.76 ± 4.02%
PROD	63.66 ± 2.88%
SUM	67.61 ± 4.79%
3,10,11 MV	59.44 ± 4.85%
PROD	61.41 ± 4.03%
SUM	61.97 ± 4.10%
4,5,6 MV	**71.83 ± 1.75%**
PROD	**71.55 ± 2.28%**
SUM	69.86 ± 1.57%
4,5,7 MV	69.01 ± 2.76%
PROD	**70.98 ± 2.35%**
SUM	68.17 ± 0.95%
4,5,8 MV	69.58 ± 4.02%
PROD	**74.65 ± 6.99%**
SUM	68.73 ± 2.28%
4,5,9 MV	67.61 ± 1.23%
PROD	**72.68 ± 2.00%**
SUM	68.17 ± 0.95%

Combinations	
4,5,10 MV	68.45 ± 2.65%
PROD	**70.70 ± 2.59%**
SUM	69.58 ± 1.99%
4,5,11 MV	69.30 ± 2.28%
PROD	**71.55 ± 2.60%**
SUM	68.45 ± 2.92%
4,6,7 MV	70.14 ± 5.15%
PROD	**72.39 ± 4.03%**
SUM	69.58 ± 6.61%
4,6,8 MV	**75.49 ± 2.65%**
PROD	**77.75 ± 2.87%**
SUM	**78.03 ± 1.56%**
4,6,9 MV	**70.98 ± 1.57%**
PROD	**71.83 ± 2.77%**
SUM	**71.55 ± 3.36%**
4,6,10 MV	**72.11 ± 4.35%**
PROD	**71.27 ± 3.18%**
SUM	**72.39 ± 4.39%**
4,6,11 MV	**70.42 ± 1.75%**
PROD	**72.96 ± 2.60%**
SUM	**72.96 ± 3.37%**
4,7,8 MV	**71.27 ± 2.65%**
PROD	**75.21 ± 2.35%**
SUM	**70.42 ± 2.47%**
4,7,9 MV	**70.14 ± 4.17%**
PROD	**71.55 ± 4.69%**
SUM	**70.14 ± 3.36%**
4,7,10 MV	65.64 ± 1.57%
PROD	69.30 ± 4.53%
SUM	67.33 ± 0.78%
4,7,11 MV	66.48 ± 2.87%
PROD	**70.98 ± 2.00%**
SUM	67.32 ± 3.13%
4,8,9 MV	**74.93 ± 2.28%**
PROD	**75.21 ± 4.21%**
SUM	**74.37 ± 1.46%**
4,8,10 MV	**71.83 ± 3.50%**
PROD	69.86 ± 1.99%
SUM	69.86 ± 2.92%
4,8,11 MV	**70.14 ± 3.79%**
PROD	**74.08 ± 4.73%**
SUM	**70.99 ± 4.03%**
4,9,10 MV	69.30 ± 4.17%
PROD	**70.14 ± 0.78%**
SUM	68.73 ± 3.79%
4,9,11 MV	69.58 ± 3.62%
PROD	**70.70 ± 3.36%**
SUM	69.30 ± 2.87%

Table C.10: Averages of 11 classifiers for the parietal and occipital features for 71 patients (refer to Table 6.17). (continued)

Combinations	
4,10,11 MV	65.64 ± 3.41%
PROD	69.29 ± 4.35%
SUM	67.32 ± 2.87%
5,6,7 MV	63.94 ± 6.73%
PROD	65.35 ± 3.83%
SUM	65.07 ± 5.16%
5,6,8 MV	**71.83 ± 3.91%**
PROD	**71.55 ± 4.18%**
SUM	**70.99 ± 4.56%**
5,6,9 MV	**70.14 ± 3.79%**
PROD	**70.42 ± 4.10%**
SUM	**70.14 ± 3.13%**
5,6,10 MV	67.04 ± 4.56%
PROD	65.63 ± 3.41%
SUM	67.61 ± 3.27%
5,6,11 MV	66.48 ± 6.23%
PROD	67.89 ± 4.69%
SUM	67.32 ± 6.71%
5,7,8 MV	**71.55 ± 2.28%**
PROD	**70.14 ± 3.36%**
SUM	68.73 ± 3.36%
5,7,9 MV	68.45 ± 3.41%
PROD	**71.55 ± 3.59%**
SUM	68.45 ± 4.72%
5,7,10 MV	64.79 ± 3.50%
PROD	66.76 ± 3.83%
SUM	67.32 ± 3.13%
5,7,11 MV	65.35 ± 6.49%
PROD	65.63 ± 5.88%
SUM	65.35 ± 3.83%
5,8,9 MV	69.02 ± 4.46%
PROD	**72.96 ± 3.37%**
SUM	69.30 ± 2.87%
5,8,10 MV	**70.14 ± 4.52%**
PROD	**70.70 ± 4.18%**
SUM	**70.42 ± 3.50%**
5,8,11 MV	**71.83 ± 4.46%**
PROD	**70.99 ± 3.18%**
SUM	69.29 ± 2.59%
5,9,10 MV	65.35 ± 6.61%
PROD	68.73 ± 5.45%
SUM	68.17 ± 5.04%
5,9,11 MV	64.51 ± 1.92%
PROD	68.73 ± 6.47%
SUM	67.61 ± 6.66%
5,10,11 MV	65.92 ± 4.18%
PROD	67.89 ± 3.99%
SUM	66.48 ± 3.79%

Combinations	
6,7,8 MV	**73.24 ± 2.77%**
PROD	69.01 ± 3.91%
SUM	69.30 ± 4.85%
6,7,9 MV	**71.27 ± 3.63%**
PROD	**71.55 ± 2.28%**
SUM	**71.55 ± 5.15%**
6,7,10 MV	67.89 ± 5.45%
PROD	67.60 ± 6.77%
SUM	69.86 ± 5.61%
6,7,11 MV	67.32 ± 4.85%
PROD	**70.42 ± 4.46%**
SUM	68.45 ± 5.19%
6,8,9 MV	**72.68 ± 2.00%**
PROD	**73.24 ± 3.27%**
SUM	**74.09 ± 2.93%**
6,8,10 MV	**70.42 ± 5.39%**
PROD	69.86 ± 3.17%
SUM	69.86 ± 2.92%
6,8,11 MV	**71.27 ± 2.00%**
PROD	**73.52 ± 4.85%**
SUM	**72.40 ± 3.83%**
6,9,10 MV	65.92 ± 3.79%
PROD	65.35 ± 4.03%
SUM	66.76 ± 5.88%
6,9,11 MV	67.61 ± 3.91%
PROD	68.73 ± 7.25%
SUM	**70.14 ± 7.66%**
6,10,11 MV	67.33 ± 3.13%
PROD	66.48 ± 3.13%
SUM	67.32 ± 2.87%
7,8,9 MV	**73.24 ± 3.50%**
PROD	**73.24 ± 2.14%**
SUM	**71.27 ± 2.00%**
7,8,10 MV	**71.83 ± 2.48%**
PROD	68.45 ± 3.62%
SUM	69.02 ± 4.46%
7,8,11 MV	69.02 ± 4.10%
PROD	69.30 ± 5.30%
SUM	69.58 ± 2.65%
7,9,10 MV	69.29 ± 1.46%
PROD	68.17 ± 1.56%
SUM	69.86 ± 2.65%
7,9,11 MV	67.32 ± 2.87%
PROD	68.17 ± 7.68%
SUM	67.61 ± 4.10%
7,10,11 MV	65.92 ± 3.36%
PROD	65.92 ± 1.92%
SUM	66.20 ± 2.76%

Combinations	
8,9,10 MV	**70.70 ± 2.28%**
PROD	69.86 ± 3.62%
SUM	**70.42 ± 3.71%**
8,9,11 MV	**70.42 ± 2.47%**
PROD	**70.98 ± 2.35%**
SUM	**70.42 ± 2.48%**
8,10,11 MV	68.17 ± 4.02%
PROD	67.04 ± 3.83%
SUM	67.04 ± 4.02%
9,10,11 MV	63.66 ± 2.88%
PROD	64.51 ± 3.58%
SUM	65.92 ± 2.87%
ALL MV	**73.80 ± 1.57%**
PROD	**73.24 ± 2.77%**
SUM	**74.37 ± 1.46%**

Table C.11: Averages of 7 classifiers for the parietal and occipital features for 71 patients (refer to Table 6.18).

Single Classifiers	
1.) TP4 1-2Hz	60.00 ± 1.99%
2.) NP8 2-4Hz	67.32 ± 4.85%
3.) TO2 1-2Hz	60.56 ± 4.46%
4.) TP7 1-2Hz	62.25 ± 3.13%
5.) NO2 1-2Hz	61.97 ± 5.80%
6.) NPZ 2-4Hz	**71.83 ± 4.46%**
7.) NP3 2-4Hz	67.89 ± 7.36%

Combinations	
1,2,3 MV	65.92 ± 3.58%
PROD	69.30 ± 3.13%
SUM	66.20 ± 3.71%
1,2,4 MV	68.17 ± 5.19%
PROD	67.89 ± 1.46%
SUM	68.45 ± 3.17%
1,2,5 MV	65.92 ± 1.46%
PROD	69.58 ± 1.56%
SUM	66.76 ± 1.99%
1,2,6 MV	69.86 ± 3.62%
PROD	**72.96 ± 3.99%**
SUM	**72.11 ± 1.46%**
1,2,7 MV	67.04 ± 4.39%
PROD	68.73 ± 3.13%
SUM	68.17 ± 4.02%
1,3,4 MV	65.35 ± 3.63%
PROD	64.23 ± 4.03%
SUM	65.35 ± 4.03%
1,3,5 MV	62.82 ± 4.88%
PROD	63.10 ± 2.28%
SUM	62.54 ± 3.41%
1,3,6 MV	67.89 ± 2.59%
PROD	69.30 ± 2.28%
SUM	67.60 ± 3.49%
1,3,7 MV	65.07 ± 2.88%
PROD	67.32 ± 3.99%
SUM	64.51 ± 3.79%
1,4,5 MV	65.35 ± 3.63%
PROD	63.94 ± 2.65%
SUM	66.20 ± 2.14%
1,4,6 MV	**70.42 ± 3.27%**
PROD	69.58 ± 2.92%
SUM	**71.27 ± 3.83%**
1,4,7 MV	69.01 ± 5.93%
PROD	65.35 ± 4.73%
SUM	69.86 ± 5.88%

Combinations	
1,5,6 MV	69.86 ± 4.56%
PROD	69.58 ± 4.02%
SUM	**70.14 ± 3.79%**
1,5,7 MV	68.17 ± 4.39%
PROD	69.01 ± 5.10%
SUM	69.01 ± 4.10%
1,6,7 MV	**72.40 ± 3.62%**
PROD	**72.39 ± 5.33%**
SUM	**72.11 ± 2.88%**
2,3,4 MV	**70.14 ± 3.13%**
PROD	**70.70 ± 2.28%**
SUM	68.45 ± 4.88%
2,3,5 MV	67.61 ± 5.10%
PROD	67.89 ± 4.17%
SUM	66.48 ± 5.85%
2,3,6 MV	**71.27 ± 4.21%**
PROD	**73.24 ± 3.50%**
SUM	**71.83 ± 4.46%**
2,3,7 MV	69.86 ± 5.04%
PROD	69.58 ± 3.63%
SUM	69.30 ± 4.85%
2,4,5 MV	68.45 ± 5.75%
PROD	69.29 ± 1.46%
SUM	68.45 ± 6.61%
2,4,6 MV	**73.52 ± 7.15%**
PROD	**74.09 ± 2.93%**
SUM	**75.77 ± 4.17%**
2,4,7 MV	**71.27 ± 4.56%**
PROD	69.86 ± 3.62%
SUM	**72.11 ± 3.99%**
2,5,6 MV	**70.71 ± 4.85%**
PROD	**72.39 ± 1.57%**
SUM	**70.14 ± 4.53%**
2,5,7 MV	67.89 ± 5.30%
PROD	**70.98 ± 4.88%**
SUM	68.73 ± 3.99%
2,6,7 MV	**72.11 ± 7.15%**
PROD	**70.70 ± 4.53%**
SUM	**71.55 ± 6.47%**
3,4,5 MV	61.97 ± 4.11%
PROD	64.79 ± 4.46%
SUM	63.94 ± 4.03%
3,4,6 MV	**70.99 ± 7.68%**
PROD	**71.83 ± 2.77%**
SUM	**71.83 ± 3.27%**

Table C.11: Averages of 7 classifiers for the parietal and occipital features for 71 patients (refer to Table 6.18). (continued)

Combinations	
3,4,7 MV	**71.27 ± 6.84%**
PROD	**72.40 ± 6.26%**
SUM	**72.96 ± 6.47%**
3,5,7 MV	69.01 ± 5.67%
PROD	**70.42 ± 6.54%**
SUM	68.73 ± 3.36%
3,6,7 MV	**73.80 ± 5.04%**
PROD	**72.39 ± 5.04%**
SUM	**73.24 ± 4.28%**
4,5,6 MV	**72.39 ± 5.88%**
PROD	68.45 ± 3.17%
SUM	**70.14 ± 7.25%**
4,5,7 MV	68.73 ± 4.35%
PROD	68.73 ± 8.33%
SUM	69.01 ± 4.10%
4,6,7 MV	**73.24 ± 4.28%**
PROD	**72.68 ± 4.56%**
SUM	**73.80 ± 3.63%**
5,6,7 MV	**73.24 ± 4.46%**
PROD	**71.27 ± 7.16%**
SUM	**72.96 ± 4.18%**
1,2,3,4,5 MV	67.33 ± 3.79%
PROD	69.86 ± 2.92%
SUM	67.04 ± 4.39%
1,2,3,4,6 MV	**71.27 ± 2.65%**
PROD	**72.96 ± 1.46%**
SUM	**72.11 ± 2.88%**
1,2,3,4,7 MV	68.73 ± 5.30%
PROD	**70.70 ± 2.28%**
SUM	69.86 ± 4.72%
1,2,3,5,6 MV	69.01 ± 1.23%
PROD	**72.11 ± 1.46%**
SUM	69.58 ± 4.56%
1,2,3,5,7 MV	69.01 ± 4.94%
PROD	**71.55 ± 1.46%**
SUM	**71.83 ± 2.77%**
1,2,3,6,7 MV	**70.14 ± 7.25%**
PROD	**73.52 ± 4.85%**
SUM	**71.55 ± 4.52%**
1,2,4,5,6 MV	69.30 ± 3.36%
PROD	**71.83 ± 3.50%**
SUM	**70.14 ± 2.28%**
1,2,4,5,7 MV	68.17 ± 3.17%
PROD	**71.55 ± 4.35%**
SUM	69.58 ± 3.62%

Combinations	
1,2,4,6,7 MV	**72.40 ± 7.38%**
PROD	**72.96 ± 4.85%**
SUM	**74.09 ± 2.00%**
1,2,5,6,7 MV	67.89 ± 3.99%
PROD	**73.52 ± 5.44%**
SUM	**70.99 ± 3.62%**
1,3,4,5,6 MV	**70.14 ± 4.85%**
PROD	**70.99 ± 3.18%**
SUM	**72.40 ± 4.73%**
1,3,4,5,7 MV	69.01 ± 4.63%
PROD	69.29 ± 3.36%
SUM	68.17 ± 5.61%
1,3,4,6,7 MV	**73.80 ± 2.00%**
PROD	**73.80 ± 4.03%**
SUM	**74.37 ± 5.72%**
1,3,5,6,7 MV	69.58 ± 5.61%
PROD	**73.52 ± 2.88%**
SUM	**70.99 ± 3.63%**
1,4,5,6,7 MV	**71.83 ± 4.95%**
PROD	**71.27 ± 5.33%**
SUM	**72.11 ± 3.13%**
2,3,4,5,6 MV	68.73 ± 3.99%
PROD	**75.21 ± 1.57%**
SUM	**70.99 ± 4.72%**
2,3,4,5,7 MV	**68.73 ± 3.36%**
PROD	**72.68 ± 3.41%**
SUM	**71.83 ± 2.48%**
2,3,4,6,7 MV	**74.08 ± 4.56%**
PROD	**73.80 ± 2.93%**
SUM	**76.34 ± 1.46%**
2,3,5,6,7 MV	**70.14 ± 4.85%**
PROD	**74.65 ± 2.76%**
SUM	**72.40 ± 4.56%**
2,4,5,6,7 MV	**71.55 ± 6.93%**
PROD	**72.68 ± 5.18%**
SUM	**72.40 ± 5.75%**
3,4,5,6,7 MV	**73.24 ± 3.50%**
PROD	**72.96 ± 4.18%**
SUM	**74.65 ± 3.91%**
ALL MV	**71.55 ± 3.36%**
PROD	**73.80 ± 1.57%**
SUM	**72.39 ± 2.00%**

Table C.12: Averages of 7 classifiers including feature-level fused Target P4 and the parietal and occipital features for 71 patients (refer to Table 6.19).

Single Classifiers	
1.) TP4 cat	62.25 ± 3.13%
2.) NP8 2-4Hz	66.76 ± 3.41%
3.) TO2 1-2Hz	58.87 ± 3.13%
4.) TP7 1-2Hz	62.25 ± 5.15%
5.) NO2 1-2Hz	58.87 ± 2.28%
6.) NPZ 2-4Hz	**73.52 ± 4.18%**
7.) NP3 2-4Hz	69.58 ± 5.61%

Combinations	
1,2,3 MV	67.32 ± 2.87%
PROD	69.58 ± 3.62%
SUM	68.17 ± 3.17%
1,2,4 MV	69.58 ± 4.03%
PROD	**70.14 ± 5.45%**
SUM	69.01 ± 6.18%
1,2,5 MV	68.17 ± 3.62%
PROD	69.30 ± 2.87%
SUM	66.76 ± 5.33%
1,2,6 MV	**73.80 ± 2.00%**
PROD	**75.21 ± 6.26%**
SUM	**73.24 ± 4.10%**
1,2,7 MV	**74.08 ± 3.18%**
PROD	**70.70 ± 4.85%**
SUM	**73.52 ± 3.13%**
1,3,4 MV	61.97 ± 5.25%
PROD	65.63 ± 5.88%
SUM	65.92 ± 3.36%
1,3,5 MV	59.15 ± 5.93%
PROD	67.32 ± 3.13%
SUM	61.41 ± 2.35%
1,3,6 MV	65.07 ± 2.28%
PROD	67.04 ± 4.21%
SUM	67.32 ± 3.36%
1,3,7 MV	64.79 ± 4.46%
PROD	**71.27 ± 2.65%**
SUM	67.89 ± 3.13%
1,4,5 MV	65.35 ± 4.21%
PROD	67.04 ± 3.41%
SUM	65.63 ± 4.89%
1,4,6 MV	**71.27 ± 2.35%**
PROD	**70.14 ± 6.81%**
SUM	**72.39 ± 1.57%**
1,4,7 MV	**73.24 ± 6.99%**
PROD	**74.09 ± 3.84%**
SUM	**74.37 ± 6.59%**

Combinations	
1,5,6 MV	**73.52 ± 3.79%**
PROD	69.58 ± 4.39%
SUM	**72.39 ± 3.63%**
1,5,7 MV	**70.70 ± 4.85%**
PROD	**73.24 ± 1.24%**
SUM	**71.55 ± 2.28%**
1,6,7 MV	**75.78 ± 4.69%**
PROD	**71.27 ± 3.18%**
SUM	**75.21 ± 4.72%**
2,3,4 MV	65.35 ± 4.03%
PROD	**70.42 ± 4.46%**
SUM	67.61 ± 3.03%
2,3,5 MV	67.04 ± 7.16%
PROD	**70.14 ± 4.85%**
SUM	67.32 ± 4.17%
2,3,6 MV	**70.42 ± 2.14%**
PROD	**74.93 ± 2.28%**
SUM	**71.55 ± 2.28%**
2,3,7 MV	69.86 ± 4.21%
PROD	69.86 ± 4.02%
SUM	69.86 ± 3.17%
2,4,5 MV	68.17 ± 4.72%
PROD	69.58 ± 2.65%
SUM	68.17 ± 3.17%
2,4,6 MV	**72.11 ± 3.13%**
PROD	**74.37 ± 2.88%**
SUM	**74.08 ± 3.63%**
2,4,7 MV	**72.11 ± 3.79%**
PROD	**72.11 ± 2.88%**
SUM	**72.39 ± 3.63%**
2,5,6 MV	**70.98 ± 2.00%**
PROD	**73.80 ± 5.04%**
SUM	**70.70 ± 3.13%**
2,5,7 MV	67.61 ± 5.93%
PROD	**70.99 ± 5.87%**
SUM	69.01 ± 5.10%
2,6,7 MV	**70.98 ± 2.00%**
PROD	**72.96 ± 5.45%**
SUM	**70.99 ± 3.63%**
3,4,5 MV	62.82 ± 5.88%
PROD	64.22 ± 4.21%
SUM	63.10 ± 7.36%
3,4,6 MV	68.45 ± 3.83%
PROD	**71.27 ± 3.63%**
SUM	69.01 ± 3.27%

Table C.12: Averages of 7 classifiers including feature-level fused Target P4 and the parietal and occipital features for 71 patients (refer to Table 6.19). (continued)

Combinations	
3,4,7 MV	69.58 ± 7.06%
PROD	**73.80 ± 5.18%**
SUM	69.86 ± 4.56%
3,5,7 MV	66.48 ± 4.53%
PROD	**72.11 ± 2.28%**
SUM	68.45 ± 1.99%
3,6,7 MV	**72.96 ± 3.36%**
PROD	**76.90 ± 4.21%**
SUM	**74.93 ± 5.30%**
4,5,6 MV	69.86 ± 3.41%
PROD	69.58 ± 2.34%
SUM	**70.14 ± 2.28%**
4,5,7 MV	69.86 ± 6.13%
PROD	**70.14 ± 5.45%**
SUM	**70.42 ± 5.25%**
4,6,7 MV	**73.52 ± 5.00%**
PROD	**73.80 ± 4.03%**
SUM	**74.37 ± 5.01%**
5,6,7 MV	**74.09 ± 6.25%**
PROD	**71.55 ± 3.37%**
SUM	**74.08 ± 5.61%**
1,2,3,4,5 MV	69.58 ± 5.75%
PROD	**72.68 ± 4.88%**
SUM	69.86 ± 4.56%
1,2,3,4,6 MV	**71.27 ± 5.19%**
PROD	**75.21 ± 5.47%**
SUM	**73.52 ± 2.87%**
1,2,3,4,7 MV	**72.68 ± 4.39%**
PROD	**72.67 ± 3.62%**
SUM	**72.68 ± 2.35%**
1,2,3,5,6 MV	**72.11 ± 1.46%**
PROD	**75.21 ± 3.41%**
SUM	**72.11 ± 3.13%**
1,2,3,5,7 MV	**71.83 ± 2.77%**
PROD	**72.11 ± 5.72%**
SUM	**72.11 ± 3.13%**
1,2,3,6,7 MV	**73.52 ± 3.79%**
PROD	**74.65 ± 4.79%**
SUM	**74.09 ± 4.72%**
1,2,4,5,6 MV	**72.96 ± 1.92%**
PROD	**74.93 ± 2.87%**
SUM	**73.24 ± 4.10%**
1,2,4,5,7 MV	**73.80 ± 5.04%**
PROD	**72.39 ± 2.65%**
SUM	**72.96 ± 4.53%**

Combinations	
1,2,4,6,7 MV	**74.93 ± 4.18%**
PROD	**74.37 ± 1.92%**
SUM	**75.21 ± 2.65%**
1,2,5,6,7 MV	**75.21 ± 3.83%**
PROD	**74.93 ± 3.99%**
SUM	**74.37 ± 3.99%**
1,3,4,5,6 MV	68.17 ± 3.41%
PROD	**70.42 ± 3.27%**
SUM	**70.70 ± 2.59%**
1,3,4,5,7 MV	**70.70 ± 3.99%**
PROD	**74.37 ± 1.46%**
SUM	**70.70 ± 5.15%**
1,3,4,6,7 MV	**72.96 ± 5.44%**
PROD	**74.65 ± 4.46%**
SUM	**74.37 ± 4.18%**
1,3,5,6,7 MV	**72.96 ± 3.37%**
PROD	**74.93 ± 3.58%**
SUM	**74.37 ± 5.72%**
1,4,5,6,7 MV	**77.18 ± 5.85%**
PROD	**74.65 ± 2.76%**
SUM	**76.90 ± 5.04%**
2,3,4,5,6 MV	69.01 ± 1.23%
PROD	**75.49 ± 3.83%**
SUM	**72.11 ± 3.79%**
2,3,4,5,7 MV	**70.70 ± 5.85%**
PROD	**71.55 ± 3.37%**
SUM	**71.83 ± 4.63%**
2,3,4,6,7 MV	**72.96 ± 1.46%**
PROD	**74.08 ± 2.65%**
SUM	**73.24 ± 2.14%**
2,3,5,6,7 MV	**71.55 ± 3.99%**
PROD	**74.65 ± 4.79%**
SUM	**72.96 ± 3.59%**
2,4,5,6,7 MV	**72.67 ± 3.83%**
PROD	**74.65 ± 2.47%**
SUM	**73.52 ± 3.36%**
3,4,5,6,7 MV	**73.52 ± 5.16%**
PROD	**74.65 ± 3.27%**
SUM	**73.24 ± 3.91%**
ALL MV	**73.81 ± 4.56%**
PROD	**74.37 ± 2.28%**
SUM	**74.09 ± 2.00%**